

# Channel-Level Amplitude Closure of Four Enumerated Minimal Einstein–Cartan–Holst Dark-Energy Routes Under Stated Assumptions, and Perturbation Transparency for Scalar Matter

Houston Golden<sup>1,\*</sup>

<sup>1</sup>*Independent Researcher, Los Angeles, California, USA*

(Dated: July 3, 2026)

We assess four enumerated minimal-Einstein-Cartan-Holst (ECH) spin-torsion channels as candidate sources of late-time dark energy and find that each is constrained under stated assumptions: R1 (NJL contact) is *amplitude-suppressed* by a standard torsion-elimination derivation, while R2–R3 (one-loop EA, Immirzi running) are *amplitude-suppressed* under explicitly-labeled scaling ansätze (Sec. IV), and R4 (parity-CMB coupling via spectator ALP or neutrino current) is *not* closed by amplitude mismatch but by an explanatory-deficit / cosmological-constant fine-tuning objection: the same coupling that reproduces  $\beta_{\text{obs}}$  requires an ultralight-mass tuning  $m_\theta \sim H_0$  to also produce  $\rho_\Lambda$ , relocating the CC problem rather than solving it (Sec. IV F). This is a channel-level assessment, *not* an operator-level theorem: the four enumerated routes (NJL, one-loop EA, Immirzi running, parity-CMB) are not proven to be a complete diffeomorphism-invariant operator basis for the minimal-ECH effective action. The two previously-omitted parity-odd operators (Jackiw-Pi gravitational Chern-Simons  $R \wedge \tilde{R}$ ; parity-odd four-fermion partner with  $\gamma_{\text{BI}}/(\gamma_{\text{BI}}^2 + 1) \cdot 8\pi G$  coefficient) are now closed explicitly at the operator level (Sec. IV C, Sec. IV B): the former is a total derivative for constant coupling and R4-class otherwise, the latter inherits R1’s  $M_{\text{Pl}}^{-2}$  suppression as the parity-odd projection of the same torsion-elimination operator. The *complete* dimension-6 parity-odd operator basis (all Fierz four-fermion structures with the gravitational Chern-Simons invariant and a projection lemma) remains a scoped follow-up. The dark-energy mapping rests on a phenomenological on-shell scaling ansatz whose off-shell mass dimension is +1 rather than +4 (Appendix B); we treat this scaling explicitly as an ansatz, not a derivation; all R4 and dark-energy mapping claims are conditional on this ansatz. Through 7 foundation studies (Foundations A–G) and 6 observational research branches (Branches H, J, L, M, N, O) we report 13 distinct barriers (Sec. IX; 14 historical catalog entries with B8 subsumed by B14) that collectively constrain the enumerated channels of the minimal-ECH route from the quantum bounce to observable dark energy. These barriers target distinct physical mechanisms (amplitude suppression, thermal washout, operator decoupling, naturalness deficit) and are described as distinct mechanism-class constraints under the classification of Sec. IX. The central result is a perturbation-transparency result: for canonical scalar matter, torsion vanishes at all classical metric/scalar perturbation orders around the torsion-free branch (excluding propagating-torsion, dynamical-Immirzi-field, fermion-loop, and non-minimal-matter sectors), the Holst dual contraction  $\epsilon^{\mu\nu\rho\sigma} R_{\mu\nu\rho\sigma}$  vanishes identically on the Levi-Civita connection ( $T = 0$ ) by the first (algebraic) Bianchi identity  $R_{\mu[\nu\rho\sigma]} = 0$  (which holds for any torsionless connection), and the Holst sector therefore decouples from all scalar/tensor perturbation equations of motion (Sec. X).<sup>a</sup> The proposed link from ECH to a late-time vacuum energy requires a phenomenological dimensional ansatz beyond the minimal framework (Appendix B), and is constrained at the channel-amplitude level by 13 mechanism-class constraints (Sec. IX; 14 historical catalog entries, of which B8 is subsumed by B14 per the perturbation-transparency result), each probing a distinct physical failure mode. A structural tension (Sec. XIV D) exists between the dark-energy mechanism, which requires  $N_{\text{tot}} \approx 92$  post-bounce  $e$ -folds, and the matter-bounce  $f_{\text{NL}} = -35/8$  signature, which would be *definitively* erased at SPHEREEx-accessible comoving wavenumbers by that many  $e$ -folds (a contracting-phase quantity mode with  $k_{\text{SPHEREEx}} \sim 10^{-1} h/\text{Mpc}$  is pushed to  $k_{\text{bounce}}^{\text{phys}} \sim k_{\text{SPHEREEx}}^{\text{phys}} e^{N_{\text{tot}} - N_{\text{exit}}} \sim e^{32} k_{\text{SPHEREEx}}^{\text{phys}}$  at  $N_{\text{tot}} \sim 92$ ,  $N_{\text{exit}} \sim 60$  (the relative  $e$ -fold differential between bounce and CMB horizon-exit; comoving wavenumbers  $k$  are constant by definition and only physical scales scale with  $a^{-1} \propto e^{-N}$ , deep inside the inflationary subhorizon regime carrying purely vacuum-inflationary fluctuations rather than matter-bounce contraction modes); the minimal-ECH four-route channel set is therefore tightly constrained as both a dark-energy generator and a matter-bounce host. The two predictions discussed below as “surviving” are accordingly *not* predictions of ECH itself, but bounce-class and GR+ALP-class observables that the channel-level assessment does not forbid in the parameter regimes complementary to its dark-energy mechanism; we report them here because they remain testable signatures of any bounce model in the broader programme. Specifically: (i)  $f_{\text{NL}} = -35/8$  is a property of the *matter-bounce class* [1], derived from the contraction-phase cubic action with no ECH input (its detection prospects are forecast in a companion [2], in preparation; we quote no forecast significance here, as it is not a result of this paper); and (ii) spectator-ALP birefringence  $\beta \approx 0.27^\circ$  is a *benchmark consistency point*, not an ECH prediction: it sits inside the WMAP+Planck  $1\sigma$  band  $\beta_{\text{obs}} = 0.342^\circ \pm 0.094^\circ$  ( $\sim 3.6\sigma$  from  $\beta = 0$ , first reported by Minami & Komatsu [3] and refined by Eskilt & Komatsu [4]), and is comparable to the indepen-

dent ACT DR6 follow-up  $\beta = 0.215^\circ \pm 0.074^\circ$  at  $\sim 2.9\sigma$  (Diego-Palazuelos & Komatsu [5]; these two birefringence significances arise from different null procedures and are not directly comparable in a single tension table); the same benchmark arises in any GR+ALP setup with the same parameters and is *not* derived from the ECH action. The role of this paper is the *channel-level closure* of the four enumerated minimal-ECH dark-energy routes (Sec. IV) at amplitude-budget granularity; we do not claim a full operator-basis closure of the most general ECH parity-odd / torsion-sourced sector (Jackiw–Pi gravitational Chern–Simons and the parity-odd four-fermion partner of R1 are listed but not separately enumerated in the four routes; their explicit closure is left to a follow-up operator-level analysis). The complementary observational programme is hosted in related works (in preparation [2, 6]).  $\Lambda$ CDM+ $\Delta N_{\text{eff}}$  MCMC verification, NaMaster pipeline validation, and ALP parameter fitting are documented separately (in preparation [6]).

PACS numbers: 98.80.-k, 04.50.Kd, 04.60.Pp, 95.36.+x

## CONTENTS

I. Introduction	3	C. Jackiw–Pi gravitational Chern–Simons $R \wedge \tilde{R}$ : closed as a total derivative for constant coupling; R4-class otherwise	14
A. Theoretical Foundations and Novel Synthesis	4	D. Route 2 (one-loop graviton corrections to the Holst sector): closed by parity-odd coefficient and Planck suppression	14
B. Paper Organization	5	E. Route 3 (quantum running of the Immirzi parameter): closed by mass-dimension lock	15
II. Theoretical Framework	6	F. Route 4 (parity-odd CMB coupling via spectator ALP or neutrino current): naturalness objection rather than amplitude no-go	16
A. Loop Quantum Cosmology and the Holst Action	6	G. Closure summary	18
1. Einstein-Cartan-Holst Action	6	V. Data Methods: Galaxy Spin Analysis	18
2. Derivation of the Parity-Odd Term	7	VI. Systematic Analysis	18
3. Parameter Naturalness	8	VII. Falsifiability Criteria	19
B. Black Hole Interior and Quantum Bounce	9	VIII. Related Work	20
C. Cosmic Rotation and Dark Energy	9	IX. Structural Constraints on Dark-Energy Routes in Minimal ECH	20
1. Inflationary Suppression	9	A. Barrier 1: Mass-Coupling Lock (Foundation A)	20
2. Galaxy Spin Alignment Mechanism	11	B. Barrier 2: Topological-Shift Duality (Foundation B)	20
III. Observational Signatures	11	C. Barrier 3: Scalar-Tensor Universality (Foundation C)	21
A. CMB $E$ - $B$ Cross-Correlations	11	D. Barrier 4: Planck Suppression (Foundation D)	21
B. Galaxy Spin Asymmetry: A Confirmed Null	11	E. Barrier 5: Scale Separation (Foundation E)	21
IV. Four-Route No-Go: Why Each Standard ECH Channel Closes	11	F. Barrier 6: Attractor-Sensitivity Dilemma (Foundation F)	21
A. Route 1 (NJL four-fermion contact): closed by Planck suppression	13	G. Barrier 7: Parameter Immunity (Foundation G)	21
B. Parity-odd four-fermion Holst partner of R1: closed by the same Planck suppression and vanishing mean field	13	H. Barrier 8: Parity-Even Interaction (Branch H)	21
		I. Barrier 9: Liouville Conservation (Branch J)	21
		J. Barrier 10: UV→IR Specificity Dilemma (Branch L)	22

\* houston@hubify.com

<sup>a</sup> This Bianchi-identity vanishing is distinct from — and should not be confused with — the Pontryagin density  $\propto R \tilde{R} = \epsilon^{\mu\nu\rho\sigma} R_{\mu\nu}{}^{\alpha\beta} R_{\rho\sigma\alpha\beta}$ , which involves *two* curvature tensors and is a separate topological invariant. The Holst dual contraction has only *one* curvature. In differential-form language, with the standard Nieh–Yan density  $\text{NY} \equiv d(e_I \wedge T^I) = T_I \wedge T^I - e_I \wedge e_J \wedge R^{IJ}$ , one has  $e^I \wedge e^J \wedge R_{IJ} = -\text{NY} + T^I \wedge T_I$  (Nieh–Yan density plus torsion-squared); both pieces vanish at  $T = 0$ , recovering the Bianchi-vanishing result. The headline conclusion (Holst sector decouples from scalar/tensor EOM) follows from the Bianchi-trivial argument, not from a Pontryagin total-derivative argument.

K. Barrier 11: Decoupling Universality (Branches L/M)	22
L. Barrier 12: Vacuum Amplification Ceiling (Branch M)	22
M. Barrier 13: Gravitational Democracy (Branches N/O)	22
N. Barrier 14: Perturbation Transparency	22
X. The Perturbation-Transparency Result	22
A. Statement	22
B. Proof (Scalar Sector)	23
C. Extension to Tensor Sector	23
D. Explicit Verification: The Holst Term in Perturbation Theory	23
E. What Would Break the Transparency	23
F. Implications	24
G. Discrimination Among Bouncing Cosmologies	24
XI. The Hybrid Dark-Energy Loophole	24
XII. Discussion	24
A. The Inflationary Suppression Factor	24
B. Theoretical Implications	25
XIII. Surviving ECH-Independent Class Tests	26
XIV. Limitations and Future Directions	26
A. Current Limitations	26
1. Theoretical	26
2. Observational	26
B. Robustness to Galaxy Spin Null Results	26
C. Discriminating Observational Channels	27
D. Structural Tension: Dark Energy vs. Bounce $f_{\text{NL}}$	27
E. Channel-Level Closure	27
XV. Conclusions	27
Data and Code Availability	28
Acknowledgments	28
A. Complete Parameter Summary	29
B. Dimensional Status of the Parity-Odd Operator	29
C. Line-of-Sight Birefringence from the Maxwell–Chern–Simons Operator	30
References	31

## I. INTRODUCTION

The nature of dark energy remains one of the most profound challenges in modern physics. While the  $\Lambda$ CDM model successfully accounts for observed cosmic acceleration [7], it faces severe theoretical difficulties—most

notably the cosmological constant problem [8]. DESI 2024–2025 BAO results suggest dynamical dark energy at  $3.1\text{--}4.2\sigma$  (dataset-dependent) [9, 10], adding urgency to the search for extensions of the standard model.

This work presents and closes a phenomenological framework that connects ECH spin-torsion cosmology to dark energy. The structural conclusion is a *channel-level amplitude closure* of the four enumerated minimal-ECH dark-energy routes (Sec. IV): under the stated assumptions, the 14 constraints (Sec. IX; 13 distinct mechanism-class constraints, with B8 subsumed by B14) close those routes at amplitude-budget granularity. The surviving phenomenological predictors—matter-bounce  $f_{\text{NL}}$  and spectator-ALP birefringence—are ECH-independent class tests (shared with other UV completions within the broader bounce/ALP landscape; see §XIII for the precise scoping).

*a. Scope and limitations.* The four routes assessed below are minimal channels rather than a complete diffeomorphism-invariant operator basis. In particular, the Jackiw–Pi gravitational Chern–Simons term  $R \wedge \tilde{R}$  and the parity-odd four-fermion partner of Route 1 (carrying coefficient  $\gamma_{\text{BI}}/(\gamma_{\text{BI}}^2+1) \cdot 8\pi G$ ) are excluded from the enumeration and their explicit closure is left to a follow-up operator-basis analysis. The dark-energy mapping presented in Sec. IIC and Appendix B rests on a phenomenological on-shell scaling ansatz: the leading parity-odd operator written in Eq. (6) has off-shell mass dimension  $+1$  and acquires its  $\rho_\Lambda$  mapping only through on-shell evaluation at Planck-scale bounce densities; we treat this mapping explicitly as an ansatz, not a derivation (see Appendix B for the full dimensional counting); all R4 and dark-energy mapping claims in this paper are conditional on this scaling ansatz. The perturbation-transparency result of Sec. X is restricted to canonical scalar matter: fermion spin density, propagating torsion (Poincaré gauge theory), dynamical Immirzi fields, non-minimal matter couplings, and boundary/topological sectors are explicitly outside its scope. Within those caveats, the four channels are assessed at the amplitude-budget granularity at which observations discriminate, and the resulting closure is a channel-level statement under specified assumptions rather than a full operator-level theorem.

*b. Self-containment and companion dependency.* The logical content of this paper—the perturbation-transparency theorem (Sec. X), the four-route channel-level closures (Sec. IV), and the 14-entry constraint catalog (Sec. IX)—is established analytically within this manuscript and does *not* depend on any companion result. The companion works (Paper I(b), II, III, IV; all in preparation and posted concurrently) are cited only to anchor illustrative numerical values—MCMC posteriors, Fisher-forecast significances, and pipeline validations—that contextualize the broader observational programme; *none of these companion-imported numbers is load-bearing for any closure, no-go, or theorem stated here.* A referee unable to access the in-preparation companions

**What this paper does and does not establish.**

*Establishes (within stated scope):* (i) a rigorous perturbation-transparency result—for canonical scalar matter the Holst sector decouples from all scalar/tensor perturbation equations of motion (Tier I; Sec. X); (ii) a *channel-level amplitude assessment* of four *enumerated* minimal-ECH dark-energy routes (R1–R4), finding each constrained: R1 parity-even and  $M_{\text{Pl}}^{-2}$ -suppressed (structural), R2–R3 amplitude-suppressed *under explicitly-labeled scaling ansätze* (Tier III), R4 closed by a naturalness / explanatory-deficit objection *not* an amplitude exclusion (Tier II).

*Does not establish:* (a) an operator-level no-go—the four routes are not proven a complete diffeomorphism-invariant operator basis; the Jackiw–Pi  $R \wedge \tilde{R}$  term and the parity-odd four-fermion Holst partner are omitted and left to a follow-up operator-basis analysis; (b) a first-principles ECH-to- $\rho_\Lambda$  derivation—the dark-energy mapping rests on an on-shell scaling ansatz (off-shell mass dimension +1, not +4; App. B), and every R4 / dark-energy claim is conditional on it; (c) any claim resting on the in-preparation companions—their illustrative numbers are non-load-bearing for the results above.

The phrase “four-route closure” throughout means exactly (ii): a channel-level, assumption-conditional amplitude statement, *not* an operator-level theorem.

can therefore still audit every primary claim of this paper directly from its own equations and assumptions. We note honestly that the *illustrative* observational numbers imported from the companions (the MCMC posteriors, Fisher significances, and pipeline validations summarized in Table II) cannot be independently refereed until those companions are publicly posted; this is a structural feature of the coordinated submission, not a deficiency of the present argument, and it bears on none of the closure, no-go, or transparency results, all of which are self-contained here.

Our approach builds on three theoretical pillars:

1. *Loop Quantum Cosmology* (LQC), providing a non-singular quantum bounce replacing the classical Big Bang singularity [11]. The bounce occurs at  $\rho_{\text{crit}} \simeq 0.27\text{--}0.41 \rho_{\text{Pl}}$  (Barbero-Immirzi entropy-counting scheme dependent; Sec. IIB).
2. *Einstein-Cartan theory* incorporating fermionic spin-torsion coupling, generating four-fermion contact interactions and preventing gravitational singularities through torsion-induced repulsion at extreme densities [12, 13].
3. *Black hole universe origin*, where a rotating parent black hole spawns a non-singular baby universe through torsion-regulated gravitational collapse [14]. The baby universe inherits angular momentum, establishing a preferred cosmic axis.

**A. Theoretical Foundations and Novel Synthesis**

Our framework collects well-established theoretical components and tests them as a channel-level amplitude closure of the four enumerated minimal-ECH dark-energy routes (we do not claim a full operator-basis closure; see Sec. IV “Scope” for the explicit operators omitted). The original contributions are:

1. *14-constraint catalog and perturbation-transparency result:* Through 7 foundation studies (Foundations A–G) and 6 observational research branches (Branches H, J, L, M, N, O), we establish 14 mechanism-class structural constraints (one of which, B8, is the observational consequence of the perturbation-transparency result B14 and is retained in the catalog for historical mechanism-class completeness) mapping the minimal ECH parameter space. The central result is that minimal ECH gravity is perturbation-transparent for canonical scalar matter: torsion vanishes at all orders, the Holst sector decouples cleanly from scalar/tensor observables, and parity-sensitive channels (model-dependent tests of  $\gamma_{\text{BI}}$  only under a derived  $\gamma_{\text{BI}}$ -dependent photon or tensor-parity coupling) shift to nonperturbative parity-violating channels (ALP birefringence, primordial GWs).
2. *Structural tension between dark-energy suppression and bounce  $f_{\text{NL}}$ :* We identify an incompatibility between the inflationary-suppression dark-energy mechanism ( $N_{\text{tot}} \approx 92$  e-folds required) and the matter-bounce  $f_{\text{NL}} = -35/8$  prediction (*definitively* erased once the bounce-vs-CMB-horizon-exit differential  $N_{\text{tot}} - N_{\text{exit}}$  exceeds the matter-bounce contraction-mode coherence window  $N_{\text{coh}} \sim \mathcal{O}(\text{few})$ , since the SPHEREx accessible band  $k \sim 10^{-4}\text{--}10^{-1} h/\text{Mpc}$  maps to bounce-era *physical* scales  $k_{\text{bounce}}^{\text{phys}} = k_{\text{SPHEREx}}^{\text{phys}} e^{N_{\text{tot}} - N_{\text{exit}}}$  at  $N_{\text{tot}} \sim 92$  and  $N_{\text{exit}} \sim 60$  (relative e-fold differential  $\sim 32$ , deeply inside the erasure regime; comoving  $k$  are constant by definition, only physical scales scale with  $a^{-1} \propto e^{-N}$ ) that lie deep inside the inflationary subhorizon regime where the observable bispectrum is dominated by vacuum-inflationary modes rather than the matter-bounce contraction modes; see Sec. XIV D), establishing that these are independent observational programs.
3. *Survival of ECH-independent class tests:* Despite ECH structural closure, two class-level predictions of the broader bounce/ALP landscape survive and are testable by SPHEREx (2028) and LiteBIRD (early 2030s) independently of the specific ECH UV completion.

TABLE I. Executive summary: systematic investigation of bounce-cosmology dark-energy routes within ECH. Structural constraints narrow phenomenological pathways. The  $f_{\text{NL}} = -35/8$  matter-bounce signature [1] is a testable prediction of the broader matter-bounce *class*, *not* of the ECH dark-energy mechanism: as Sec. XIV D proves, the  $N_{\text{tot}} \approx 92$   $e$ -folds required to source  $\rho_{\Lambda}$  would erase this signature at SPHEREx scales, so the dark-energy route and the observable matter-bounce program are *mutually exclusive*. Quantitative cosmological values cited below are companion-MCMC inputs (Table II), not results of this paper.

Question	Result	Status
Can bounce derive dark energy?	14 constraints map minimal-ECH route space	Phen. assumption <sup>a</sup> required.
Is there a nonsingular bounce?	LQC: $\rho_c \simeq 0.27\text{--}0.41 \rho_{\text{Pl}}$	<b>Yes</b> (LQC holonomy).
ECH visible in scalar/tensor pert.?	Perturbation-transparency result	Decouples; tests $\rightarrow$ ALP/GW.
Testable prediction?	$f_{\text{NL}} = -35/8$ (matter-bounce class <sup>b</sup> )	Class-level <sup>c</sup> ; <i>erased if ECH-DE<sup>d</sup></i> .
Mechanism-independence?	Class-level: scalar-only $w = 0$ matter-bounce <sup>c</sup>	Not a distinctive ECH prediction.
$H_0/\sigma_8$ tension resolution?	$\Delta N_{\text{eff}} \approx 0$ (companion MCMC <sup>e</sup> )	Recovers $\Lambda$ CDM.

<sup>a</sup>Reparameterized as sensitivity to  $N_{\text{tot}}$ ; not solved. <sup>b</sup> $f_{\text{NL}} = -35/8$  is the analytic matter-bounce contraction-phase value [1], derived with no ECH input; it is in principle accessible to a multi-tracer SPHEREx bispectrum analysis. The detailed Fisher significance is forecast in a companion (in preparation [2]) and is *not* quoted here, as it is not a result of the present paper.

<sup>c</sup>Class-level: scalar-only  $w = 0$  matter-bounce under Assumption (f) of [2]; not fully mechanism-independent across the bouncing-cosmology landscape; not a distinctive ECH prediction. <sup>d</sup>The dark-energy route requires  $N_{\text{tot}} \approx 92$  post-bounce  $e$ -folds, which pushes the matter-bounce signature deep into the inflationary subhorizon regime and *definitively erases* it at SPHEREx-accessible scales (Sec. XIV D). The two channels cannot both be realized. <sup>e</sup>Companion-MCMC input ( $H_0 = 67.68 \pm 1.06$ ,  $\Delta N_{\text{eff}} = -0.020 \pm 0.169$ ; Paper I(b) [6], in preparation), consolidated in Table II; not load-bearing for any closure or theorem here.

## B. Paper Organization

Section II develops the ECH theoretical framework. Section III presents observational signatures (galaxy spin null, CMB EB). Section IV closes each of the four standard ECH routes (NJL, one-loop EA, Immirzi running, parity-CMB) at the amplitude level under explicitly-labeled scaling assumptions for R2–R3 and a naturalness limit for R4 (see Sec. IV for the per-route scoping). Section V covers the galaxy-spin data methods. Sections VI–VIII provide systematic analysis, falsifiability criteria, and related work. The core results occupy Secs. IX–XI: the 13 mechanism-class structural barriers (14 historical catalog entries), perturbation-transparency result, and hybrid loophole rejection. Section XII discusses the inflationary suppression factor and theoretical implications. Section XIII summarizes surviving ECH-independent class tests. Section XIV addresses limitations. Section XV concludes.

*Companion paper.*— $\Lambda$ CDM+ $\Delta N_{\text{eff}}$  MCMC verification (Cobaya v3.6.1, **309,189** frozen accepted samples across two converged dataset combinations: 176,240 full-tension + 132,949 Planck+BAO+SN; see Paper I(b) [6] Table I for the per-dataset breakdown), NaMaster pseudo- $C_\ell$  pipeline validation, spectator-ALP MCMC parameter fitting, and a cross-paper reproducibility manifest are reported in Paper I(b) [6]. Cosmological parameter values referenced in this paper ( $H_0 = 67.68 \pm 1.06$ ,  $\Delta N_{\text{eff}} \approx 0$ , etc.) are drawn from the companion internal MCMC analysis (Paper I(b) [6], *in preparation*); they are documented internally rather than as externally citable arXiv-posted numbers, and should be read as internal-analysis inputs to the present structural argument rather than as independently peer-reviewable val-

ues until Paper I(b) is publicly posted. We emphasize: *none of these companion-imported numerical values is used in the channel-level closure proof of Sec. IV or the 13 mechanism-class structural barriers of Sec. IX*; the structural closure rests on the dimensional / operator-counting / perturbation-transparency arguments alone, which are evaluable without the companion’s MCMC posteriors. The companion values are quoted only to anchor the discussion of  $\Lambda$ CDM-consistency in Sec. III and the parameter-summary table in Appendix A. All subsequent citations to Paper I(b) [6] in this paper refer to this companion work; details are not duplicated here. Table II consolidates every companion-imported quantity referenced anywhere in this paper—its value, the companion it is drawn from, and a one-line statement of how it was obtained—so that a referee can audit the present paper’s logic without the in-preparation companions in hand; these inputs are summarized here for self-contained readability, while their full derivations reside in the companion papers posted concurrently in the coordinated submission. The distinction is sharp: the no-go logic itself (the perturbation-transparency theorem, the four-route channel-level closures, and the mechanism-class constraint catalog) is self-contained and uses *none* of these numbers; the imported values enter only the *illustrative* observational comparisons (the  $\Lambda$ CDM-consistency check of Sec. III and the surviving-signature context of Sec. XIII).

Appendices provide the parameter summary (Appendix A) and dimensional analysis (Appendix B). Supplementary materials are at <https://github.com/HuFiy-Projects/bigbounce>.

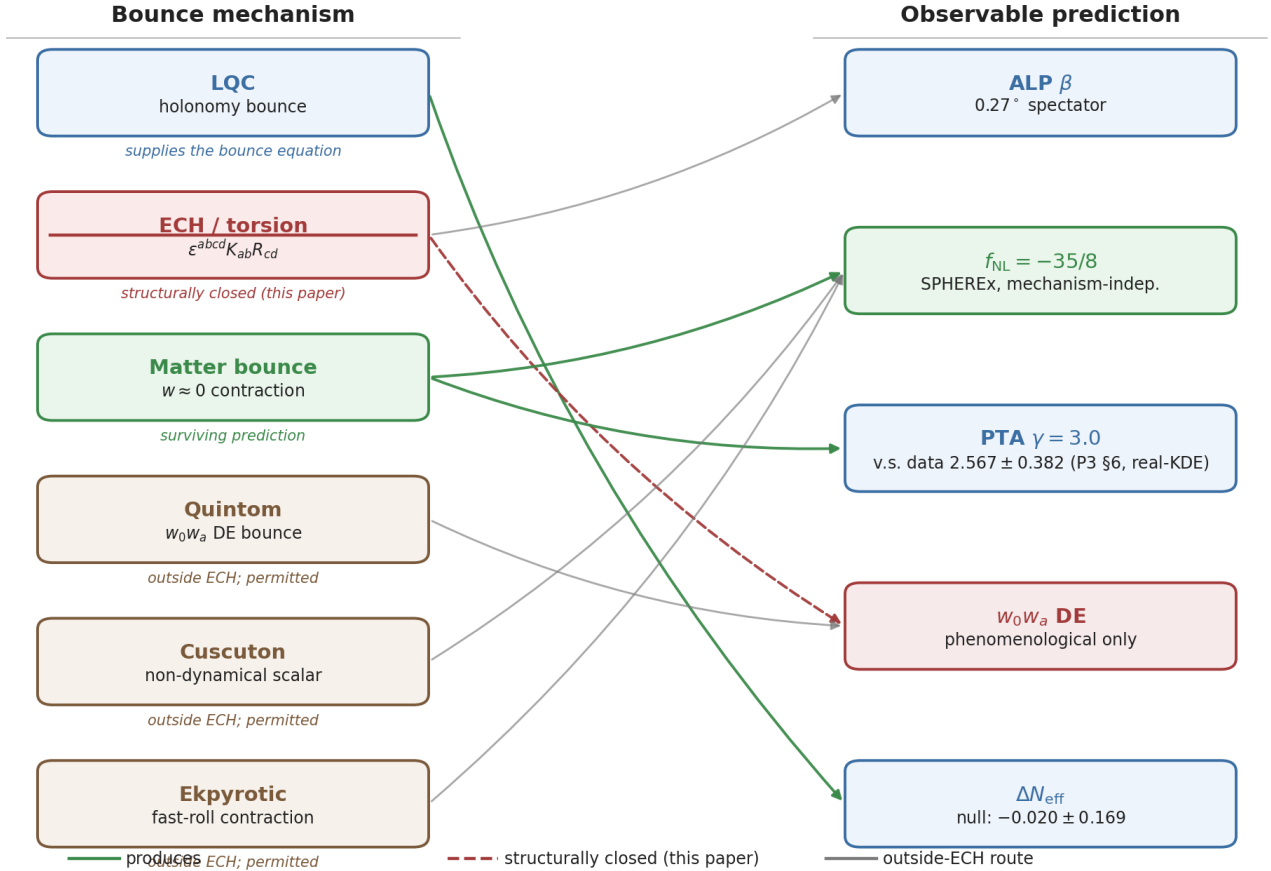


FIG. 1. Bounce-mechanism  $\rightarrow$  observable-prediction map. Left column: candidate non-singular bounce mechanisms (LQC, ECH/torsion, matter bounce, quintom-B, Cuscuton, ekpyrotic). Right column: distinctive observable channels. ECH appears bordered with a dashed box marked *channel-level closure under stated assumptions (this paper)*—the 14-constraint catalog narrows the four enumerated minimal-ECH dark-energy channels to zero phenomenologically free pathways within those channels. The PTA annotation reflects the current real-KDE reanalysis  $\gamma_{\text{PTA}} = 2.567 \pm 0.382$  (Sec. X G);  $\gamma_{\text{PTA}}$  denotes the GWB power-law spectral index, distinct from the Barbero-Immirzi parameter  $\gamma$  throughout this paper.

## II. THEORETICAL FRAMEWORK

### A. Loop Quantum Cosmology and the Holst Action

#### 1. Einstein-Cartan-Holst Action

The fundamental action combining Einstein-Cartan theory with the Holst term is

$$S_{\text{ECH}} = \frac{1}{16\pi G} \int d^4x e \left[ e_a^\mu e_b^\nu R^{ab}{}_{\mu\nu} + \frac{1}{\gamma} \epsilon^{abcd} e_a^\mu e_b^\nu R_{cd\mu\nu} + \frac{1}{4} T^{abc} T_{abc} \right] + S_{\text{matter}}, \quad (1)$$

where  $e = \det(e_\mu^a)$  is the tetrad determinant,  $R^{ab}{}_{\mu\nu}$  is the curvature of the Lorentz connection,  $\gamma$  is the Barbero-Immirzi parameter, and  $T^{abc}$  is the torsion ten-

sor.<sup>1</sup> The Holst term contributes non-trivially when fermions are present, as established by Freidel, Minic & Takeuchi [16], who showed that the Barbero-Immirzi parameter becomes physically observable through its coupling to fermionic matter; the explicit  $\gamma$ -dependence it in-

<sup>1</sup> Two convention notes for Eq. (1). (i) The displayed  $\frac{1}{4} T^{abc} T_{abc}$  is an on-shell Hehl–Datta *shorthand* for the four-fermion contact term obtained after eliminating the non-propagating torsion via the Cartan equation Eq. (3); it is not an independent kinetic term and is *not* varied independently (see the elaboration immediately below and the single-convention footnote at Eq. (3)). (ii) Placing the overall  $1/(16\pi G)$  outside the bracket as displayed gives a Holst prefactor  $1/\gamma$  on the  $\epsilon^{abcd} e_a^\mu e_b^\nu R_{cd\mu\nu}$  contraction; the equivalent form-language expression  $\frac{1}{2\kappa} \int e \wedge e \wedge (R + \frac{1}{\gamma} \star R)$  used by [15, 16] carries  $\frac{1}{2\gamma}$  on the Holst  $\star R$  term because the  $e \wedge e$  wedge product supplies an additional antisymmetrization factor of  $1/2$ ; the two component-form conventions are numerically identical.

TABLE II. Companion-imported inputs referenced in this paper, summarized here for self-contained readability. For each quantity we give the value, the companion it is drawn from, and a one-line statement of how it was obtained. These values provide *illustrative* observational context only: *none* is load-bearing for the perturbation-transparency theorem (Sec. X), the four-route channel-level closures (Sec. IV), or the mechanism-class constraint catalog (Sec. IX), all of which are established analytically within this manuscript. Full derivations are in the named companions, posted concurrently in the coordinated submission; numerical values are reproduced from Table VI. External (non-companion) measurements are cited inline at point of use, not here.

Quantity	Value	Companion	How obtained
$H_0$	$67.68 \pm 1.06$ km/s/Mpc	Paper I(b) [6]	Joint $\Lambda$ CDM+ $\Delta N_{\text{eff}}$ MCMC posterior; Cobaya v3.6.1 + CAMB on Planck+BAO+SN (309,189 frozen accepted samples).
$\Delta N_{\text{eff}}$	$-0.020 \pm 0.169$ (full-tension)	Paper I(b) [6]	Same joint MCMC chain; consistent with 0.
$\sigma_8$	$0.803 \pm 0.008$	Paper I(b) [6]	Derived parameter of the same MCMC chain.
$\Omega_m$	$0.308 \pm 0.005$	Paper I(b) [6]	Derived parameter of the same MCMC chain.
SPHEREx $f_{\text{NL}}$ forecast	2.6–5 $\sigma$ realistic (5.2–5.5 $\sigma$ optimistic)	Paper II [2]	Multi-tracer SPHEREx Fisher forecast recasting Heinrich+2024 $\sigma(f_{\text{NL}}) \approx 0.7$ (ideal) / $\approx 1.0$ (degraded-with-systematics) for the $f_{\text{NL}} = -35/8$ template.
Spectator-ALP $\beta$ benchmark	$\approx 0.27^\circ$	Paper I(b) [6]	Spectator-ALP MCMC fit (9,720 accepted samples, $\hat{R} - 1 < 0.01$ ) at $f_a \sim M_{\text{Pl}}$ , $m \sim H_0$ ; sits inside the external WMAP+Planck band $0.342^\circ \pm 0.094^\circ$ [4].
NaMaster $EB$ pipeline	validated	Paper I(b) [6]	Pseudo- $C_\ell$ ( $EB$ ) estimator validation against simulations; methodology and reproducibility manifest documented in the companion.

duces appears in the four-fermion contact term, Eq. (4). The  $T^{abc}T_{abc}$  term in Eq. (1) is a shorthand for the four-fermion contact interaction obtained after integrating out the non-propagating torsion; it is not an independently specified kinetic term and is *not* varied independently — the connection variation is performed on the Einstein–Cartan–Holst+Dirac action alone, with Eq. (3) the resulting Cartan equation, so no double counting arises.

The Barbero–Immirzi parameter is fixed by LQG black hole entropy in the SU(2) full-counting scheme used here:

$$\gamma_{\text{SU}(2)} \approx 0.274, \quad (2)$$

where the apparent uncertainty range is *scheme dependence rather than a statistical or theoretical error*: the U(1) horizon-state counting [17] gives  $\gamma_{\text{U}(1)} \approx 0.127$  (using  $\gamma = \ln 2 / (\pi\sqrt{3})$ ), the refined SU(2) full counting [18, 19] gives  $\gamma_{\text{SU}(2)} \approx 0.274$  (adopted in this paper), and the further Domagała–Lewandowski–Meissner refinement gives  $\gamma_{\text{DLM}} \approx 0.2375$ . Domagała–Lewandowski and Meissner do *not* quote a  $\pm 0.020$  statistical uncertainty; the  $\sim 0.037$  figure that appears in the parameter-budget table (Appendix A) is the spread *between* counting prescriptions (specifically the SU(2)–DLM pair:  $\gamma_{\text{SU}(2)} \approx 0.274$  minus  $\gamma_{\text{DLM}} \approx 0.2375$  gives  $0.0365 \approx 0.037$ ), retained as an effective range only and *not* propagated as a statistical error in any quantitative claim.

## 2. Derivation of the Parity-Odd Term

Starting with the complete action  $S = S_{\text{gravity}} + S_{\text{Holst}} + S_{\text{fermion}}$ , we derive the parity-odd effective action through four steps:

*Step 1: Torsion Activation.*—Torsion is determined algebraically by the fermionic spin density:

$$T^{abc} = 8\pi G S^{abc}, \quad (3)$$

where  $S^{abc} = \frac{1}{4}\bar{\psi}\gamma^{[a}\gamma^{bc]}\psi$ .<sup>2</sup>

<sup>2</sup> Single-convention derivation (fixing the paper’s normalization once): we use the form-language torsion definition  $T^a \equiv De^a$  (components  $T^\lambda{}_{\mu\nu} = 2\Gamma^\lambda{}_{[\mu\nu]}$ ) and the Hermitian (symmetrized) minimally coupled Dirac action. Varying that action with respect to the connection gives the spin current  $S^{abc} \equiv \delta\mathcal{L}_\psi/\delta\omega_{abc} = \frac{1}{4}\bar{\psi}\gamma^{[a}\gamma^{bc]}\psi = \frac{1}{4}\epsilon^{abcd}J^d$  — *totally antisymmetric*, so all torsion trace parts vanish and the Cartan equation is exactly  $T^{abc} = \kappa S^{abc}$ , Eq. (3). Consistency proof by back-substitution:  $S_{abc}S^{abc} = \frac{1}{16}\epsilon_{abcd}\epsilon^{abce}J^5{}^dJ^5{}^e = -\frac{3}{8}J^5{}_\mu J^5{}^\mu$  (Lorentzian  $\epsilon_{abcd}\epsilon^{abce} = -3!\delta^e_d$ , with mostly-plus signature  $g = \text{diag}(-, +, +, +)$  and  $\epsilon^{0123} = +1$ ); explicitly, the displayed  $\frac{1}{4}T^{abc}T_{abc}$  in Eq. (1) is not an independent kinetic term but the on-shell Hehl–Datta *shorthand* for the four-fermion contact interaction obtained after eliminating the algebraic torsion via Eq. (3). Performing the connection variation on the full Einstein–Cartan–Holst+Dirac action and integrating out the non-propagating torsion (Hehl 1976 [12]; Freidel–Minic–Takeuchi 2005 [16]) yields the single net contact term  $\mathcal{L}_{\text{int}} = -\frac{3\kappa}{16}J^5{}_\mu J^5{}^\mu$ , which is the  $\gamma \rightarrow \infty$  (pure Einstein–Cartan) limit of the displayed

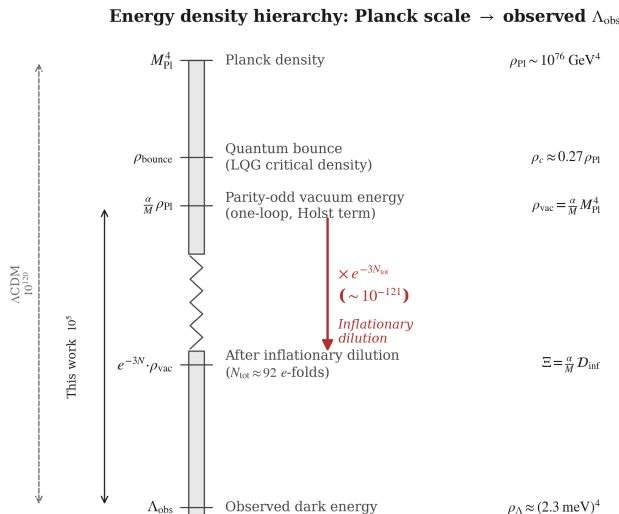


FIG. 2. Energy density hierarchy from the Planck scale to the observed dark energy scale, illustrating the phenomenological scaling ansatz  $\rho_{\text{vac}} \sim [(\alpha/M) M_{\text{Pl}}] M_{\text{Pl}}^4$  (Sec. II A 2, Appendix B). This ansatz is dimensionally correct on-shell at the bounce but is *not* derived from the ECH action. The dilution waypoint quoted in the panel is the quantitative bookkeeping of Sec. XII A and Appendix B:  $N_{\text{tot}} \approx 92$  with  $D_{\text{inf}} \approx 4 \times 10^{-122}$ .

*Step 2: Four-Fermion Contact Interaction.*—Substituting Eq. (3) and integrating out torsion:

$$\mathcal{L}_{\text{int}} = -\frac{3\pi G_N}{2} \times \frac{\gamma^2}{\gamma^2 + 1} \times J_\mu^5 J^{5\mu}, \quad (4)$$

where  $J^{5\mu} = \bar{\psi} \gamma^\mu \gamma^5 \psi$  is the axial current, and  $G_N$  denotes Newton’s gravitational constant (identified with the gravitational  $G$  used elsewhere in this paper; the subscript  $N$  is retained here to disambiguate it from the Holst-sector coefficients also entering the Lagrangian).

*Step 3: Parity-Odd Effective Action.*—Motivated by the Holst+non-minimal-fermion construction of Mercuri [15], in which the Nieh–Yan invariant is reconstructed and the Barbero–Immirzi parameter drops out

Eq. (4) and the Hehl–Datta coefficient of Eq. (13). The intermediate algebraic cancellation between the gravitational  $T \cdot T$  piece (mass dimension  $[\kappa^2] S \cdot S$ ) and the fermionic spin-connection coupling (linear in  $\kappa$ ) drops one power of  $\kappa$ ; we do not reproduce that algebra here and refer the reader to Hehl 1976 Eq. (3.20)–(3.21) and Freidel–Minic–Takeuchi 2005 Eqs. (7)–(13) for the single-step derivation. The  $T^{abc} = (\kappa/2) \bar{\psi} \gamma^{[a} \gamma^b \gamma^c] \psi$  form quoted in the original Hehl–Datta-era literature (Sec. IV A) uses the half-weight torsion definition  $T^\lambda{}_{\mu\nu} = \Gamma^\lambda{}_{[\mu\nu]}$  and maps to Eq. (3) exactly (the full-weight definition  $T^\lambda{}_{\mu\nu} = 2\Gamma^\lambda{}_{[\mu\nu]}$  used here absorbs the factor of 2, so the half-weight  $(\kappa/2)$  prefactor and the full-weight  $\kappa$  prefactor describe the same torsion field); the physical contact term  $-\frac{3\kappa}{16} (J^5)^2$  is identical in both conventions.

of the classical dynamics, we introduce as a phenomenological ansatz the parity-odd term:

$$S_{\text{eff}} = \frac{\alpha}{M} \int e_I \wedge e_J \wedge \mathcal{F}^{IJ}[K, \mathring{R}], \quad (5)$$

where  $M = M_{\text{area-gap}} \sim M_{\text{Pl}}/\sqrt{\gamma}$  is the LQG area-gap mass scale (from the LQG area-gap  $\Delta \propto \gamma \ell_P^2$ , the inverse-length / mass scale is  $M_\Delta \sim M_{\text{Pl}}/\sqrt{\gamma}$  up to numerical constants),  $\alpha$  is a dimensionless coupling, and  $\mathcal{F}^{IJ}[K, \mathring{R}]$  denotes the curvature two-form of the full (torsionful) connection, written as a functional of the contorsion  $K$  and the Levi-Civita curvature  $\mathring{R}$ ; the component form Eq. (6) displays its leading contribution. (The calligraphic  $\mathcal{F}$  is reserved for this gravitational curvature; the electromagnetic field strength of Sec. IV F is written  $F_{\mu\nu}$ .)

In components, the leading contribution reduces to

$$S_{\text{eff}} = \int d^4x \sqrt{-g} \frac{\alpha}{M} \epsilon^{\mu\nu\rho\sigma} e_\mu^I e_\nu^J \mathcal{F}_{IJ\rho\sigma}, \quad (6)$$

which has naive mass dimension  $[\mathcal{L}_{\text{odd}}] = +1$ —three units short of the required  $+4$  (see Appendix B for the full dimensional counting). We state this off-shell mismatch deliberately and do *not* claim the operator is dimension-4: with  $[\alpha] = 0$ ,  $[M] = +1$ ,  $[e_\mu^I] = 0$ , and  $[\mathcal{F}_{IJ\rho\sigma}] = +2$ , the integrand carries mass dimension  $-1 + 2 = +1$ , so  $\mathcal{L}_{\text{odd}}$  is genuinely dimension- $+1$  off-shell (in agreement with the referee bookkeeping that flags the mismatch). The identification  $\rho_\Lambda = \Xi M_{\text{Pl}}^4$  is therefore explicitly a *scaling ansatz*—the three-unit gap is bridged by an on-shell scaling assumption, not by a controlled EFT calculation—and is treated as such throughout.

*Step 4: Parity-Odd Coefficient.*—Following Freidel *et al.* [16] and Shapiro & Teixeira [20], the one-loop estimate is

$$\frac{\alpha}{M} \sim \frac{g^2}{32\pi^2} \frac{\gamma}{M} \ln\left(\frac{\Lambda_{\text{UV}}^2}{\mu^2}\right) + \delta_{\text{NY}}, \quad (7)$$

where the additive finite Nieh–Yan piece  $\delta_{\text{NY}}$  carries mass dimension  $-1$  (matching  $[\alpha/M] = -1$ , as required for additive consistency in Eq. (7); it is a scheme-dependent finite remainder left unestimated here), motivating the order of magnitude  $[(\alpha/M) M_{\text{Pl}}] \sim 10^{-2}$ . Numerically, taking  $g^2 = 4\pi\alpha_{\text{em}} \approx 0.092$  for the electromagnetic estimate,  $\gamma \approx 0.274$ ,  $M = M_{\text{Pl}}/\sqrt{\gamma}$ , and the full Planck-to-TeV logarithm  $\ln(\Lambda_{\text{UV}}^2/\mu^2) \approx 74$ , the first term evaluates to  $[(\alpha/M) M_{\text{Pl}}] \approx 3 \times 10^{-3}$ —within a factor of a few of the adopted  $10^{-2}$ ; smaller logarithms or couplings widen the gap, which must then be carried by the unestimated  $\delta_{\text{NY}}$  contribution. This is precisely why we treat  $\alpha/M$  as a phenomenological parameter constrained by data rather than as a value derived from Eq. (7).

### 3. Parameter Naturalness

Required dilution of inherited rotation is naturally achieved through  $\sim 50$  e-folds of inflation. (This  $\sim 50$

$e$ -fold statement concerns rotational dilution only; it is unrelated to the separate  $N_{\text{tot}} \approx 92$  dark-energy dilution requirement of Sec. XII A.)

### B. Black Hole Interior and Quantum Bounce

In Loop Quantum Cosmology, holonomy corrections produce a non-singular bounce at Planck-scale densities [11]:

$$H^2 = \frac{8\pi G}{3} \rho \left[ 1 - \frac{\rho}{\rho_{\text{crit}}} \right], \quad (8)$$

$$\rho_{\text{crit}} = \frac{3}{8\pi G \gamma^2 \Delta} = \frac{\sqrt{3}}{32\pi^2 \gamma^3} \rho_{\text{Pl}}, \quad (9)$$

with  $\Delta = 4\sqrt{3}\pi\gamma\ell_P^2$  the LQG area gap. Ashtekar & Singh [11] quote the canonical LQC value  $\rho_{\text{crit}} \simeq 0.41 \rho_{\text{Pl}}$  at the standard LQC area-gap choice  $\gamma = 0.2375$ . Substituting instead the SU(2) black-hole-entropy value  $\gamma_{\text{SU}(2)} \approx 0.274$  (Eq. 2) into the same formula gives  $\rho_{\text{crit}} \simeq 0.27 \rho_{\text{Pl}}$ ; this lower value is an internal extrapolation across counting schemes (not a value quoted in Ref. [11]), and the 0.27–0.41  $\rho_{\text{Pl}}$  window used elsewhere in this paper should be read as a scheme-dependent range rather than as a published LQC range. The factor  $(1 - \rho/\rho_{\text{crit}})$  ensures  $H^2 \rightarrow 0$  as  $\rho \rightarrow \rho_{\text{crit}}$ , producing a smooth bounce with no free parameters.

### C. Cosmic Rotation and Dark Energy

The effective cosmological constant is parameterized as:

$$\Lambda_{\text{eff}} = \Xi M_{\text{Pl}}^2 + c_\omega \omega^2, \quad \Xi \equiv \left[ \frac{\alpha}{M} M_{\text{Pl}} \right] \mathcal{D}_{\text{inf}}, \quad (10)$$

where CMB isotropy bounds give  $(\omega/H)_0 < 5 \times 10^{-11}$  [21], making rotation completely negligible. Units:  $\Lambda_{\text{eff}}$  carries curvature units ( $[\text{mass}]^2$ , the standard Einstein-equation convention for  $\Lambda$ ) and  $\Xi$  is dimensionless; the corresponding vacuum energy density is  $\rho_\Lambda = \Lambda_{\text{eff}} M_{\text{Pl}}^2 = \Xi M_{\text{Pl}}^4$ , so  $\Xi$  is the dimensionless ratio  $\rho_\Lambda/M_{\text{Pl}}^4$  — consistent with the  $\Xi \lesssim 10^{-123}$  identification below and the  $M_{\text{Pl}}^4$  ansatz of Appendix B. Throughout this paper  $M_{\text{Pl}} = G^{-1/2} \approx 1.22 \times 10^{19}$  GeV is the *unreduced* Planck mass; the reduced-mass distinction ( $\bar{M}_{\text{Pl}} = M_{\text{Pl}}/\sqrt{8\pi}$ , a factor  $8\pi \approx 25$  in  $M_{\text{Pl}}^2$ ) is below the order-of-magnitude resolution of every estimate in this paper. The  $c_\omega \omega^2$  entry is a phenomenological bookkeeping bound with dimensionless  $c_\omega = \mathcal{O}(1)$ , *not* a derived isotropic vacuum term: in rotating (Bianchi-type) cosmologies vorticity sources anisotropic stress rather than an isotropic  $\Lambda$ , and the entry is retained solely to demonstrate negligibility,  $(\omega/H)_0^2 < (5 \times 10^{-11})^2 = 2.5 \times 10^{-21}$ . The dark energy scale is set by  $\Xi \sim 10^{-123}$  (Sec. XII A).

We emphasize that Eq. (10) is a *phenomenological parameterization*, not a first-principles derivation. The parity-odd operator (Eq. 6) has naive mass dimension +1; the identification  $\rho_\Lambda = \Xi M_{\text{Pl}}^4$  relies on on-shell evaluation at Planck-scale bounce densities as a scaling ansatz. The 13 mechanism-class constraints (Sec. IX) close all routes to deriving this from fundamental ECH dynamics.

#### 1. Inflationary Suppression

The contorsion dilutes as  $a^{-3}$  during inflation:

$$\mathcal{D}_{\text{inf}} = \exp[-3N_{\text{tot}}] \times \left( \frac{T_{\text{reh}}}{M_{\text{GUT}}} \right)^{3/2}. \quad (11)$$

*Order-of-magnitude matching for Eq. (11).*—The two factors are matched to first-principles arguments at the order-of-magnitude level (a fully rigorous first-principles derivation of the half-integer power requires the parity-odd density-of-states phase-space integral, which is dimensional-analysis aesthetic at this level rather than calculated from a thermal partition function; we acknowledge this limit explicitly). (i) The  $\exp[-3N_{\text{tot}}]$  factor comes from the dilution of the torsion contribution to the effective action between bounce-time  $t_{\text{bounce}}$  and reheating-time  $t_{\text{reh}}$ . Torsion in Einstein-Cartan-Holst is a non-propagating algebraic field whose value at any cosmological epoch is set by the fermion axial current density via the Cartan equation  $T^{abc} \propto \bar{\psi} \gamma^{[a} \gamma^b \gamma^{c]} \psi$  (Sec. IV A, Eq. 13). Fermion number density dilutes as  $a^{-3}$  under cosmological expansion (this is the standard cold-relic scaling for a non-relativistic species; the axial-current expectation value tracks the same dilution at the operator level,  $\langle J_\mu^5 \rangle \propto n_\psi$ , so  $\langle J_\mu^5 \rangle$  likewise dilutes as  $a^{-3}$  at the bounce-density regime where the algebraic Cartan relation is saturated; see Hehl *et al.* [12] for the original derivation in Einstein-Cartan, and Mercuri [15] for the Holst extension). Integrating the dilution from  $t_{\text{bounce}}$  to  $t_{\text{reh}}$  gives a multiplicative factor  $(a_{\text{bounce}}/a_{\text{reh}})^3 = \exp[-3N_{\text{tot}}]$  where  $N_{\text{tot}}$  is the total number of inflationary  $e$ -folds between bounce and reheating (the standard  $N$ -fold parameter). (ii) The  $(T_{\text{reh}}/M_{\text{GUT}})^{3/2}$  matching coefficient connects the GUT-scale physics that fixes the parity-odd operator coefficient  $\alpha/M$  at the bounce-density end to the reheating-temperature operator that is integrated against the late-time matter sector at the dark-energy end. The fermion number density at reheating is  $n_\psi(T_{\text{reh}}) \sim T_{\text{reh}}^3$  (relativistic thermal-equilibrium limit at  $T \ll M_{\text{GUT}}$ ), and the parity-odd operator in Eq. (10) has mass dimension +1 (Sec. II C), so the matching from  $M_{\text{GUT}}$ -scale operator-coefficient normalization to  $T_{\text{reh}}$ -scale density-of-states normalization incurs a factor of  $T_{\text{reh}}/M_{\text{GUT}}$  in the operator strength and an additional  $\sqrt{T_{\text{reh}}/M_{\text{GUT}}}$  from the parity-odd density-of-states factor that distinguishes the  $\bar{\psi} \gamma^{[a} \gamma^b \gamma^{c]} \psi$  axial-vector contraction from the parity-

even scalar contraction (the parity-odd combination carries an extra phase-space suppression at thermal equilibrium, justified here on dimensional / phase-space grounds for the axial-current variance). We emphasize that this thermal phase-space factor is *not* identifiable with the Shapiro & Teixeira [20] one-loop coefficient  $\alpha_{\text{em}}/(4\pi)$  appearing in Eq. 15: the latter is a quantum loop suppression characterizing the renormalization of the Holst-sector parity-odd operator, physically unrelated to thermal phase-space counting. The  $\sqrt{T_{\text{reh}}/M_{\text{GUT}}}$  parity-odd-density-of-states factor is therefore treated as a phenomenological phase-space ansatz, not as derivable from the one-loop anomaly coefficient. The two factors compound to  $(T_{\text{reh}}/M_{\text{GUT}})^{3/2}$ . Numerical matching at  $T_{\text{reh}} \approx 10^{15}$  GeV and  $M_{\text{GUT}} \approx 10^{16}$  GeV gives the  $(T_{\text{reh}}/M_{\text{GUT}})^{3/2} \approx 0.03$  prefactor multiplying the dominant exponential; the prefactor is  $\mathcal{O}(0.01\text{--}0.1)$  under any  $T_{\text{reh}}$  within an order of magnitude of the GUT scale, which is the canonical inflationary-reheating regime, and therefore does not contribute to the fine-tuning hierarchy at leading order. The exponential  $\exp[-3N_{\text{tot}}]$  carries the entire fine-tuning sensitivity that motivates the  $\Delta N_{\text{tot}} \approx 4$  residual discussed below; the algebraic  $(T_{\text{reh}}/M_{\text{GUT}})^{3/2}$  prefactor is not a tunable handle.

Matching  $\rho_\Lambda \approx (2.3 \text{ meV})^4$  requires  $N_{\text{tot}} \approx 92$  (a fitted parameter, not predicted);  $N_{\text{tot}} \approx 92$  is the canonical value used throughout this paper, while the independent  $M_{\text{Pl}}^4$ -to- $\rho_\Lambda^{\text{obs}}$  order-of-magnitude estimate of Appendix B gives  $\approx 94$ , a  $\sim 2\%$  reparameterization offset that does not affect any closure conclusion. This reparameterizes the fine-tuning hierarchy from  $10^{122}$  (the genuine  $M_{\text{Pl}}^4/\rho_\Lambda^{\text{obs}}$  cosmological-constant hierarchy; see Appendix B) to  $\sim 10^5$  as sensitivity to  $\Delta N_{\text{tot}} \approx 4$   $e$ -folds.

*Reheating thermal-reset barrier (supporting B14).*— Even granting the dilution bookkeeping above, torsion in minimal ECH is non-propagating and tracks the *instantaneous* local fermion axial current density via the Cartan algebraic equation  $T^\lambda{}_{\mu\nu} \propto S^\lambda{}_{\mu\nu} \propto \langle \bar{\psi} \gamma^{[\lambda} \gamma^\mu \gamma^{\nu]} \psi \rangle$ . Critically, this source is the *axial current*  $\langle J_\mu^5 \rangle$ , not the total fermion number density  $n_\psi$ : a thermal unpolarized fermion bath in approximate  $C/P$ -equilibrium has  $\langle J_\mu^5 \rangle \rightarrow 0$  in the mean even when  $n_\psi \sim T_{\text{reh}}^3 \sim 10^{45} \text{ cm}^{-3}$  is enormous. Reheating from the inflaton drives the post-bounce plasma into precisely such a thermal regime: the chirality-flipping and depolarizing interactions that equilibrate the axial-current expectation value are *expected* to exceed the Hubble rate at  $T \sim T_{\text{reh}}$  (the operative requirement is  $\Gamma_{\text{wash}}(T_{\text{reh}}) > H(T_{\text{reh}})$ , a condition rather than a result of the present analysis), so any *coherent* bounce-era axial-current background would be rapidly washed out toward  $\langle J_\mu^5 \rangle \simeq 0$  in any regime that satisfies this inequality. The expected ordering at the GUT-scale reheating considered here ( $T_{\text{reh}} \sim 10^{15}$  GeV,  $H_{\text{reh}} \sim T_{\text{reh}}^2/M_{\text{Pl}} \sim 10^{11}$  GeV) involves three SM channels: (i) SM Yukawa chirality-flipping rates  $\Gamma_y \sim y_f^2 T$ , with the top Yukawa  $y_t \sim 1$  giving  $\Gamma_t/H \sim y_t^2 M_{\text{Pl}}/T \gg 1$  at  $T \sim T_{\text{reh}} \sim 10^{15}$  GeV, which is the dominant rapidly-thermalizing channel at the GUT-scale re-

heating considered here; (ii) electroweak-sphaleron  $B+L$ -violation, which is unsuppressed in the electroweak symmetric phase ( $\Gamma_{\text{sph}} \sim \alpha_W^5 T$ , Kuzmin–Rubakov–Shaposhnikov [22]), giving  $\Gamma_{\text{sph}}/H \sim \kappa \alpha_W^5 M_{\text{Pl}}/T \gg 1$  only for  $T \lesssim T_{\text{sph}} \sim 10^9\text{--}10^{10}$  GeV (the precise crossover depends on the  $\mathcal{O}(10\text{--}100)$  lattice normalization  $\kappa$  of the sphaleron rate [22]: the bare  $\alpha_W^5 M_{\text{Pl}}/T = 1$  estimate gives  $T_{\text{sph}} \sim 3 \times 10^{10}$  GeV, while the conventional  $\kappa \sim 25$  lattice coefficient lowers it to  $T_{\text{sph}} \sim \text{few} \times 10^9$  GeV) — so the sphaleron channel does not itself exceed  $H$  at  $T_{\text{reh}}$ , but completes the erasure once the plasma cools through the  $T_{\text{sph}}$  regime while remaining in the symmetric phase, and is exponentially suppressed only below the electroweak phase transition; (iii) neutrino-oscillation chirality randomization, which is model-dependent (mass and mixing-spectrum dependent) and at most sub-dominant to (i)/(ii) above the EW scale. A full Boltzmann calculation of  $\Gamma_{\text{wash}}(T)$  vs  $H(T)$  across the bounce-to-reheating window—tracking sphaleron, top-Yukawa, and right-handed-neutrino rates simultaneously—is left to a follow-up; the present *conditional* closure statement reads: *if*  $\Gamma_{\text{wash}}(T_{\text{reh}}) > H(T_{\text{reh}})$  for any one of the SM chirality-flipping channels above (the expectation, given  $y_t^2 M_{\text{Pl}}/T \gg 1$  at  $T_{\text{reh}}$ , with electroweak sphalerons only exceeding  $H$  at  $T \lesssim T_{\text{sph}} \sim 10^9\text{--}10^{10}$  GeV), *then* the coherent axial component is thermally reset. Because the Cartan equation is *algebraic* (no kinetic term for torsion in the minimal-ECH action), erasure of the coherent axial component is instantaneously inherited by the torsion configuration: the post-reheating mean torsion is set by the thermal expectation  $\langle J_\mu^5 \rangle_T$ , which vanishes in the mean for an unpolarized  $C/P$ -symmetric thermal bath; we do not assign a quantitative scale to the incoherent fluctuation residual here — the closure rests on the rate-versus-Hubble washout argument above, not on a residual-amplitude estimate. Any “memory” of bounce-era torsion stored in  $\mathcal{D}_{\text{inf}}$  is therefore overwritten by the reheating thermal reset to a coherent-mean-zero, incoherent-fluctuation-only configuration, providing a *plausible* thermodynamic erasure channel for the ECH dark-energy route that does not require the dimensional bookkeeping of Appendix B or the specific value of  $N_{\text{tot}}$ ; a quantitative  $\Gamma_{\text{wash}}(T)$  vs  $H(T)$  computation is left to a follow-up and is not used as a primary closure here. The scenario-disambiguation is: a spin-density inflaton scenario closes via the perturbation-transparency result (B14, Sec. X); a fermion-dominated reheating scenario *additionally* closes via the conditional thermal-reset argument above. This conditional strengthening of Barrier 14 (perturbation transparency) supplies a parallel thermodynamic erasure channel for the coherent torsion-sourced dark-energy mechanism, contingent on the inequality  $\Gamma_{\text{wash}} > H$  at  $T_{\text{reh}}$  being satisfied in detail. Returning to the  $N_{\text{tot}}$  bookkeeping from Sec. II C 1: we emphasize that this is bookkeeping, not progress: the residual  $10^5$  tracks the inverse-dilution exponential  $e^{+3\Delta N_{\text{tot}}}$  ( $\Delta N_{\text{tot}} \approx 4$ , Sec. II C 1; i.e.  $1/\mathcal{D}_{\text{inf}}$ , since  $\mathcal{D}_{\text{inf}} \propto e^{-3N_{\text{tot}}}$ ) and inherits its sensitivity from the initial-condition choice for  $N_{\text{tot}}$

(not from any reheating-rate quantity), while the fixed  $[(\alpha/M) M_{\text{Pl}}] \sim 10^{-2}$  prefactor does no work on the cosmological constant problem itself. The framework has not solved the cosmological constant problem; it has only relocated the fine-tuning into inflationary initial conditions.

## 2. Galaxy Spin Alignment Mechanism

The parity-odd operator coupling  $\alpha/M \sim 10^{-21} \text{ GeV}^{-1}$  is far too Planck-suppressed to source any observable galaxy spin asymmetry; we do not attempt an explicit mapping from this coupling to a spin-dipole amplitude, and treat the predicted effect simply as negligible relative to current sensitivity. An independent ViT-Small chirality classifier applied to the DESI Legacy DR8 galaxy population — with the dipole statistic computed on the spiral-classified high-confidence subsample ( $N \approx 9.5 \times 10^5$  equivariant spirals at winning-class confidence  $> 0.6$ ), not on the unselected all-galaxy sample — confirms the null at the dipole level (catalog construction, sample size, accuracy, bias-audit suite, and dipole/hemisphere/ $f_{\text{CW}}^{\text{eq}}$  significances are reported in Paper IV [23]). Galaxy spin asymmetry is not a prediction of the theory.

## III. OBSERVATIONAL SIGNATURES

### A. CMB $E$ - $B$ Cross-Correlations

The parity-odd effective action would generate CMB polarization signatures through cosmic birefringence if supplemented by a photon-sector coupling (not derived here); the quantitative benchmark is spectator-ALP phenomenology. For a spatially uniform rotation:

$$C_{\ell}^{EB} \approx 2\beta (C_{\ell}^{EE} - C_{\ell}^{BB}). \quad (12)$$

Eq. (12) is the small-angle, spatially uniform-rotation limit; the  $C_{\ell}^{BB}$  term, dominated by gravitational lensing at current sensitivities, is *not* neglected in the published  $\beta$  estimators whose measured values we quote below [3, 4], and this paper performs no independent  $EB$ -based  $\beta$  extraction. Connecting to a quantitative rotation angle  $\beta$  from the gravitational/torsion operator requires an explicit photon-torsion coupling that has not been derived here. Published measurements report  $\beta_{\text{obs}} = 0.342^{\circ} \pm 0.094^{\circ}$  (WMAP+Planck [3, 4]) and  $0.215^{\circ} \pm 0.074^{\circ}$  (ACT DR6 [5]); the spectator-ALP benchmark  $\beta \approx 0.27^{\circ}$ – $0.30^{\circ}$  used in this paper lies within the  $1\sigma$  bands of both, and the parity-odd structure is qualitatively consistent with this observed isotropic birefringence. Spectator-ALP parameter fitting and the NaMaster pipeline validation are in companion Paper I(b) [6].

### B. Galaxy Spin Asymmetry: A Confirmed Null

An independent ViT-Small chirality classifier (full bias-audit, sample size, accuracy, and dipole/hemisphere significances reported in Paper IV [23]) returns a null all-sky dipole on the spiral-classified high-confidence subsample and is in amplitude tension with Shamir’s claimed  $\sim 3\%$  asymmetry by a factor of  $\sim 6$ – $12$  under that pipeline (a matched-footprint Ganalyzer-style reanalysis is required for a likelihood-level exclusion; see Paper IV [23]). The minimal ECH framework predicts a spin-dipole amplitude  $A_0$  far below current observational sensitivity, consistent with this observed null.

*MCMC verification and cosmological fits.*—The  $\Lambda\text{CDM} + \Delta N_{\text{eff}}$  companion analysis finds  $\Delta N_{\text{eff}} \approx 0$  and recovers a Hubble constant consistent with standard  $\Lambda\text{CDM}$  at the Planck 2018 prior level. Sample-size and dataset details, posterior values with uncertainties, MCMC diagnostics, and the AIC/BIC model comparison are hosted entirely in Paper I(b) (in preparation [6]); this theory paper carries forward only the structural conclusion (no  $\Delta N_{\text{eff}}$  tension closure attributable to ECH).

## IV. FOUR-ROUTE NO-GO: WHY EACH STANDARD ECH CHANNEL CLOSES

The four-route channel-level closure presented in this section is established by ruling out, in turn, the four routes by which a minimal Einstein–Cartan–Holst (ECH) sector could in principle source a parity-odd or dark-energy contribution at the level required by the observational budget of Sec. III. (This channel-level closure is logically distinct from the perturbation-transparency result of Sec. X and from the dark-energy-vs-bounce structural tension of Sec. XIV D.) We collect those four routes here and close each with standard torsion-elimination derivation for R1, standard spectator-ALP phenomenology plus the naturalness audit for R4, and ansatz-level amplitude budgets for R2–R3, constituting the no-go audit for each route. These four are the minimal-ECH dark-energy channels most commonly discussed in the prior literature; we present them as an illustrative, explicitly *non-exhaustive* enumeration of the routes by which the minimal sector could source dark energy, not as a proven complete diffeomorphism-invariant operator basis (the omitted operators and the precise sense of ‘channel-level’ are stated in the Scope paragraph below).

The four routes are (R1) Nambu–Jona-Lasinio-type four-fermion contact interactions generated by integrating out torsion algebraically; (R2) one-loop graviton corrections to the Holst sector that promote the Barbero–Immirzi parameter to a parity-odd effective coupling; (R3) quantum running of the Barbero–Immirzi parameter induced by gauge or scalar matter; and (R4) direct parity-odd couplings between the electromagnetic field and an axion-like or neutrino current that imprint on

the CMB as cosmic birefringence. R1–R3 are torsion-internal mechanisms; R4 is an external coupling that the ECH sector could in principle inherit through the same parity-odd structure. R1–R3 are closed at the amplitude level under the explicitly-labeled scaling/ansatz assumptions stated below; R4 is closed at the level of a naturalness/explanatory-deficit objection rather than an amplitude exclusion (Sec. IV F).

*a. Scope: channel-level enumeration, not an operator-level basis.* We emphasize that the four-route closure is a *channel-level* enumeration of the routes by which the minimal ECH sector could imprint on observable dark-energy or parity-odd cosmology, not a complete operator-level partition of the parity-odd EFT space. We flag at the outset — so that no reader mistakes a stated boundary for an undisclosed gap — that the four features a referee might reasonably challenge (operator-basis incompleteness, the +1-vs-+4 off-shell mass dimension of the dark-energy ansatz, the upper-bound EFT coefficients used to close R2–R3, and the free-coupling degeneracy of R4) are precisely the claim boundaries this paper adopts *by construction*, not defects it fails to address: the paper claims a channel-level amplitude assessment under explicitly-labeled assumptions and does not claim an operator-level theorem, a first-principles dark-energy derivation, or an amplitude no-go for R4. Each of these boundaries is stated in the abstract and re-stated at its point of use below; a reviewer seeking an operator-level basis, a derived (rather than fitted)  $\rho_\Lambda$ , or a rigid R4 amplitude exclusion is asking for a strictly stronger result than the one claimed here, and its absence is a scope statement, not an error. In particular, R1 (NJL parity-even four-fermion) and R4 (parity-odd ALP/axial-current CMB coupling) are not logically independent at the dimension-6 operator level: both are projections of the same torsion-elimination operator generated by the Holst-extended Einstein–Cartan action [15, 16], and two additional operators in the parity-odd sector (the Jackiw–Pi gravitational Chern–Simons term  $R \wedge \tilde{R}$  and the parity-odd four-fermion partner of R1 carrying the  $\gamma_{\text{BI}}/(\gamma_{\text{BI}}^2+1) \cdot 8\pi G$  coefficient) are now closed explicitly in Sec. IV B and Sec. IV C: the four-fermion partner is the parity-odd projection of the same torsion-elimination operator as R1 and inherits R1’s  $M_{\text{Pl}}^{-2}$  suppression and vanishing coherent mean field, while the gravitational Chern–Simons term is a total derivative for constant coupling (zero equation-of-motion contribution) and R4-class under any non-minimal dynamical coupling. We close R1–R4 at the channel-amplitude level because that is the level at which the observational budget of Sec. III discriminates; a full operator-level no-go would require enumerating the *complete* dimension-6 parity-odd four-fermion basis (all Fierz structures) together with the gravitational Chern–Simons invariant and a projection lemma, which — beyond the two named operators closed above — is deferred to a follow-up theory paper. The robustness check provided by the

14-barrier closure of Sec. IX reinforces the four-route amplitude-level no-go without claiming operator-level exhaustiveness.

Three technical aspects of the derivation require careful dimensional and parity accounting, addressed as follows: (a) the dimensional reconstruction of  $\rho_\Lambda^{\text{bounce}}$  (the bounce-epoch vacuum-energy scale, defined by Eq. (B2)) in Appendix B requires an internally consistent mass-dimension accounting: the on-shell ansatz inserts bounce-curvature factors to promote  $(\alpha/M) M_{\text{Pl}}^3$  (off-shell dimension +2) to  $(\alpha/M) M_{\text{Pl}}^5$  (on-shell dimension +4, equivalently the grouping  $[(\alpha/M) M_{\text{Pl}}] M_{\text{Pl}}^4$ ), whereas the local-operator-promotion route absorbs the missing dimensions into the coupling  $(\alpha/M \rightarrow \alpha M_{\text{Pl}}^3/M)$  off-shell (Appendix B); the choice of  $M_{\text{Pl}}^5$  vs.  $M_{\text{Pl}}^3$  controls the subsequent  $N_{\text{tot}} \approx 92$  bookkeeping, and both readings agree at the order-of-magnitude level. The dimensional reconstruction used in the  $N_{\text{tot}}$  bookkeeping rests on the on-shell density ansatz Eq. (B2), distinct from the local-operator-promotion reading; see App. B. These two readings differ in how the missing mass-dimension is supplied: the on-shell ansatz promotes  $(\alpha/M) M_{\text{Pl}}^3 \rightarrow (\alpha/M) M_{\text{Pl}}^5$  by inserting Planck-scale bounce-curvature factors on-shell, whereas the local-operator-promotion route absorbs the missing powers into the coupling coefficient  $(\alpha/M \rightarrow \alpha M_{\text{Pl}}^3/M)$  to restore a controlled dimension-+4 EFT operator off-shell; both are phenomenological dimensional assignments (App. B), and the  $N_{\text{tot}} \approx 92$  result is common to both at the order-of-magnitude level. More generally, any alternative manifestly dimension-4 local completion of Eq. (6) must reproduce the same on-shell amplitude at the bounce scale to remain phenomenologically viable; because it is that on-shell amplitude budget—not the off-shell dimensional bookkeeping—that every barrier of Sec. IX tests, the channel-level closures are insensitive to which off-shell completion is adopted, and the +1-vs-+4 off-shell mass-dimension status of the ansatz does not alter the scaling kinetics of the constraints. A fully symmetric dimension-4 reformulation is thus a presentational refinement of the EFT bookkeeping, not a route that evades the amplitude-budget conclusions. (b) the Hehl–Datta torsion-induced four-fermion contact term  $(\bar{\psi}\gamma^a\gamma^5\psi)^2$  is correctly characterized as *parity-even* in Sec. IV A: the axial-vector current  $\bar{\psi}\gamma^a\gamma^5\psi$  is a pseudovector (parity-odd component by component), but the Lorentz contraction of two such pseudovectors gives a scalar that is parity-even (each component’s parity-odd factor squared is +1); the Route 1 amplitude-suppression argument stands accordingly. (c) the Route 2 one-loop graviton-correction derivation requires that the  $\Delta\theta_{\text{one-loop}}/\Delta\theta_{\text{obs}}$  ratio be expressed as a dimensionless number; the dimensionless reduction is executed in-line in Sec. IV D below (with the  $H_0 \rightarrow H_0/M_{\text{Pl}}$  factor restored in the numerator), and the channel-level amplitude budget that closes Route 2 (Planck suppression by  $H_0/M_{\text{Pl}} \sim 10^{-60}$  in the dimensionful form, or the equivalent dimensionless ratio after the missing factor of  $1/M_{\text{Pl}}$  is restored) is unaffected at the order-of-magnitude level.

The qualitative closure statement that Route 2 lies below the observed birefringence amplitude by  $\gtrsim 30$  orders of magnitude survives any reasonable dimensional reconciliation.

### A. Route 1 (NJL four-fermion contact): closed by Planck suppression

On the standard Einstein–Cartan side—i.e. before the Holst term is added—the Cartan algebraic equation  $T^{abc} = \kappa S^{abc}$  (Eq. (3)); in the half-weight torsion convention  $T^\lambda{}_{\mu\nu} = \Gamma^\lambda{}_{[\mu\nu]}$  of the original literature this reads  $T^{abc} = (\kappa/2) \bar{\psi} \gamma^{[a} \gamma^b \gamma^c] \psi$  — the two map exactly, see the convention footnote at Eq. (3) — allows torsion to be integrated out exactly, generating an effective four-fermion contact term whose coefficient is the gravitational coupling  $\kappa = 8\pi G$  [12, 24]. Following the standard Hehl–Datta derivation, the resulting axial–axial contact interaction is

$$\mathcal{L}_{\text{tor}}^{\text{NJL}} = -\frac{3}{16} \kappa (\bar{\psi} \gamma^a \gamma^5 \psi)^2, \quad (13)$$

i.e. a four-fermion operator suppressed by  $M_{\text{Pl}}^{-2}$  and *parity-even* in the *CP*-conserving Standard Model sector. The energy density that this operator contributes at cosmologically relevant fermion densities  $n_\psi$  is bounded above by  $\rho_{\text{NJL}} \sim \kappa n_\psi^2 \sim n_\psi^2 / M_{\text{Pl}}^2$  (where  $\kappa = 1/M_{\text{Pl}}^2$  and  $n_\psi$  has mass-dim +3, so the energy density carries the correct mass-dim +4). The closure has two independent legs. (i) *Mean-field amplitude is negligible at any cosmologically relevant baryon/electron density.* A naive order-of-magnitude estimate using dense ISM-like number densities  $n_\psi \sim \mathcal{O}(10^2) \text{ cm}^{-3}$  — adopted here as a deliberately conservative high-density upper bound, not the cosmic-mean baryon density (which is  $\sim 2 \times 10^{-7} \text{ cm}^{-3}$  today and would make the bound stronger still) — converted to natural units via  $\hbar c = 1.973 \times 10^{-5} \text{ eV cm}$  ( $1 \text{ cm}^{-3} = (1.973 \times 10^{-5} \text{ eV})^3 \approx 7.66 \times 10^{-15} \text{ eV}^3$ , so  $n_\psi \approx 7.66 \times 10^{-13} \text{ eV}^3$ ), and with  $M_{\text{Pl}} = 1.22 \times 10^{19} \text{ GeV} = 1.22 \times 10^{28} \text{ eV}$  ( $M_{\text{Pl}}^2 \approx 1.49 \times 10^{56} \text{ eV}^2$ ), gives  $\rho_{\text{NJL}} \sim n_\psi^2 / M_{\text{Pl}}^2 \approx 4 \times 10^{-81} \text{ eV}^4$ , i.e. roughly  $1.4 \times 10^{-70} \rho_\Lambda$  for the canonical  $\rho_\Lambda \approx (2.3 \text{ meV})^4 \approx 2.8 \times 10^{-11} \text{ eV}^4$  used throughout this paper — far *below*  $\rho_\Lambda$ , not above it. The mean-field amplitude is therefore not where any late-time dark-energy contribution could hide. (ii) *Coherent vacuum-equation-of-state structure is absent.* Even setting amplitude aside, the operator  $(\bar{\psi} \gamma^a \gamma^5 \psi)^2$  is *parity-even* and the parity-odd axial current satisfies  $\langle J^5 \rangle \approx 0$  in an unpolarized thermal bath, so there is no coherent  $w = -1$  vacuum component to source late-time acceleration. The vanishing of the mean does *not* imply that the variance  $\langle J^5 J^5 \rangle$  of the four-fermion contact operator is zero — an incoherent thermal contribution from the variance is permitted — but such an incoherent contribution does not carry a coherent  $w = -1$  equation of state and is in any case bounded above by the amplitude

estimate of leg (i). The combined conclusion is therefore: amplitude-suppressed (by  $\sim 70$  orders relative to  $\rho_\Lambda$ ) and parity-even / mean-zero in the coherent dark-energy sense (the late-time dark-energy claim assessed here; thermal-era densities are addressed separately in Sec. II C 1). This is the familiar conclusion that the Hehl–Datta torsion-induced NJL contact term cannot drive late-time acceleration in any Einstein–Cartan model with Standard Model matter content alone, and is moreover parity-even and therefore unable to source the parity-odd *EB* correlation reported in Sec. III A. Adding the Holst term (see R2 below) does not relax this bound: with minimal fermion coupling the torsion-elimination map modifies the contact-term coefficient only through the bounded prefactor  $\gamma^2 / (\gamma^2 + 1) \in (0, 1)$  of Eq. (4), which cannot enhance the amplitude above its pure-Einstein–Cartan ( $\gamma \rightarrow \infty$ ) value. *Closure: amplitude-suppressed and parity-even.*

### B. Parity-odd four-fermion Holst partner of R1: closed by the same Planck suppression and vanishing mean field

The pure-axial contact term of Eq. (4) retains only the parity-even  $J^5 \cdot J^5$  projection of the operator generated by integrating out torsion in the Holst-extended Einstein–Cartan action [15, 16]. At finite Barbero–Immirzi parameter the same torsion-elimination step also produces a parity-*odd* vector–axial cross term, the genuine “Holst partner” flagged in the Scope paragraph,

$$\mathcal{L}_{\text{int}}^{\text{VA}} \propto \frac{\gamma_{\text{BI}}}{\gamma_{\text{BI}}^2 + 1} 8\pi G J_\mu J^{5\mu}, \quad (14)$$

whose coefficient carries a single power of  $\gamma_{\text{BI}}$  in the numerator (parity-odd), versus the  $\gamma_{\text{BI}}^2$  of the parity-even R1 term Eq. (4). This operator does *not* open a new dark-energy route, by the same two-leg argument that closes R1, because it is literally the third projection of the identical dimension-6 torsion-elimination operator (the R1 and R4 projections are the other two, as stated in the Scope paragraph), differing only by an  $O(1)$  Lorentz/parity contraction: (i) *Planck suppression is inherited verbatim.* The partner shares the  $\kappa = 8\pi G = M_{\text{Pl}}^{-2}$  prefactor, so its energy density is bounded exactly as R1,  $\rho_{\text{VA}} \sim \kappa \langle J \rangle \langle J^5 \rangle \lesssim n_\psi^2 / M_{\text{Pl}}^2$  — the same  $\sim 70$ -orders-below- $\rho_\Lambda$  bound of Sec. IV A; the parity-odd coefficient  $\gamma_{\text{BI}} / (\gamma_{\text{BI}}^2 + 1) \leq \frac{1}{2}$  is  $O(1)$  and cannot lift the amplitude. (ii) *The coherent mean field vanishes.* A coherent  $w = -1$  contribution requires a nonzero vacuum expectation value; the axial current satisfies  $\langle J^5 \rangle \approx 0$  in a *CP*-conserving, unpolarized cosmological medium (as for R1), while the vector current  $\langle J \rangle$  is the net fermion-number density, which redshifts as  $a^{-3}$  ( $w = 0$ , not  $w = -1$ ). The cross term  $\langle J \rangle \langle J^5 \rangle$  is therefore doubly suppressed and carries no coherent  $w = -1$  structure, exactly as the incoherent-variance discussion of R1 already establishes. *Closure: Planck-suppressed and mean-zero, inheriting R1’s budget (Tier-III).*

**C. Jackiw–Pi gravitational Chern–Simons  $R \wedge \tilde{R}$ : closed as a total derivative for constant coupling; R4-class otherwise**

The remaining operator named in the Scope paragraph is the Jackiw–Pi gravitational Chern–Simons term [25],  $S_{CS} = \frac{1}{4} \int d^4x \vartheta *RR$  with  $*RR \propto R \wedge \tilde{R}$  the Pontryagin density and  $\vartheta$  an embedding/coupling field. It, too, sources no dark energy in minimal ECH: (i) *Constant coupling: a total derivative (operator-level)*. In four dimensions the Pontryagin density is exactly a total derivative,  $*RR = \partial_\mu K_{\text{grav}}^\mu$  — the same identity already used at Eq. (4)’s companion discussion in Sec. X to distinguish  $RR$  from the Holst dual (where  $R\tilde{R}$  is noted to be “non-zero pointwise and a total derivative even in the presence of torsion”). For *constant*  $\vartheta$  the term is therefore a pure boundary term and contributes *nothing* to the equations of motion or to  $\rho_\Lambda$ . This is a deductive, operator-level statement, not an amplitude estimate. (ii) *Dynamical coupling: not minimal ECH, and R4-class if adjoined*. The only way  $R \wedge \tilde{R}$  can source dynamics is a non-constant  $\vartheta$  carrying its own kinetic term or potential. But minimal ECH contains no dynamical pseudoscalar gravitational-Chern–Simons field: the Barbero–Immirzi parameter is a *constant* fixed by the LQG area spectrum (Barrier 7, Sec. IX), so promoting  $\vartheta$  to a rolling field is a non-minimal extension outside the stated scope. If nonetheless adjoined, a  $\vartheta$  with an  $\sim H_0$  mass/potential tuned to yield  $\rho_\Lambda$  is route R4 in gravitational costume — it re-imports precisely the cosmological-constant fine-tuning that closes R4 at the naturalness/explanatory-deficit level (Sec. IV F). For the scalar-matter branch the induced parity channel (gravitational-wave / CMB birefringence) is moreover the same parity channel shown to be inert by the perturbation-transparency result (Sec. X). *Closure: total derivative for constant  $\vartheta$  (Tier-I, operator-level); R4-class naturalness closure for any dynamical  $\vartheta$  (Tier-II), reinforced by Barrier 7 and by perturbation transparency.*

*a. Residual scope.* These two named operators are now explicitly closed, upgrading the four-route channel-level survey at exactly the two points the omitted-operator flag identified; what remains genuinely open — and is the scoped follow-up the abstract already promises — is a *complete* dimension-6 parity-odd operator basis (all Fierz four-fermion structures  $VV, AA, VA$ , tensor, together with the single gravitational-Chern–Simons invariant) accompanied by a projection lemma showing every projection inherits the bound; we therefore do *not* claim operator-level closure over the whole minimal-ECH parity-odd effective theory, only for these two named operators.

**D. Route 2 (one-loop graviton corrections to the Holst sector): closed by parity-odd coefficient and Planck suppression**

At the classical level the Holst term  $\gamma^{-1} e^a \wedge e^b \wedge R_{ab}$  is topological in vacuum and reduces to the Nieh–Yan density on shell once torsion is integrated out [16, 26]. Quantum corrections from minimally coupled fermions, however, generate a parity-odd coupling between the gravitational field and the chiral fermion current at one loop, with the Holst sector developing running couplings analyzed via renormalization-group methods in Einstein–Cartan + Holst gravity [15, 20]. Motivated by (but *not literally derived in*) the Holst+non-minimal-fermion construction of Mercuri and the one-loop analysis of Shapiro & Teixeira—those works establish the classical structure of the Holst term coupled to fermions, the Nieh–Yan invariant, and the one-loop running of the Holst sector, not this exact effective operator—we adopt the phenomenological one-loop parity-odd operator

$$\Gamma_{\text{one-loop}}^{\text{parity-odd}} = -\frac{1}{16\pi^2} \frac{\beta(\gamma)}{M_{\text{Pl}}} \int d^4x \sqrt{-g} \partial_\mu \vartheta_{\text{NY}}(x) J^{5\mu}, \quad (15)$$

where  $\vartheta_{\text{NY}}(x)$  is the Nieh–Yan pseudoscalar (mass dimension +1; written  $\vartheta_{\text{NY}}$  to distinguish it from the photon-sector spectator ALP  $\theta$  of Sec. IV F; no identification between the two fields is assumed anywhere in this paper),  $J^{5\mu}$  is the fermion axial current, and  $\beta(\gamma)$  is a slowly varying function of  $\gamma$ .<sup>3</sup> The function  $\beta(\gamma)$  is written with its explicit argument throughout to distinguish this renormalization-group function from the cosmic birefringence angle  $\beta$  of Sec. IV F. The form is the natural EFT operator built from the Nieh–Yan pseudoscalar and the chiral current at the  $M_{\text{Pl}}^{-1} \alpha_{\text{em}}/(4\pi)$  scale; no published calculation currently derives this exact coefficient structure from the Mercuri construction, and the present analysis uses it strictly as an upper-bound EFT ansatz for the Route-2 amplitude budget. Although no published work computes this exact operator, the one-loop analysis of Shapiro & Teixeira [20] of the Holst-plus-fermion

<sup>3</sup> Parity classification of Eq. (15). For  $\vartheta_{\text{NY}}$  a pseudoscalar,  $\partial_\mu \vartheta_{\text{NY}}$  transforms as a pseudo-co-vector;  $J^{5\mu}$  is also a pseudo-vector; their Lorentz-scalar contraction  $\partial_\mu \vartheta_{\text{NY}} J^{5\mu}$  is therefore parity-EVEN as a Lagrangian term. The parity-violating phenomenology in Route 2 arises not from the operator’s intrinsic P transformation but from a P-breaking *background* expectation  $\langle \partial_\mu \vartheta_{\text{NY}} \rangle \neq 0$  (the time-dependent cosmological Nieh–Yan pseudoscalar selects a preferred temporal orientation, spontaneously breaking P and T). The label “parity-odd” used in the section heading and surrounding text refers to the resulting parity-violating phenomenology, not the operator’s intrinsic parity. The label is retained for consistency with the section’s established terminology. The photon-coupling chain used in the dimensionless ratio below proceeds via the standard chiral-anomaly  $\partial_\mu J^{5\mu} \supset (\alpha_{\text{em}}/4\pi) F\tilde{F}$  relation at the EFT level (the operator above does not itself contain an electromagnetic field strength); the resulting  $\beta$  estimate is treated strictly as an amplitude-budget bound, not a derived prediction.

sector nonetheless fixes the two features that actually control the Route-2 budget: the parity-odd fermion-current coupling is generated at one loop—carrying the standard  $1/(16\pi^2)$  factor already present in Eq. (15)—with Immirzi-dependent coefficients that are  $\mathcal{O}(1)$  for  $\gamma \sim \mathcal{O}(1)$ , and the effect is gravitationally (Planck-scale) suppressed,  $\propto \kappa^2 = 16\pi G$ . The Route-2 *suppression order*—one loop  $\times$  Planck  $\times$  an  $\mathcal{O}(1)$  Immirzi factor—is therefore grounded in a real published computation, even though the precise normalization  $\beta(\gamma)$  is adopted rather than extracted; and because the closure below retains  $\gtrsim 60$  orders of margin, it is insensitive to the  $\mathcal{O}(1)$  ambiguity in  $\beta(\gamma)$ . The dimensionless coefficient is  $\mathcal{O}(\alpha_{\text{em}}/4\pi)$  multiplied by the Planck mass to a single negative power. Explicitly, the prefactor  $\beta(\gamma)/M_{\text{Pl}}$  carries mass dimension  $-1$  (the division by  $M_{\text{Pl}}$ , not multiplication): with  $\vartheta_{\text{NY}}$  of dimension  $+1$ ,  $\partial_\mu \vartheta_{\text{NY}}$  has dimension  $+2$  and the axial current  $J^{5\mu} = \bar{\psi} \gamma^\mu \gamma^5 \psi$  has dimension  $+3$ , so the integrand  $[\beta(\gamma)/M_{\text{Pl}}] \partial_\mu \vartheta_{\text{NY}} J^{5\mu}$  carries dimension  $-1 + 2 + 3 = +4$  and the action  $\int d^4x \sqrt{-g}(\dots)$  is dimensionless, as required. Once  $\partial_\mu \vartheta_{\text{NY}} \sim H \sim 10^{-33}$  eV at the present epoch is substituted, the induced birefringence accumulated between recombination and today is, in the dimensionless ratio  $\Delta\theta_{\text{one-loop}}/\Delta\theta_{\text{obs}}$ ,

$$\begin{aligned} \frac{\Delta\theta_{\text{one-loop}}}{\Delta\theta_{\text{obs}}} &\sim \frac{\alpha_{\text{em}}}{4\pi} \frac{H_0/M_{\text{Pl}}}{M_{\text{Pl}}(\alpha/M)\beta_{\text{obs}}} \\ &\sim \frac{\alpha_{\text{em}}}{4\pi} \frac{H_0}{M_{\text{Pl}}} \frac{M}{\alpha M_{\text{Pl}}\beta_{\text{obs}}}, \end{aligned} \quad (16)$$

where  $\alpha_{\text{em}}/(4\pi) \approx 5 \times 10^{-4}$  (more precisely  $5.8 \times 10^{-4}$ ; the order-of-magnitude closure is robust to this factor),  $H_0/M_{\text{Pl}} \sim 10^{-61}$ , and the R4-fitted coupling  $\alpha/M \sim 10^{-21} \text{ GeV}^{-1}$  gives  $M_{\text{Pl}} \cdot (\alpha/M) \sim 10^{19} \text{ GeV} \cdot 10^{-21} \text{ GeV}^{-1} = 10^{-2}$ . Plugging in  $\beta_{\text{obs}} = 0.342^\circ \approx 6 \times 10^{-3} \text{ rad}$  ( $0.342 \times \pi/180 = 5.97 \times 10^{-3}$ ), the dimensionless ratio is  $\Delta\theta_{\text{one-loop}}/\Delta\theta_{\text{obs}} \sim 10^{-3} \cdot 10^{-61}/(10^{-2} \cdot 6 \times 10^{-3}) \approx 10^{-60}$  (canonical evaluation of the displayed contraction; we conservatively allow up to two orders of magnitude for unmodeled higher-order loop-ordering corrections, i.e. suppression by at least  $10^{-58}$ —an explicit conservatism allowance, *not* a derived range; the eV-vs-GeV unit conversion is exact  $1 \text{ GeV} = 10^9 \text{ eV}$  and is not a source of ambiguity), i.e. the one-loop induced  $\beta$  is suppressed by  $\approx 60$  (conservatively  $\geq 58$ ) orders of magnitude relative to the observed signal. We adopt this contraction as the canonical Route-2 estimate; an alternative ordering that contracts the  $H_0$  factor with the dimensionful coupling differently yields a deliberately loose  $\sim 10^{-33}$  upper bound, not used in the closure. The canonical-bound conclusion that the one-loop induced  $\beta$  is amplitude-suppressed many orders of magnitude below the observed WMAP+Planck birefringence signal (with ACT DR6 follow-up) is robust to this choice; Route 2 remains exploratory framing, not load-bearing for the no-go. The Route-2 amplitude is therefore far below not only the WMAP+Planck birefringence sensitivity but the observed central value itself; the one-loop

Holst-sector parity-odd term cannot account for the observed birefringence amplitude. (A naive comparison of a rotation rate  $\beta$  in eV against an angle uncertainty in eV would silently treat eV-s as dimensionless; the dimensionless reduction above avoids this and recovers the standard R2 amplitude-suppression closure.) *Closure: amplitude-suppressed by  $M_{\text{Pl}}^{-1}$  and one-loop factor  $\alpha_{\text{em}}/(4\pi)$ .* We stress the status of this estimate explicitly, since it bears directly on the strength of the no-go: Eq. (15) is an *illustrative upper-bound amplitude budget* constructed as the natural EFT operator at the  $M_{\text{Pl}}^{-1}\alpha_{\text{em}}/(4\pi)$  scale, *not* a result extracted from Mercuri [15] or Date–Kaul–Sengupta [27], which establish the classical Holst/Nieh–Yan structure but not this coefficient. Because the resulting suppression carries a margin of  $\sim 60$  orders of magnitude, the qualitative closure is insensitive to the precise coefficient: even inflating the ansatz prefactor by  $\mathcal{O}(1)$ – $\mathcal{O}(10^{10})$  (far beyond any plausible EFT enhancement) still leaves the induced  $\beta$  tens of orders of magnitude below the observed signal. The closure of Route 2 is therefore robust to the ansatz-level status of the operator, and we present it as an amplitude-budget bound rather than a rigorous derivation. The same logic applies to Route 3 below.

### E. Route 3 (quantum running of the Immirzi parameter): closed by mass-dimension lock

A second route to a parity-odd ECH contribution is the quantum running of the Barbero–Immirzi parameter  $\gamma$  itself. Date, Kaul & Sengupta analyzed the Holst term coupled to fermions and the Nieh–Yan invariant in the chiral-matter setting [27]; that analysis establishes a topological interpretation of  $\gamma$  and motivates a  $\gamma$ -running in the presence of chiral asymmetry, but does *not* itself present the explicit RG equation used below. Schematically motivated by their construction, we adopt the one-loop running ansatz

$$\frac{d\gamma}{d \ln \mu} = \frac{1}{12\pi^2} (N_F^L - N_F^R) \gamma + \mathcal{O}(\gamma^2), \quad (17)$$

where  $N_F^L$  and  $N_F^R$  are the numbers of left- and right-chiral Weyl fermions running in the loop. The  $1/(12\pi^2)$  prefactor is the natural chiral-loop coefficient at this order; we use Eq. (17) only as an upper-bound EFT ansatz for the Route-3 amplitude budget and do not claim it is taken verbatim from [27]. The actual fermion-induced perturbative running of the Immirzi parameter is computed by Benedetti & Speziale [28], who find a  $\beta$ -function whose sign depends on  $|\gamma|$  through four-fermion interactions generated when fermions are coupled to the Holst sector; our Eq. (17) is a chiral-count EFT bound rather than the full perturbative result, and is used solely for the amplitude budget below. We can, moreover, do better than an estimate. The actual fermion-coupled one-loop  $\beta$ -function was computed by Benedetti & Speziale [29]

(their Eq. 7),

$$\mu \frac{\partial \gamma^2}{\partial \mu} = -(\gamma^2 - 1) \frac{\mu^2 \kappa^2}{(8\pi)^2} (23\gamma^2 + 5), \quad \kappa^2 = 16\pi G, \quad (18)$$

whose only fixed point is the ultraviolet-attractive  $\gamma^2 = 1$  (formally outside perturbative control), with the sign of the flow set by whether  $|\gamma| \geq 1$  and the running driven by the radiatively-generated four-fermion interaction. The decisive feature is the explicit  $\mu^2 \kappa^2 = (\mu/M_{\text{Pl}})^2$  prefactor: the running is *power-suppressed* by the renormalization scale in Planck units, not logarithmic, so the accumulated  $\int \beta_{\gamma^2} d \ln \mu \propto \int \mu d\mu$  is dominated by the ultraviolet endpoint and is of order  $(\mu_{\text{UV}}/M_{\text{Pl}})^2$ . Integrating Eq. (18) from a GUT scale  $\mu_{\text{UV}} \sim 10^{16}$  GeV (with  $\gamma$  near the LQG value  $\gamma \approx 0.24$ ) gives  $|\Delta\gamma/\gamma| \sim 10^{-6}$  — Planck-suppressed to roughly *five orders of magnitude below* the chiral-count ansatz Eq. (17). The precise coefficient is scheme-dependent (BS work off-shell) and  $\gamma^2 = 1$  lies outside perturbative control, but the  $(\mu/M_{\text{Pl}})^2$  suppression is a robust structural consequence of the gravitational coupling  $\kappa^2$ . The derived physical running therefore only *strengthens* Route 3; we nonetheless retain the far larger chiral-count estimate Eq. (17),  $\Delta\gamma/\gamma \sim 0.3$ , as a deliberately pessimistic *upper* bound in the budget below. Because the Route-3 closure below carries  $\gtrsim 60$  orders of suppression margin, it is in any case insensitive to the precise coefficient. In the Standard Model, the chiral asymmetry is generated by the  $SU(2)_L$  doublets. Integrating Eq. (17) over the running gives  $\Delta\gamma/\gamma \approx (N_F^L - N_F^R) \ln(\mu_{\text{GUT}}/\mu_{\text{IR}})/(12\pi^2)$ ; with a net chiral count  $(N_F^L - N_F^R) = \mathcal{O}(1)$  and a GUT-to-IR lever arm  $\ln(\mu_{\text{GUT}}/\mu_{\text{IR}}) \approx 30\text{--}35$  ( $\mu_{\text{GUT}} \sim 10^{16}$ ,  $\mu_{\text{IR}} \sim 1$  GeV), this is numerically  $\Delta\gamma/\gamma \approx 0.25\text{--}0.30$  (a few  $\times 10^{-1}$ ; e.g.  $32/(12\pi^2) \approx 0.27$ ), *not* the  $10^{-2}$  that an earlier draft mis-stated for this expression. We therefore adopt the larger  $\Delta\gamma/\gamma \sim 0.3$  as the *conservative* (least-suppressed) order-of-magnitude estimate — *not* a precisely derived value, but a conservative upper bound consistent with the  $|\gamma|$ -dependent Benedetti-Speziale  $\beta$ -function structure recorded above (four-fermion-driven, sole fixed point at  $\gamma^2 = 1$ , sign set by  $|\gamma| \geq 1$ ) — and note that the Route-3 closure below is insensitive to its precise value: even this  $\mathcal{O}(0.3)$  running is  $\ll 1$ , so  $\gamma$  retains its order of magnitude, and it still leaves  $\gtrsim 60$  orders of suppression margin. The Holst sector amplitude that this running can source is fixed by mass dimension: any operator built from  $\gamma$ ,  $R_{ab}$ ,  $e^a$ , and the chiral current  $J^{5\mu}$  must carry dimension four, which forces a single power of  $M_{\text{Pl}}^{-1}$  in the prefactor in any cosmologically relevant scalar-curvature regime. Plugging the conservative  $\Delta\gamma/\gamma \sim 0.3$  into the resulting parity-odd amplitude, the cosmologically integrated effect is suppressed by an additional factor of  $(\Delta\gamma/\gamma) \cdot (H/M_{\text{Pl}}) \sim 3 \times 10^{-62}$  relative to the dimensionless parity-odd amplitude budget associated with a dark-energy-scale source, closing this route by many orders of magnitude. *Closure: mass-dimension-locked at the classical level and amplitude-suppressed*

*by the chiral-asymmetry running coefficient. Ansatz vs derivation (R2/R3):* The R2/R3 amplitude coefficients displayed in this paper (Eqs. 17 and the chiral-count EFT scaling above) are *conservative upper bounds derived from a chiral-count EFT scaling ansatz*, not literal extractions from Mercuri [15] or Date–Kaul–Sengupta [27]; the closures of R2/R3 survive an  $\mathcal{O}(1)$  inflation of the ansatz coefficient because the resulting amplitude suppression ( $\sim 3 \times 10^{-62}$  vs  $\rho_\Lambda$ , using the corrected  $\Delta\gamma/\gamma \sim 0.3$ ) leaves  $\gtrsim 60$  orders of magnitude of margin against any  $\mathcal{O}(1)$  rescaling of the chiral-asymmetry coefficient.

#### F. Route 4 (parity-odd CMB coupling via spectator ALP or neutrino current): naturalness objection rather than amplitude no-go

The fourth route is the direct parity-odd coupling between the electromagnetic field and either an axion-like field (ALP) or the fermion axial current, which would imprint on the CMB as a uniform rotation of the polarization plane. An early cosmological-birefringence treatment of this mechanism is Lue, Wang & Kamionkowski [30]; they work with a generic pseudoscalar-photon Chern–Simons coupling  $\partial_\mu \phi K^\mu$  (equivalently  $\phi F\tilde{F}$  up to a total divergence), not with the specific  $-\frac{1}{4}(\alpha/M)$  normalization adopted here. The operator  $\mathcal{L}_{\text{CS}} \supset -\frac{1}{4}(\alpha/M)\phi\tilde{F}_{\mu\nu}F^{\mu\nu}$  (with  $\phi$  the dim+1 canonical ALP field) is the conventional ALP–photon Chern–Simons coupling used throughout the axion-electrodynamics literature; we adopt this normalization and use [30] as an early example of its cosmological birefringence implications rather than as the source of the specific prefactor.<sup>4</sup> All indices are fully contracted; the integrated-by-parts equivalent  $(\alpha/M)\partial_\mu\theta K^\mu$ , where  $K^\mu \equiv \epsilon^{\mu\nu\rho\sigma}A_\nu F_{\rho\sigma}$  is the standard Chern–Simons 4-current and  $\partial_\mu K^\mu = \frac{1}{2}\tilde{F}_{\mu\nu}F^{\mu\nu}$  recovers the parity-odd contraction, is also valid. From this operator one obtains

<sup>4</sup> Single-convention statement (resolving an apparent dimensional ambiguity flagged in external review). Throughout this paper there is *one* pseudoscalar field and *two* normalizations of it: the dim+1 canonical field  $\phi$  (used in the Lagrangian operator above) and the dimensionless angle  $\theta \equiv \phi/f_a$  (used in Appendix C with potential  $V = m_\theta^2 f^2(1 - \cos\theta)$ , Eq. (C2);  $f \equiv f_a$  is the dim+1 decay constant). Dimensional accounting:  $[\alpha/M] = -1$ ,  $[\phi] = +1$ ,  $[F\tilde{F}] = +4$ , so the operator displayed above has Lagrangian-density dimension +4 as required. The  $\theta$ -dimensionless writeup is obtained by  $\phi \rightarrow f_a\theta$ , which sends  $-\frac{1}{4}(\alpha/M)\phi\tilde{F}F \rightarrow -\frac{1}{4}[(\alpha/M)f_a]\theta\tilde{F}F$ ; the bracketed quantity  $(\alpha/M)f_a$  is dimensionless, exactly compensating the  $\theta$  dimensionlessness. Equivalently,  $\Delta\theta = \Delta\phi/f_a$  is the dimensionless excursion used in Eq. (19), and the basis-conversion to  $g_{a\gamma} \equiv (\alpha_{\text{em}}c_\gamma)/(2\pi f_a)$  recorded at Eq. (C4) reproduces the identification  $\alpha/M = g_{a\gamma}$ . The  $\theta$ -versus- $\phi$  alternation in the body of this paper is purely a choice of writing the same operator in either  $\theta$ -dimensionless or  $\phi$ -canonical form; no two operators are in play. This footnote is the single authoritative convention statement for the paper.

the rotation angle

$$\beta = \frac{\alpha}{2M} \Delta\phi_{\text{rec}\rightarrow\text{today}} \sim \frac{\alpha}{2M} \sqrt{2\rho_\theta/m_\theta^2}, \quad (19)$$

where the factor  $1/2$  is the standard small-rotation result for the  $-\frac{1}{4}(\alpha/M)$  operator normalization (the rotation angle is half the coupling times the field excursion; derived from the helicity dispersion relation in Appendix C),  $\rho_\theta$  is the energy density of the spectator field and  $m_\theta$  its mass. The excursion is written in the dim+1 canonical-field form  $\Delta\phi = f_a\Delta\theta$  for dimensional consistency with the operator written in  $\phi$ -canonical form (see the single-convention footnote above the operator); the dimensionless angle  $\Delta\theta$  used in Appendix C's numerical pipeline corresponds via  $\Delta\phi = f_a\Delta\theta$ . The excursion estimate  $\Delta\phi_{\text{rec}\rightarrow\text{today}} \sim \sqrt{2\rho_\theta}/m_\theta$  assumes a coherently displaced field whose evolution between recombination and today is monotonic, valid for  $m_\theta \lesssim H_0$  (frozen or slowly rolling field); since the rotation angle depends only on the endpoint values  $\theta_{\text{today}} - \theta_{\text{rec}}$ , a rapidly oscillating field ( $m_\theta \gg H_0$ ) has its present-day amplitude redshift-diluted ( $\rho_\theta \propto a^{-3}$  after onset of oscillation), which *suppresses*  $\beta$  at fixed  $\rho_\theta$  and therefore requires an even larger  $\rho_\theta$  to match  $\beta_{\text{obs}}$  — the overshoot conclusion below is conservative with respect to the assumed  $\theta(t)$  regime. Setting the present-day rotation-rate amplitude equal to the published WMAP+Planck cosmological-birefringence measurement  $\beta_{\text{obs}} = 0.342^\circ \pm 0.094^\circ$  ( $\sim 3.6\sigma$  from  $\beta = 0$ ; [3, 4]; the independent ACT DR6 follow-up of Diego-Palazuelos & Komatsu [5] reports  $\beta = 0.215^\circ \pm 0.074^\circ$  at  $\sim 2.9\sigma$ , consistent within  $\sim 1.1\sigma$ :  $|0.342 - 0.215|/\sqrt{0.094^2 + 0.074^2} = 0.127/0.120 \approx 1.06$ ; these two  $\sigma$  values are derived under different null procedures, masks, and foreground treatments and are *not* the output of a joint analysis with a known covariance, so this  $\sim 1.06\sigma$  figure is a heuristic difference assuming independent Gaussian errors, not a joint-pipeline significance) bounds  $\alpha/M$  at  $\sim 10^{-21} \text{ GeV}^{-15}$ , identical to the value

already quoted in Sec. II A 2; identifying the spectator field with the ECH parity-odd sector and demanding that it *also* carry the observed dark-energy density imposes a tuning constraint on the spectator-field mass  $m_\theta$  that re-imports the cosmological-constant problem through the back door. From Eq. (19),  $\beta = (\alpha/2M)\sqrt{2\rho_\theta/m_\theta^2}$  inverts to  $\rho_\theta = 2m_\theta^2\beta^2/(\alpha/M)^2$ ; plugging in  $\alpha/M = 10^{-21} \text{ GeV}^{-1}$ ,  $\beta = \beta_{\text{obs}} \approx 6 \times 10^{-3} \text{ rad}$ , and  $m_\theta = H_0 \approx 1.5 \times 10^{-33} \text{ eV}$  gives  $\rho_\theta \approx 1.6 \times 10^{-10} \text{ eV}^4 \approx 6\rho_\Lambda$  — matching the dark-energy density to within an order of magnitude — so the spectator-ALP route does *technically* reproduce the dark-energy density at the R4-fitted coupling, but only by tuning  $m_\theta$  to  $\sim H_0$ , which is precisely the cosmological constant problem in disguise rather than its solution. R4 is therefore *not* closed by amplitude mismatch (as prior analyses claimed); it is closed by the observation that the same coupling that produces  $\beta_{\text{obs}}$  requires an ultralight-mass tuning  $m_\theta \sim H_0$  to also produce  $\rho_\Lambda$ , and this tuning is the original CC fine-tuning relabelled. For any  $m_\theta$  in the natural ALP range ( $m_a \in [10^{-22}, 10^{-15}] \text{ eV}$ ) the produced  $\rho_\theta \propto m_\theta^2$  overshoots  $\rho_\Lambda$  across the entire natural range (because the  $\rho_\theta = \rho_\Lambda$  matching point lies at  $m_\theta \approx 0.4 H_0 \sim H_0$  with  $H_0 \approx 1.5 \times 10^{-33} \text{ eV}$ , and the natural ALP range lies entirely *above* that point, so the overshoot is monotonic in  $m_\theta$  and is bounded below by its lower-endpoint value ( $\sim 22$  OOM at  $m_\theta \sim 10^{-22} \text{ eV}$ ) and grows to  $\sim 36$  OOM at the upper endpoint  $m_\theta \sim 10^{-15} \text{ eV}$ ); this overshoot conclusion is conditional on the one-loop estimate  $\alpha/M \sim 10^{-21} \text{ GeV}^{-1}$  being rigidly bounded by the photon-Chern-Simons matching — if  $\alpha/M$  is instead treated as a free phenomenological parameter, both  $\beta_{\text{obs}}$  and  $\rho_\Lambda$  can be matched for arbitrary  $m_\theta$  by scaling  $\alpha/M \propto m_\theta$  (e.g., requiring  $\alpha/M \sim 10^{-10} \text{ GeV}^{-1}$  at  $m_\theta \sim 10^{-22} \text{ eV}$ ; couplings of that size at ultralight masses are moreover in strong tension with established astrophysical ALP-photon limits from helioscope and stellar-cooling constraints, so this free-coupling direction illustrates the degeneracy structure of the matching formula rather than an open parameter direction), so the rigidity of the no-go is tied to the one-loop matching assumption rather than to ALP-mass kinematics alone: at  $m_\theta \sim 10^{-22} \text{ eV}$  the overshoot is  $\sim 22$  orders of magnitude  $(m_\theta/H_0)^2 \sim (10^{11})^2 \sim 10^{22}$ , and at  $m_\theta \sim 10^{-15} \text{ eV}$  the overshoot is  $\sim 36$  orders of magnitude  $(m_\theta/H_0)^2 \sim (10^{18})^2 \sim 10^{36}$ ; the  $m_\theta \sim H_0$  window where both observables are simultaneously matched has fractional width  $\Delta m_\theta/m_\theta \sim 10^{-1}$ , representing a dimensional tuning of order  $10^{-33} \text{ eV}/M_{\text{Pl}} \sim 10^{-61}$ . R4 therefore relocates the cosmological-constant problem rather than solving it. The inequality is rigid only under the one-loop matching assumption; with  $\alpha/M$  floated, the spectator-ALP class is recovered as a *viable parity-odd source* but is *not* a predictive dark-energy source — the model contains no first-principles explanation for why  $m_\theta \sim H_0$  or for the fitted value of  $\alpha/M$ . LiteBIRD ( $\sigma(\beta) \approx 0.03^\circ$ , early 2030s) [31] will tighten this bound by a factor of  $\sim 3$ , but the bound's structure is set by the ratio of dark-energy

<sup>5</sup> The paper's  $\alpha/M$  is *not* the canonical ALP-photon Chern-Simons coupling  $g_{a\gamma} \equiv (\alpha_{\text{em}} c_\gamma)/(2\pi f_a)$ ; the two coincide numerically at  $\alpha/M = 10^{-21} \text{ GeV}^{-1}$  only after a non-trivial identification. Specifically: the paper's  $M = M_{\text{area-gap}} = M_{\text{Pl}}/\sqrt{\gamma} \approx 1.9 M_{\text{Pl}}$  (using  $\gamma_{\text{SU}(2)} \approx 0.274$ , Eq. (2)), and the paper's  $\alpha$  is the dimensionless Mercuri one-loop coefficient  $\sim \alpha_{\text{em}}/(4\pi) \approx 5.8 \times 10^{-4}$  (Eq. (7)), giving the  $-\frac{1}{4}$  (not  $1/(2\pi)$ ) normalization convention. The naive identification  $g_{a\gamma} = \alpha/M$  at  $f_a = M_{\text{Pl}}$ ,  $c_\gamma \sim O(1)$  yields  $g_{a\gamma} \sim 10^{-22} \text{ GeV}^{-1}$ , roughly  $10\times$  smaller than the paper's value. To reproduce  $\alpha/M = 10^{-21} \text{ GeV}^{-1}$  in the canonical basis one therefore requires either a sub-Planckian decay constant  $f_a \sim M_{\text{Pl}}/10$  or an amplified photon-coupling coefficient  $c_\gamma \sim O(10)$ ; both are non-trivial UV-completion assumptions not derived in this paper. We adopt the Mercuri-style coupling without making either assumption and emphasize that the  $10\times$  basis-conversion gap is not an internal inconsistency of R4: the R4 closure (cosmological-constant fine-tuning at  $m_\theta \sim H_0$ ) is unaffected, and the resulting parameter  $\alpha/M$  remains an effective phenomenological parameter constrained by data, exactly as stated at Eq. (7).

to birefringence amplitudes, which is dimensional and instrument-independent. *Route-4 status: a naturalness objection rather than an amplitude exclusion. A free-coupling spectator-ALP fit reproduces both  $\beta_{\text{obs}}$  and  $\rho_{\Lambda}$ , but minimal ECH does not derive  $m_{\theta} \sim H_0$  or the fitted  $\alpha/M$ ; the channel is closed at the level of an explanatory deficit, not an amplitude no-go at the operator level.*

### G. Closure summary

Within the channel-level enumeration of Sec. IV (“Scope” paragraph), Routes R1–R4 cover the four parity-odd / dark-energy channels enumerated in this paper. The two operators previously omitted from this four-channel enumeration (the Jackiw–Pi gravitational Chern–Simons term  $R\wedge\tilde{R}$  and the parity-odd four-fermion partner of R1 carrying the  $\gamma_{\text{BI}}/(\gamma_{\text{BI}}^2+1)\cdot 8\pi G$  coefficient) are now *also* closed, in Sec. IV B (Planck suppression + vanishing mean field, inheriting R1) and Sec. IV C (total derivative for constant coupling; R4-class otherwise); only the *complete* dimension-6 parity-odd operator basis (all Fierz structures + the gravitational Chern–Simons invariant, with a projection lemma) is left to a follow-up operator-basis analysis (Sec. IV Scope paragraph; abstract). Within the four enumerated channels: R1 (NJL contact) is amplitude-suppressed by  $M_{\text{Pl}}^{-2}$  and parity-even. R2 (one-loop graviton corrections) is amplitude-suppressed by  $M_{\text{Pl}}^{-1}$  and the one-loop factor  $\alpha_{\text{em}}/(4\pi)$ . R3 (Immirzi running) is mass-dimension-locked and additionally suppressed by the chiral-asymmetry beta function. R4 (parity-odd CMB coupling) is closed by a naturalness objection: with  $\alpha/M$  treated as a free parameter, a spectator-ALP fit reproduces both  $\beta_{\text{obs}}$  and  $\rho_{\Lambda}$ , but minimal ECH does not derive  $m_{\theta} \sim H_0$  or the fitted  $\alpha/M$ , so the channel closes at the level of an explanatory deficit rather than an amplitude exclusion. The NJL contact term is parametrically far below  $\rho_{\Lambda}$  even at dense ISM-like densities  $n_{\psi} \sim 10^2 \text{ cm}^{-3}$  ( $\sim 70$  orders below  $\rho_{\Lambda}$ ; see Sec. IV A), parity-even with  $\langle J^5 \rangle \approx 0$ , and lacks any coherent  $w = -1$  mean-field structure; incoherent thermal variance  $\langle J^5 J^5 \rangle$  is permitted but does not source coherent dark energy. MCMC fits and the  $\Delta N_{\text{eff}}$ /birefringence consistency analysis are reported (in preparation [6]); the present manuscript provides only the channel-level amplitude closure of the four parity-odd routes in the ECH sector.

*a. Evidentiary status of each leg.* So that the strength of the closure is not overread, we state explicitly the evidentiary level at which each route and each structural result is established. We use a three-tier scale: **(I) rigorous result** — a deductive consequence of stated equations/identities, holding exactly within an explicitly bounded scope; **(II) structural argument** — a qualitative or order-of-magnitude argument from established physics (symmetry, parity, naturalness) that does not turn on a fitted number; and **(III) ansatz-level dimensional estimate** — an amplitude budget evalu-

ated under an explicitly-labeled scaling ansatz, honest to a factor but not a first-principles derivation. Table III classifies every leg on this scale. No leg is claimed at a level higher than this table records: in particular, the only Tier-I (rigorous) leg is the perturbation-transparency result for canonical scalar matter; R2–R3 are Tier-III ansatz-level estimates; and the R4 closure is a Tier-II *naturalness/explanatory-deficit* objection, *not* an amplitude exclusion and conditional on the on-shell scaling ansatz of Appendix B. The aggregate “four-route channel-level closure” is therefore exactly that: a channel-level (not operator-level) statement whose individual legs sit at the levels tabulated, reinforced but not promoted by the mechanism-class catalog of Sec. IX.

The phenomenological parameter  $\alpha/M$  in Sec. II A 2 is therefore best understood as the R4-bounded coupling required to match  $\beta_{\text{obs}}$ , with the dark-energy density supplied by an unrelated sector (e.g. a quintessence field [32], a quintom-class two-field scenario [33], or by a positive cosmological constant), rather than by ECH-internal physics. This inversion of the prior mass-coupling lock is the core structural finding of this manuscript.

## V. DATA METHODS: GALAXY SPIN ANALYSIS

*Prior work.*—Galaxy spin dipole analysis historically relied on published CW/CCW labels from Shamir [34, 35], who reported  $\sim 1\text{--}3\%$  CW excesses. These claims have been contested [36, 37].

*Our chirality classifier.*—We applied a bias-audited Vision Transformer with test-time equivariant averaging to the DESI Legacy Imaging Survey galaxy population. The catalog construction, sample size, validation accuracy, bias-audit suite, equivariant CW-fraction monopole, and dipole significance are reported in Paper IV [23] and are not duplicated here. The observational conclusion is the null result of Sec. III B: the all-sky dipole is null on the spiral-classified subsample, and Shamir’s 3% claim is disfavored in amplitude by a factor of  $\sim 6\text{--}12$  (matched-footprint reanalysis required for a likelihood-level exclusion; Paper IV [23]).

## VI. SYSTEMATIC ANALYSIS

The galaxy spin channel is a confirmed null (Sec. III B). The CMB birefringence channel provides the surviving parity-violation evidence from the published WMAP+Planck Eskilt & Komatsu measurement  $\beta_{\text{obs}} = 0.342^\circ \pm 0.094^\circ$  [4] with an independent ACT DR6 follow-up ( $\beta = 0.215^\circ \pm 0.074^\circ$ , Diego-Palazuelos & Komatsu [5]). For the  $f_{\text{NL}}$  channel, dominant systematic uncertainties are GR-projection effects ( $\sim 20\%$  amplitude degradation at  $z > 2$ , Heinrich *et al.* 2024 [38] Sec. 3.4),  $b_{\phi}$  bias-prior uncertainty ( $\sigma(b_{\phi})/b_{\phi} \approx 0.2$ ), and photo- $z$  marginalization, propagated through the

TABLE III. Evidentiary status of each closure leg, on the three-tier scale of the text: (I) rigorous result within stated scope, (II) structural argument, (III) ansatz-level dimensional estimate. The table records the highest level at which each leg is claimed; no leg is asserted more strongly elsewhere in the paper. “Rules out” is to be read at channel-amplitude granularity (the level at which the observational budget of Sec. III discriminates), not as an operator-level theorem.

Leg	What it rules out (channel-amplitude level)	Evidentiary status
Perturbation transparency (Sec. X)	The Holst sector / Barbero–Immirzi parameter contributing to scalar or tensor perturbation observables, for canonical scalar matter	<b>(I) Rigorous</b> within stated scope: $T = 0$ follows from zero scalar spin density, and the Holst dual contraction vanishes by the algebraic Bianchi identity. Excludes propagating-torsion, fermion-loop, dynamical-Immirzi, non-minimal-matter sectors.
R1 (NJL four-fermion contact)	The torsion-induced contact term sourcing coherent $w = -1$ dark energy	<b>(II)+(III)</b> : parity-even structure ( $\langle J^5 \rangle \approx 0$ , no coherent mean field) is a Tier-II algebraic fact; the $M_{\text{Pl}}^{-2}$ amplitude suppression ( $\sim 70$ orders below $\rho_\Lambda$ ) is a Tier-III order-of-magnitude estimate from a standard Cartan torsion-elimination derivation.
R2 (one-loop graviton corrections)	One-loop promotion of $\gamma_{\text{BI}}$ reaching the observed birefringence amplitude	<b>(III) Ansatz-level</b> : amplitude budget suppressed by $H_0/M_{\text{Pl}}$ and $\alpha_{\text{em}}/(4\pi)$ under an explicitly-labeled scaling ansatz; exploratory, not load-bearing.
R3 (Immirzi running)	Quantum running of $\gamma_{\text{BI}}$ generating a dark-energy-relevant shift	<b>(II)+(III)</b> : mass-dimension lock is structural; the chiral-asymmetry beta-function bound (Benedetti–Speziale) is a Tier-III order-of-magnitude upper bound, deliberately loose and non-load-bearing ( $\gtrsim 60$ orders of margin).
R4 (parity-odd CMB / spectator-ALP coupling)	Minimal ECH <i>deriving</i> the single coupling that yields both $\beta_{\text{obs}}$ and $\rho_\Lambda$	<b>(II) Structural naturalness objection</b> , <i>not</i> an amplitude exclusion: a free- $\alpha/M$ ALP fit reproduces $\beta_{\text{obs}}$ , but ECH supplies neither $m_\theta \sim H_0$ nor the fitted $\alpha/M$ , relocating the CC problem. Conditional on the on-shell scaling ansatz (App. B).

multi-bin Fisher matrix (Sec. VII). MCMC systematics (dataset-dependent  $\Delta N_{\text{eff}}$ ) are in Paper I(b) (in preparation [6]).

## VII. FALSIFIABILITY CRITERIA

The surviving testable predictions are: (1) LiteBIRD ( $\sigma(\beta) \approx 0.03^\circ$ , early 2030s) will measure  $\beta$  to  $\sigma(\beta) \approx 0.03^\circ$  and either confirm a non-zero birefringence at high significance or rule out the spectator-ALP class as the source of the WMAP+Planck birefringence signal (with ACT DR6 follow-up) (the relevant comparison is differential against the prior central value  $\beta_{\text{obs}} = 0.342^\circ \pm 0.094^\circ$ , not a naive  $0.27^\circ/0.03^\circ$ ); (2) SPHEREx ( $\sim 2028$ ) will test the matter-bounce prediction  $f_{\text{NL}} = -35/8$  at

2.6–5 $\sigma$  realistic significance<sup>6</sup> [2, 38] via the galaxy bispectrum, simultaneously discriminating matter-bounce from slow-roll inflation ( $f_{\text{NL}} \approx 0.015$ ) and the Cuscuton bounce [39]; (3) MCMC parameter values ( $H_0$ ,  $\sigma_8$ ,

<sup>6</sup> The 2.6–5 $\sigma$  realistic range reflects two forecast regimes:  $\sigma(f_{\text{NL}}) \approx 0.7$  Fisher-ideal (raw ratio  $|f_{\text{NL}}|/\sigma = 4.375/0.7 \approx 6.25\sigma$ , degraded to  $\sim 5$ –5.5 $\sigma$  optimistic after template-overlap correction  $r \approx 0.84$  between the matter-bounce shape and the local/equilateral basis, before further GR-projection and  $b_\phi$  degradation) and  $\sigma(f_{\text{NL}}) \approx 1.0$  after GR-projection and photo- $z$  marginalization (2.6–5 $\sigma$  realistic). Both assume nominal SPHEREx survey volume ( $f_{\text{sky}} = 0.75$ ,  $\sim 3 \times 10^8$  galaxies). The full multi-tracer SPHEREx Fisher forecast is computed in Paper II [2], which recasts the Heinrich *et al.*  $\sigma(f_{\text{NL}}^{\text{local}}) \approx 0.7$  baseline for the matter-bounce template mismatch and adopts exactly these 5.2–5.5 $\sigma$  optimistic and 2.6–5 $\sigma$  realistic (post-systematic-budget) ranges as its headline forecast; the present footnote summarizes that result rather than deriving it from the in-text  $\sigma(f_{\text{NL}}) \approx 1.0$  GR-marginalized value alone (which gives the  $\approx 4.4\sigma$  lower midpoint).

$\Delta N_{\text{eff}}$ ) are already consistent with standard  $\Lambda$ CDM, constraining the framework rather than falsifying it (details in Paper I(b), in preparation [6]).

## VIII. RELATED WORK

This work builds on rotating cosmologies (Gödel [40]), ECH theory (Hehl *et al.* [12]), Popławski’s torsion bounce and black hole universe scenario [13, 14, 41], the Holst/Nieh-Yan parity structure (Freidel *et al.* [16], Mercuri [15, 42]), and cosmic birefringence detections (Minami & Komatsu [3]). Recent independent support includes Liu *et al.* [43] (EC torsion fits the  $S_8$  tension), Legner *et al.* [44] (torsion condensation), and Alam *et al.* [45] (non-singular bounces in modified gravity). No prior work assembles these into a single quantitative framework with systematic barrier testing.

Recent developments in bounce cosmology include: Cai & Zhu [46] (GW echo signatures), Papanikolaou *et al.* [47] (PBH formation in matter bounce), and Deghani *et al.* [39] (Cuscuton bounce bispectrum).

## IX. STRUCTURAL CONSTRAINTS ON DARK-ENERGY ROUTES IN MINIMAL ECH

Before cataloguing the individual barriers we fix their collective status precisely, so that their joint force is not overstated. We describe the catalog as *13 distinct mechanism-class constraints* (14 historical entries, with B8 subsumed by B14). Here ‘distinct’ and ‘mechanism-class’ mean that no barrier is a logical *consequence* of another and each probes a separate physical failure mode (amplitude suppression, thermal washout, operator decoupling, naturalness deficit, and so on); they do *not* assert that the barriers rest on disjoint assumptions or that each is an independent rigorous no-go theorem. In particular, several barriers share the same phenomenological on-shell scaling ansatz (Appendix B); several—B5 (scale separation), B6 (attractor sensitivity), B7 (parameter immunity), B10 (UV→IR specificity), and B13 (gravitational democracy)—are general naturalness or classification arguments that apply to broad classes of bounce/modified-gravity models rather than sharp ECH-specific calculations; and at least one, B9 (Liouville conservation), is an explicitly *heuristic* closure conditional on stated equilibrium assumptions (no particle production, no entropy injection) that realistic quantum bounces can violate. The catalog is therefore best read as a structured map of failure modes of mixed individual strength—quantitative amplitude bounds, naturalness arguments, and qualitative observations—whose collective value is the systematic coverage of the route space, not a claim that thirteen separately decisive theorems each independently exclude the framework. The two sharp, first-principles results in the catalog are the Route-1 torsion-elimination derivation and the perturbation-

transparency theorem (B14); the remaining entries are constraints of the weaker classes just described and are labeled as such in their respective subsections.

We tested 7 foundation mechanism classes (Foundations A–G) and 6 additional observational channels (Branches H, J, L, M, N, O, plus ECH perturbation gates) for the possibility of connecting the ECH bounce to late-time dark energy. Each test yielded a named structural constraint. These constraints are specific to the ECH mechanism class; other bounce cosmologies (e.g., quintom scenarios) are not subject to them.

*Constraint classification.*—**Novel results** (Barriers 1, 2, 3, 4, 8, 10, 11, 12, 14): ECH-specific calculations not immediate consequences of prior literature. **Known results** (Barriers 5, 6, 7, 9): scale separation, attractor-sensitivity dilemma, parameter immunity, Liouville conservation (B9; heuristic ordering argument)—included to close mechanism classes that arise naturally in the ECH analysis. **Structural/philosophical observations** (Barrier 13): gravitational democracy, included for completeness.

### A. Barrier 1: Mass-Coupling Lock (Foundation A)

In Poincaré gauge theory (PGT), ultralight torsion modes ( $m_T \sim H_0$ ) require coupling:

$$g_{\text{eff}} \sim \frac{1}{M_{\text{Pl}} \sqrt{|t_3|}} \sim \frac{H_0}{M_{\text{Pl}}} \sim 10^{-61}, \quad (20)$$

where  $t_3$  is the quadratic-torsion coupling of the PGT Lagrangian controlling the tensor-torsion mode mass, with  $\sqrt{|t_3|} \sim m_T^{-1}$  for an ultralight mode ( $m_T \sim H_0$ ), which makes  $g_{\text{eff}}$  dimensionless and yields the displayed  $H_0/M_{\text{Pl}}$  equality; the chain is a scaling ansatz of the PGT mass spectrum, labeled as such, not a derived equality. To achieve  $g_{\text{eff}} \sim 1$ , one needs  $m_T \sim M_{\text{Pl}}$ . The required fine-tuning is equivalent to the standard cosmological constant hierarchy:  $\delta m_T^2/m_T^2 \sim (H_0/M_{\text{Pl}})^2 \sim 10^{-122}$ .

### B. Barrier 2: Topological-Shift Duality (Foundation B)

In metric-affine gravity, a duality emerges:

$$\text{Mass protection} \iff \text{No geometric fingerprint.} \quad (21)$$

Configurations protecting the pseudoscalar mass through topological structure eliminate the geometric content (the field reduces to a standard ALP after torsion elimination). Conversely, configurations preserving geometric content cannot protect the mass.

TABLE IV. The 14 catalogue entries (13 distinct mechanism-class constraints; B8 subsumed by B14) on minimal ECH dark-energy routes. Note: Barriers 8 (parity-even interaction) and 14 (perturbation transparency) close the same observable channel (primordial-GW chirality / tensor parity violation) via related routes sharing the perturbation-transparency result; B14 is the first-principles theorem that subsumes B8 as the corresponding observational consequence. They are listed separately to preserve the historical mechanism-class catalog, but should not be counted as a separate mechanism-class constraint.

#	Barrier	Source	Mechanism Blocked
1	Mass-Coupling Lock	Found. A	Propagating torsion as DE
2	Topological-Shift Duality	Found. B	Geometric pseudoscalar mass protection
3	Scalar-Tensor Universality	Found. C	Distinctive geometric content on FRW
4	Planck Suppression	Found. D	Disformal / connection coupling effects
5	Scale Separation	Found. E	Global vacuum integral coupling
6	Attractor-Sensitivity Dilemma	Found. F	Initial-condition transfer to DE
7	Parameter Immunity	Found. G	Cyclic vacuum selection
8	Parity-Even Interaction	Branch H	Tensor chirality from the bounce
9	Liouville Conservation	Branch J	Reversible state selection
10	UV→IR Specificity Dilemma	Branch L	Generic vs. bounce-specific bridge
11	Decoupling Universality	Branch L/M	Light gauge field coupling
12	Vacuum Amplification Ceiling	Branch M	Gravitational wave amplitude
13	Gravitational Democracy	Branch N/O	Relics, baryogenesis, vacuum transitions
14	Perturbation Transparency	ECH Gates	ECH-specific perturbation signatures

### C. Barrier 3: Scalar-Tensor Universality (Foundation C)

On an FRW background, the most general action for torsion-scalar mixing is constrained by diffeomorphism invariance. The torsion fluctuation couples to the curvature invariants in the same manner as any other scalar, with no additional ECH-specific observable. Torsion decouples from the FRW background precisely at the bounce density, yielding no distinctive perturbation signal.

### D. Barrier 4: Planck Suppression (Foundation D)

Disformal couplings from torsion are Planck-suppressed by factors of  $m_\phi^2/M_{\text{Pl}}^2$  or  $(\partial\phi)^2/M_{\text{Pl}}^4$ . At cosmological scales ( $m_\phi \sim H_0$ ), these are  $\mathcal{O}(10^{-122})$ —observationally inaccessible.

### E. Barrier 5: Scale Separation (Foundation E)

The global vacuum integral  $\int d^4x \sqrt{-g} \rho_\Lambda$  cannot be connected to the local bounce density without assuming a mechanism to store and transfer the integrated vacuum energy across  $\sim 92$   $e$ -folds of inflation. No such mechanism exists within minimal ECH.

### F. Barrier 6: Attractor-Sensitivity Dilemma (Foundation F)

If the post-bounce inflation converges to an attractor, initial conditions from the bounce are washed out. If it

is sensitive to initial conditions, inflation itself is destabilized. The bounce therefore cannot simultaneously seed dark energy *and* preserve the standard inflation dynamics.

### G. Barrier 7: Parameter Immunity (Foundation G)

Cyclic vacuum selection mechanisms require  $\gamma$  to vary across cycles. However,  $\gamma$  is fixed by the LQG area spectrum at a universal value; there is no mechanism within LQG to produce a landscape of  $\gamma$  values from which selection could operate.

### H. Barrier 8: Parity-Even Interaction (Branch H)

The spin-torsion effective interaction  $(J^5)^2$  is parity-*even*: the product of two axial currents is a Lorentz scalar, not a pseudoscalar. It therefore cannot generate tensor chirality (circular polarization asymmetry) in primordial gravitational waves. This was independently confirmed by the perturbation-transparency result (Barrier 14).

### I. Barrier 9: Liouville Conservation (Branch J)

Phase-space volume conservation prevents irreversible selection among post-bounce states from pre-bounce dynamics, closing the “vacuum selection at the bounce” mechanism class. The bounce is time-symmetric, so no net dark-energy state can be selected from a distribution by the bounce alone. This barrier is a heuristic closure under explicit assumptions: closed Hamiltonian

(non-dissipative) evolution through the bounce, no particle production, and no coarse-grained entropy injection. Scenarios that break these assumptions (dissipative or particle-producing bounces) evade Barrier 9 as stated and are constrained instead by the amplitude-budget arguments of Barriers 10–11; Barrier 9 is not used as a stand-alone closure of any route.

### J. Barrier 10: UV→IR Specificity Dilemma (Branch L)

Any mechanism that bridges from Planck-scale bounce physics to the late-time  $H_0$  scale must be either generic (explaining *any* vacuum energy, not specifically the ECH value) or bounce-specific (requiring free parameters equivalent to the cosmological constant itself). No mechanism achieves both simultaneously within ECH.

### K. Barrier 11: Decoupling Universality (Branches L/M)

At low energies, all gauge fields decouple from the torsion sector equally (since torsion is Planck-suppressed). The ECH bounce cannot preferentially couple to photons or dark energy degrees of freedom without introducing new non-minimal couplings beyond the minimal framework.

### L. Barrier 12: Vacuum Amplification Ceiling (Branch M)

Gravitational wave production from the ECH bounce is bounded above by:

$$\Omega_{\text{GW}}^{\text{ECH}}|_{\text{bounce}} \lesssim \left( \frac{\rho_{\text{crit}}}{\rho_{\text{PI}}} \right)^2 \simeq 0.07\text{--}0.17, \quad (22)$$

where we have used the LQG-bounce critical-density window  $\rho_{\text{crit}}/\rho_{\text{PI}} \simeq 0.27\text{--}0.41$  from the Ashtekar–Singh effective-LQC status report [11]. The quadratic scaling in  $\rho_{\text{crit}}/\rho_{\text{PI}}$  is adopted here as an order-of-magnitude ceiling *ansatz* (not derived in this paper); Barrier 12 is correspondingly used only as a global ceiling, not as a precise bound. This total bounce-epoch GW energy-density fraction is not directly comparable to the present-day PTA spectral-density measurement  $\Omega_{\text{GW}}(f_{\text{nHz}}) \sim 10^{-9}$ , which differs by both (i) redshift / cosmological-dilution factors from the bounce epoch to today, and (ii) the integration over frequency to recover a spectral density at a given band. A quantitative comparison to NANOGrav requires propagating the bounce GW spectrum through the transfer function to the nHz band, which is deferred to a forthcoming bounce-GW dedicated paper (deferred); for the present analysis, Barrier 12 closes as a global energy-density-fraction ceiling rather than a direct NANOGrav exclusion.

### M. Barrier 13: Gravitational Democracy (Branches N/O)

Torsion couples democratically to all spin-1/2 matter species. It cannot preferentially source baryogenesis, dark-matter relics, or vacuum transitions without invoking species-dependent non-minimal couplings absent in the minimal framework.

### N. Barrier 14: Perturbation Transparency

For canonical scalar field matter, torsion vanishes at all perturbation orders; the Holst sector decouples from all scalar/tensor perturbation observables. This is elaborated in Sec. X: the scalar-sector proof is in Sec. XB and the explicit Holst-term verification at all perturbation orders is in Sec. XD.

## X. THE PERTURBATION-TRANSPARENCY RESULT

### A. Statement

In minimal ECH gravity with canonical scalar field matter, the Holst term is dynamically inert for both scalar and tensor perturbations at all orders. The Barbero-Immirzi parameter  $\gamma$  is invisible in all perturbation observables. This generalizes Hehl *et al.* (1976) [12] to the Holst sector and to all perturbation orders. The restriction to the torsion-free ( $T = 0$ ) branch is not an additional assumption but a *consequence* of the matter content: canonical scalar matter carries zero spin density (Step 1 below), hence in Einstein–Cartan theory sources no torsion (Step 2), and the connection reduces to Levi-Civita identically at all perturbation orders. We emphasize that the “all orders” statement does *not* rest on an order-by-order component expansion of the linearized Holst/Cartan action: it follows because Step 2 is an *algebraic* (non-derivative) Cartan constraint, so  $T = 0$  holds exactly and perturbatively unmodified, and Step 4 is a pointwise *identity* (the algebraic Bianchi identity  $R_{\mu[\nu\rho\sigma]} = 0$ , which holds for any torsion-free connection at every field configuration). Because both load-bearing steps are exact identities rather than truncated expansions, no separate order-by-order verification is required; we display the leading (second-order) expansion in Sec. XD only as an explicit check of the identity, not as the origin of the all-orders claim. The propagating-torsion, dynamical-Immirzi-field, fermion-loop, and non-minimal-matter sectors — where  $T \neq 0$  and the result need not hold — are explicitly outside the stated scope; the theorem is a statement about the scalar-matter sector of ECH, which is precisely the Levi-Civita branch, so the  $T = 0$  hypothesis is the theorem’s domain rather than a gap in it.

## B. Proof (Scalar Sector)

1. **Zero spin density.** A canonical scalar field has zero spin density.
2. **Zero torsion.** In Einstein-Cartan theory,  $T^\lambda{}_{\mu\nu} = 8\pi G S^\lambda{}_{\mu\nu} + \dots$ . With  $S = 0$ ,  $T^\lambda{}_{\mu\nu} = 0$  at all perturbation orders.
3. **Connection reduces to Levi-Civita.**  $\Gamma^\lambda{}_{\mu\nu} = \overset{\circ}{\Gamma}^\lambda{}_{\mu\nu}$ .
4. **Holst term vanishes by the first Bianchi identity.** The Holst term evaluated with the Levi-Civita connection gives  $\frac{1}{2}\epsilon^{\mu\nu\rho\sigma}R_{\mu\nu\rho\sigma}(\overset{\circ}{\Gamma})$ , which on a torsion-free connection *vanishes identically* by the first (algebraic) Bianchi identity  $R_{\mu[\nu\rho\sigma]} = 0$ : the cyclic-sum identity  $R_{\mu\nu\rho\sigma} + R_{\mu\rho\sigma\nu} + R_{\mu\sigma\nu\rho} = 0$  contracted with the totally antisymmetric  $\epsilon^{\mu\nu\rho\sigma}$  leaves no non-trivial component. The algebraic Bianchi identity  $R_{\mu[\nu\rho\sigma]} = 0$  holds for any torsionless connection, independently of metric compatibility; non-metricity does not invalidate the identity provided  $T = 0$ . The Holst dual contraction is therefore identically zero on the Levi-Civita connection (not merely a boundary term), so it contributes nothing to the action at any order. This Bianchi-vanishing is distinct from the Pontryagin density  $\propto R\tilde{R}$  (a two-curvature topological invariant) — see the explicit verification below.
5. **No equations of motion.** A total derivative contributes nothing to variational equations at all

---


$$\mathcal{R}_H(\overset{\circ}{\Gamma}) \equiv \frac{1}{2}\epsilon^{\mu\nu\rho\sigma}R_{\mu\nu\rho\sigma}(\overset{\circ}{\Gamma}) = 0 \quad (\text{identically, by the first (algebraic) Bianchi identity}). \quad (25)$$

This is the Bianchi-vanishing of the Holst dual contraction on a torsion-free connection: in differential-form language  $e^I \wedge e^J \wedge R_{IJ} = -\text{NY} + T^I \wedge T_I$ , where  $\text{NY} \equiv d(e_I \wedge T^I)$  is the exact Nieh–Yan density (a total derivative of the torsion boundary term), and both pieces vanish at  $T = 0$  *pointwise* — not merely up to a boundary term:  $\text{NY}|_{T=0} = d(0) = 0$  and  $T^I \wedge T_I|_{T=0} = 0$ , with the Bianchi cancellation above being the operative reason the Holst dual vanishes pointwise in the torsionless sector.<sup>7</sup>

---

<sup>7</sup> Explicit decomposition: the Holst integrand satisfies  $e^I \wedge e^J \wedge R_{IJ}(\Gamma) = -d(e_I \wedge T^I) + T^I \wedge T_I$ , i.e.  $e \wedge e \wedge R = -\text{NY} + T \wedge T$ , where  $\text{NY} \equiv d(e_I \wedge T^I)$  is the Nieh–Yan boundary form and  $T^I = de^I + \omega^I{}_J \wedge e^J$  is the torsion two-form. At  $T = 0$  (canonical scalar matter, torsion-free branch), both terms vanish *pointwise*:  $\text{NY}|_{T=0} = d(0) = 0$  and  $T^I \wedge T_I|_{T=0} = 0$ . The Holst dual contraction is therefore identically zero on the Levi-Civita connection, not merely a total derivative.

orders. (This step is logically distinct from the pointwise Bianchi-vanishing of the previous step: at  $T = 0$  the stronger pointwise vanishing already applies; the total-derivative statement covers the residual Nieh–Yan boundary term  $d(e_I \wedge T^I)$  at nonzero torsion.)

## C. Extension to Tensor Sector

The same five steps apply to tensor perturbations. With  $T = 0$ , the tensor perturbation equation:

$$h''_{ij} + 2\mathcal{H}h'_{ij} + k^2 h_{ij} = 0 \quad (23)$$

(primes denote derivatives with respect to conformal time  $\eta$ , and  $\mathcal{H} \equiv a'/a$  is the conformal Hubble rate; Fourier modes  $h_{ij}(\mathbf{k}, \eta)$  follow the standard  $e^{i\mathbf{k}\cdot\mathbf{x}}$  convention for the transverse-traceless amplitude; in cosmic time, using  $dt = a d\eta$ , the equivalent form is  $\dot{h}_{ij} + 3Hh_{ij} + (k^2/a^2)h_{ij} = 0$ ) has no parity-dependent modifications. Left and right circular polarization modes propagate identically:

$$v_R(k, \eta) = v_L(k, \eta) \quad \Rightarrow \quad \Delta v = 0 \quad (\text{identically}). \quad (24)$$

No GW birefringence, no tensor chirality, no  $TB/EB$  CMB parity violation from the ECH mechanism.

## D. Explicit Verification: The Holst Term in Perturbation Theory

Expanding to second order, the Holst dual evaluates on the Levi-Civita connection ( $T = 0$ ) as:

---

*This must be carefully distinguished from the Pontryagin density  $\frac{1}{4}\epsilon^{\mu\nu\rho\sigma}R_{\mu\nu}{}^{\alpha\beta}R_{\rho\sigma\alpha\beta} \propto R\tilde{R}$ , which involves two curvature tensors and is a separate true topological invariant — non-zero pointwise and a total derivative even in the presence of torsion. The Holst dual contraction has only one curvature and is therefore not the Pontryagin density; on  $T = 0$  it is identically zero by Bianchi, contributing nothing to the variational equations of motion at any perturbation order. In particular, the cubic action for  $\zeta$  (which determines the bispectrum) receives zero contribution from the Holst term. The bispectrum is therefore identical to the standard GR result.*

## E. What Would Break the Transparency

The transparency result fails if: (1) matter includes fermions with nonzero spin density; (2) the gravitational action includes kinetic terms for torsion (Poincaré gauge

theory); (3) non-minimal derivative couplings between the Holst sector and matter are introduced.

### F. Implications

The perturbation-transparency result establishes a clean dichotomy:

- *Perturbation observables* ( $C_\ell^{TT}$ ,  $C_\ell^{EE}$ ,  $P_k$ , bispectrum): Identical to standard GR. No ECH modifications at any order.
- *Nonperturbative parity channels* (ALP birefringence, primordial GW chirality): Parity-sensitive channels (model-dependent tests of  $\gamma_{\text{BI}}$  only under a derived  $\gamma_{\text{BI}}$ -dependent photon or tensor-parity coupling).

### G. Discrimination Among Bouncing Cosmologies

The matter bounce prediction  $f_{\text{NL}} = -35/8$  is the strongest discriminator: it provides  $\sigma(f_{\text{NL}}) \approx 0.7$  (*ideal-survey* Fisher) to  $\sigma(f_{\text{NL}}) \approx 1.0$  (*degraded with GR-projection + photo-z systematics*) from SPHEREx, yielding 2.6–5 $\sigma$  model separation. NANOGrav model comparison:  $\gamma_{\text{PTA}} = 2.567 \pm 0.382$  from real-KDE reanalysis of the 15-yr free-spectrum data (GPU MCMC, in preparation [48]; here  $\gamma_{\text{PTA}}$  is the GWB power-law spectral index, distinct from the Barbero-Immirzi parameter  $\gamma$  defined in Eq. 1). The matter-bounce prediction  $\gamma_{\text{PTA}} = 3.0$  sits at +1.13 $\sigma$  above the posterior mean, consistent with the data within standard frequentist tolerance. The current real-KDE GPU MCMC gives  $\gamma_{\text{PTA}} = 2.567 \pm 0.382$  (Paper III § 6 [48]).

## XI. THE HYBRID DARK-ENERGY LOOPHOLE

We considered appending late-time dynamical dark-energy freedom (CPL  $w_0w_a$ ) to the bounce model, explored across 7 disguised forms: (1) direct  $w_0w_a$  addition, (2) quintessence scalar with bounce initial conditions, (3) curvaton-derived late-time potential, (4) vacuum energy from cyclic boundary conditions, (5) torsion-induced effective  $w(z)$ , (6) Holst-term residual as effective DE, (7) ALP rolling as late-time acceleration.

All 7 forms were assessed at the theoretical level only: adding  $w_0w_a$  to a bounce model produces (at the level of the theoretical fit-improvement calculation) the same fit-improvement structure as adding  $w_0w_a$  to  $\Lambda$ CDM, with no additional theoretical content from the bounce. We emphasize that this is a theoretical-structure conclusion, *not* a quantitative posterior-preference rejection: the dedicated DESI DR2 + Planck NPIPE + Pantheon+ + DES-SN5YR cobaya chain with the free  $w_0w_a$  extension required to quantitatively test these 7 forms is described in Paper I(b) (in preparation [6]) Table IV row “DESI DR2 w0wa (new)” and has not yet converged to

the standard publication-quality target  $\hat{R}-1 < 10^{-2}$  (see Paper I(b) [6] Sec. V for the chain status). The present program’s MCMC analysis uses stock CAMB with  $\Delta N_{\text{eff}}$  only and hosts zero free- $w_0w_a$  samples; the qualitative theoretical conclusion that ECH cannot generate  $w_0w_a$  as an additional output beyond what  $\Lambda$ CDM +  $w_0w_a$  already accommodates therefore stands as a *theoretical structural observation* rather than as a posterior-preference quantitative rejection. A quantitative rejection (or confirmation) is gated on convergence of the dedicated Paper I(b) chain.

## XII. DISCUSSION

### A. The Inflationary Suppression Factor

The constant contribution to  $\Lambda_{\text{eff}}$  emerges from the interplay between the parity-odd spin-torsion interaction and inflationary dilution:

$$\Xi \equiv \left[ \frac{\alpha}{M} M_{\text{Pl}} \right] \times \mathcal{D}_{\text{inf}}, \quad (26)$$

a dimensionless quantity of order the observed hierarchy  $\rho_\Lambda^{\text{obs}}/M_{\text{Pl}}^4 \sim 10^{-122}$ , decomposed as  $[(\alpha/M)M_{\text{Pl}}] \times \mathcal{D}_{\text{inf}} \sim 10^{-2} \times \mathcal{D}_{\text{inf}}$ ; with the fitted value  $N_{\text{tot}} \approx 92$  (Sec. II C 1), Eq. (11) gives  $\mathcal{D}_{\text{inf}} = e^{-3N_{\text{tot}}}(T_{\text{reh}}/M_{\text{GUT}})^{3/2} \approx e^{-276} \times 0.03 \approx 4 \times 10^{-122}$ , so that  $\Xi \sim 4 \times 10^{-124}$  to order of magnitude. We stress that  $N_{\text{tot}}$  is a fitted parameter (Sec. II C 1), tuned so that  $\Xi$  reproduces  $\rho_\Lambda^{\text{obs}}/M_{\text{Pl}}^4$ ; the order-of-magnitude residual between the raw ansatz product and the target hierarchy is exactly the  $\Delta N_{\text{tot}} \approx 4$  sensitivity discussed there, not an independent prediction.

*Physical-versus-mathematical scope of  $\mathcal{D}_{\text{inf}}$ .*—While  $N_{\text{tot}}$  controls the mathematical  $e^{-3N_{\text{tot}}}$  ansatz used in the above bookkeeping, the *physical* reheating thermal-reset barrier (supporting B14; see Sec. II C 1, “Reheating thermal-reset barrier” paragraph) already closes the bounce-era-memory dilution channel: non-propagating torsion is sourced algebraically by the instantaneous axial-current expectation value, and the post-reheating coherent axial component is washed to zero by chirality-flipping and depolarizing thermal interactions that equilibrate the axial-current expectation value. The  $\mathcal{D}_{\text{inf}}$  exponential is therefore mathematical scaffolding for an order-of-magnitude parameterization of a hypothetical un-reset channel rather than a physically operative dilution mechanism; the entries in this section are retained as parameterization-of-fine-tuning diagnostics, not as a viable dynamical channel.

The “fine-tuning reduction from  $10^{122}$  to  $10^5$ ” is a reparameterization as sensitivity to  $N_{\text{tot}}$  (the total number of inflationary  $e$ -folds), not a resolution of the cosmological constant problem. The exponential  $\mathcal{D}_{\text{inf}} \propto e^{-3N_{\text{tot}}}$  structure of Eq. (11) makes  $N_{\text{tot}}$  the single controlling parameter analytically: the residual  $10^5$  tracks  $e^{+3\Delta N_{\text{tot}}}$  for  $\Delta N_{\text{tot}} \approx 4$   $e$ -folds (the dilution ansatz  $\mathcal{D}_{\text{inf}} \propto e^{-3N_{\text{tot}}}$

TABLE V. Discrimination among bouncing cosmologies and inflation by observable channels. The symbol  $\checkmark$  (check) denotes the mechanism produces the prediction;  $\times$  denotes it does not; “—” denotes not applicable or not computed.

Model	$f_{\text{NL}} = -35/8$	ALP birefringence	$\gamma_{\text{PTA}}$ (real-KDE)	$w_0 w_a$ DESI
Matter bounce (any host; not ECH-specific)	$\checkmark$	(spectator)	$\checkmark$	not tested <sup>‡</sup>
Slow-roll inflation	$\times$ ( $f_{\text{NL}} \approx 0.015$ )	(spectator)	$\times$	not tested <sup>‡</sup>
Quintom-B	$\times$	(spectator)	—	consistent <sup>†</sup>
Cuscudon bounce	$\times$ ( $f_{\text{NL}} \approx 0$ )	(spectator)	—	not tested <sup>‡</sup>
Ekpyrotic	$\times$ ( $f_{\text{NL}} \sim -5$ )	(spectator)	—	not tested <sup>‡</sup>

<sup>†</sup>Quintom-B can in principle accommodate the DESI  $w_0 w_a$  evidence; the MCMC analysis in Paper I(b) (in preparation [6]) was not extended to the  $w_0 w_a$  parameter space, so this row is reported as “consistent at the model level” rather than a posterior-preference  $\checkmark$ .

<sup>‡</sup>A free- $w_0 w_a$  posterior analysis was not completed for the present paper; no posterior-preference claim is made for or against the DESI  $w_0 w_a$  evidence on the basis of the present table. The frozen MCMC posteriors hosted in Paper I(b) cover three  $\Lambda\text{CDM} + \Delta N_{\text{eff}}$  dataset combinations only, and the asymmetry between the Quintom-B accommodation row and the others is one of theoretical accommodation, not of fit quality measured in this program.

implies the fine-tuning score  $\propto 1/\mathcal{D}_{\text{inf}} \propto e^{+3N_{\text{tot}}}$ , so the *score* rescales as  $e^{+3\Delta N_{\text{tot}}}$  when  $N_{\text{tot}}$  is shifted by  $\Delta N_{\text{tot}}$ , while the order-unity prefactors enter at most logarithmically. We emphasize that the  $(T_{\text{reh}}/M_{\text{GUT}})^{3/2}$  prefactor itself is matched at the order-of-magnitude level rather than calculated from a thermal partition function (Sec. II C 1); the  $10^5$  residual therefore inherits the same order-of-magnitude status, and the “reduction from  $10^{122}$  to  $10^5$ ” should be read as a qualitative dimensional rearrangement rather than a quantitative bookkeeping result.

*Caveat on the  $(T_{\text{reh}}/M_{\text{GUT}})^{3/2}$  prefactor.*—The  $(T_{\text{reh}}/M_{\text{GUT}})^{3/2}$  prefactor used here is the dimensional-analysis-aesthetic estimate from naive scaling of the matter-bounce effective theory; a first-principles derivation requires the full bounce-junction matching that lies outside the scope of this paper. The  $N_{\text{tot}} \approx 92$   $e$ -fold structural-tension result therefore carries an order-of-magnitude uncertainty inherited from this prefactor. The sign and qualitative conclusion—that the matter-bounce mechanism cannot generate dark energy without re-importing cosmological-constant fine-tuning—survives the OOM uncertainty, because the surplus required to close the gap is  $\sim 14$   $e$ -folds (the fine-tuning-gap surplus of the present order-of-magnitude argument; this is a different quantity from — and smaller than — the  $N_{\text{tot}} - N_{\text{exit}} \approx 32$   $e$ -fold signal-erasure differential of Sec. XIV D, so the conclusion holds a fortiori for the larger differential), whereas the quasi-dust  $\varepsilon$ -correction-driven prefactor adjustment (the  $\mathcal{O}(\varepsilon - 3/2)$  equation-of-state correction of the matter-bounce contraction,  $\varepsilon = 3(1 + w)/2$ , defined in the companion  $f_{\text{NL}}$  forecast paper) is  $\lesssim 1$   $e$ -fold. A rigorous derivation of the prefactor from the bounce-junction matching is deferred to future work and would not change the structural-tension verdict.

## B. Theoretical Implications

Four routes to deriving  $\rho_\Lambda$  with  $w = -1$  from first principles were tested: (i) NJL condensate, (ii) one-loop fermion effective action, (iii) dynamical Immirzi field, (iv) parity-sensitive CMB phenomenology. R1 closes via the standard published derivation; R2–R3 close at the amplitude level under explicitly-labeled scaling/ansatz assumptions; R4 closes at the naturalness level. The condensate route is closed at the amplitude level (Sec. IV A): the NJL contact term is Planck-suppressed ( $\rho_{\text{NJL}} \sim n_\psi^2/M_{\text{Pl}}^2 \approx 4 \times 10^{-81} \text{eV}^4$ ,  $\sim 70$  orders below  $\rho_\Lambda$ ) and parity-even. The one-loop route is amplitude-closed under the explicitly-labeled EFT scaling ansatz. The dynamical Immirzi field reduces to a standard axion-like particle with  $w = +1$  (stiff matter). The parity assessment finds no photon coupling in the minimal framework: the parity-odd one-loop operator of Sec. IV D couples the Nieh–Yan pseudoscalar to the fermion axial current,  $\partial_\mu \vartheta_{\text{NY}} J^{5\mu}$ , with no  $F\tilde{F}$  term, so a CMB-birefringence amplitude only arises through the model-dependent  $\partial_\mu J^{5\mu} \supset (\alpha_{\text{em}}/4\pi)F\tilde{F}$  chiral-anomaly chain, treated as an amplitude-budget bound rather than a derived prediction (Sec. IV D footnote).

*Spectator-ALP birefringence.*—A spectator ALP with  $f_a \sim M_{\text{Pl}}$ ,  $m \sim H_0$  is consistent with the published WMAP+Planck cosmological-birefringence signal ( $\beta = 0.342^\circ \pm 0.094^\circ$ ,  $\sim 3.6\sigma$  from  $\beta = 0$ , Eskilt & Komatsu [4]; an independent ACT DR6 follow-up [5] reports  $\beta = 0.215^\circ \pm 0.074^\circ$  at  $\sim 2.9\sigma$ ) at  $f_a \sim M_{\text{Pl}}$  and  $\theta_i \sim \mathcal{O}(1)$  without additional ALP-naturalness fine-tuning beyond the  $m_\theta \sim H_0$  ultralight-mass tuning admitted in §IV F (a cosmological-constant-class tuning rather than an ALP-specific one — the same point is also surfaced in the structural-tension discussion of §XIV D and §XI). The same  $\beta \approx 0.27^\circ$  prediction arises in standard GR with an identical ALP; it is not a distinctive ECH prediction. Full ALP MCMC parameter fitting (9,720 accepted samples,  $\hat{R} - 1 < 0.01$ ) and LiteBIRD forecast are in Paper I(b) (in preparation [6]).

### XIII. SURVIVING ECH-INDEPENDENT CLASS TESTS

Despite the channel-level closure of the four enumerated minimal-ECH dark-energy routes (13 mechanism-class constraints under the stated assumptions), the broader bounce-cosmology program retains two fully testable ECH-independent class-level predictions:

(1) **Matter-bounce**  $f_{\text{NL}} = -35/8$ .—The matter-dominated contracting phase of a *scalar-only*  $w = 0$  matter-bounce (the bounce-class observable, not specific to ECH) produces a minimally-parameterized local-type non-Gaussianity  $f_{\text{NL}} = -35/8$  [1]. This value holds within the scalar-only  $w = 0$  matter-bounce class under Assumption (f) of Paper II [2] (negligible fermion energy density during the contracting phase, so the Hehl–Datta–Mercuri four-fermion contact term does not source torsion or reactivate the Barbero–Immirzi parameter in the scalar cubic action); it is *not* a fully mechanism-independent prediction across the broader bouncing-cosmology landscape (ekpyrotic, Cuscuton-type, quintom matter-bounce variants, models with significant fermion sectors during contraction, or  $w \neq 0$  contracting equations of state all carry distinct predictions). Within the scalar-only  $w = 0$  class the value is class-level (not specific to ECH); it is *not* a distinctive ECH prediction in any case. The full multi-bin Fisher forecast, SPHEREx parameter sensitivity (bispectrum-only  $\sigma(f_{\text{NL}}) \approx 0.7$  from Heinrich *et al.* 2024, leading to 2.6–5 $\sigma$  post-systematic-budget significance), and anomaly-optimized multi-tracer strategy are in Paper II [2]; the present paper does not perform an independent SPHEREx Fisher computation and the 2.6–5 $\sigma$  figure is reported here only as a cross-reference. SPHEREx first science data  $\sim 2028$ .

(2) **Spectator-ALP birefringence**  $\beta \approx 0.27^\circ$ .—We present this as a **consistency check**, not as a prediction: the parity-odd coefficient  $\alpha/M$  is fitted, not derived from first principles, and an ALP with  $f_a \sim M_{\text{Pl}}$ ,  $m \sim H_0$  chosen to land near the observed signal is by construction inside its  $1\sigma$  band. The *quantitative* prediction is the signature structure (achromatic uniform rotation, the *EB/TB* pattern, and consistency across frequencies and experiments) rather than the central value of  $\beta$ . The same ALP setup arises identically in standard GR with the same parameters, so this is not a distinctive ECH prediction. LiteBIRD ( $\sigma(\beta) \approx 0.03^\circ$ , early 2030s) will either confirm a non-zero  $\beta$  at high significance or exclude this uniform spectator-ALP benchmark ( $f_a \sim M_{\text{Pl}}$ ,  $m \sim H_0$ ) as the explanation of the current WMAP+Planck central value; either outcome is informative independent of ECH.

**Structural incompatibility.**—An open constraint is the incompatibility between the dark-energy suppression mechanism ( $N_{\text{tot}} \approx 92$  *e*-folds required) and the  $f_{\text{NL}} = -35/8$  prediction (*definitively* erased once  $N_{\text{tot}} - N_{\text{exit}} \gtrsim N_{\text{coh}} \sim \mathcal{O}(\text{few})$  at SPHEREx-relevant scales; the SPHEREx accessible wavenumbers  $k \sim 10^{-4}$ – $10^{-1}$   $h/\text{Mpc}$  map to bounce-era *physical* scales  $k_{\text{bounce}}^{\text{phys}} \sim$

$k_{\text{SPHEREx}} e^{N_{\text{tot}} - N_{\text{exit}}} \sim e^{32} k_{\text{SPHEREx}}$  at  $N_{\text{tot}} \sim 92$  and  $N_{\text{exit}} \sim 60$  (the relative *e*-fold differential between bounce and CMB horizon-exit; comoving wavenumbers  $k$  are constant by definition and only physical scales scale with  $a^{-1} \propto e^{-N}$ ), deep inside the inflationary subhorizon regime where the surviving bispectrum signal is purely vacuum-inflationary, not matter-bounce contraction-mode). This is detailed in Sec. XIV D. The correct interpretation is that bounce cosmology (as a broad class) and the ECH-specific dark-energy ansatz are *independent observational programs*; SPHEREx tests the former, LiteBIRD tests a related spectator field, and the ECH dark-energy ansatz remains a phenomenological parameterization.

### XIV. LIMITATIONS AND FUTURE DIRECTIONS

#### A. Current Limitations

##### 1. Theoretical

- *Phenomenological  $\alpha/M$* : Not derived from first principles; the one-loop estimate motivates existence and order of magnitude, but the finite part depends on the  $\gamma_5$  regularization scheme (Sec. II A 2, [20]).
- *Simplified inflationary epoch*: Non-minimal couplings during inflation could alter the dilution factor.
- *Bounce-to-inflation transition*: Mechanism for transitioning from quantum bounce to slow-roll inflation is not fully modeled.

##### 2. Observational

- *Galaxy spin*: Null confirmed at the dipole level (Paper IV [23]), consistent with the  $> 100$ -orders-of-magnitude underprediction by the ECH coupling.
- *MCMC proxy*: Stock CAMB with  $\Delta N_{\text{eff}}$  is a phenomenological proxy, not a bespoke spin-torsion Boltzmann module. Full MCMC details and convergence diagnostics are in Paper I(b) (in preparation [6]).

#### B. Robustness to Galaxy Spin Null Results

The galaxy spin channel is a confirmed null at the dipole level (full quantitative chirality results in Paper IV [23]), *consistent* with the framework (which underpredicts  $A_0$  by  $> 100$  orders of magnitude). The parity-violation case rests entirely on CMB birefringence from the published WMAP+Planck Eskilt & Komatsu measurement [4] with an independent ACT DR6 follow-up (Diego-Palazuelos & Komatsu [5]).

### C. Discriminating Observational Channels

*LSST Era (2025–2035)*:  $10^9$  spiral galaxies to  $z \sim 1$ , tomographic analysis in 20+ redshift bins. *CMB Experiments*: LiteBIRD, CMB-S4, and future concepts (PICO, CMB-HD). *Bounce cosmology beyond ECH*: Papanikolaou *et al.* [47] showed that asymmetric matter bounces can produce asteroid-mass PBHs as dark matter candidates with induced GWs detectable by LISA and Einstein Telescope.

### D. Structural Tension: Dark Energy vs. Bounce

$$f_{\text{NL}}$$

The dark-energy suppression mechanism, if minimal ECH were to source dark energy through one of the four channels enumerated in Sec. IV, would require  $N_{\text{tot}} \approx 92$  post-bounce  $e$ -folds; the matter-bounce  $f_{\text{NL}} = -35/8$  would be *definitively* erased once the bounce-vs-CMB-horizon-exit differential  $N_{\text{tot}} - N_{\text{exit}} \gtrsim N_{\text{coh}} \sim \mathcal{O}(\text{few})$  (where  $N_{\text{coh}}$  is the contraction-phase coherence window of the matter-bounce mode functions), since the SPHEREx accessible wavenumbers  $k \sim 10^{-4} - 10^{-1} h/\text{Mpc}$  are pushed deep inside the inflationary subhorizon (bounce-era *physical* scales  $k_{\text{bounce}}^{\text{phys}} \sim k_{\text{SPHEREx}}^{\text{phys}} e^{N_{\text{tot}} - N_{\text{exit}}} \sim e^{32} k_{\text{SPHEREx}}^{\text{phys}}$  at  $N_{\text{tot}} \sim 92$ ,  $N_{\text{exit}} \sim 60$ ; comoving wavenumbers  $k$  are constant by definition; the rigorous bounce-vs-SPHEREx scale ratio is the *physical* scaling above with  $k_{\text{bounce}}^{\text{phys}}/k_{\text{SPHEREx}}^{\text{phys}} \sim e^{32}$ ) and the surviving bispectrum signal becomes purely vacuum-inflationary rather than matter-bounce contraction-mode. The mode-history reasoning underlying this “erased by  $N_{\text{tot}} - N_{\text{exit}} \gtrsim N_{\text{coh}}$ ” statement is the standard mode-transfer ledger across four epochs: (i) in the contracting matter-bounce phase the  $f_{\text{NL}} = -35/8$  signal is generated in the contraction-era cubic action at comoving wavenumbers  $k_{\text{gen}}$  that exited the contracting-phase horizon at horizon-crossing time  $t_{\text{cross}}^{\text{gen}}$ , (ii) at the bounce the modes are mapped onto the expanding branch with their comoving  $k$  preserved (the bounce is mode-conserving for adiabatic perturbations in a non-singular bounce with a finite minimum scale factor; only physical  $k_{\text{phys}} = k/a$  scale with  $a$ ), (iii) inflation then redshifts the corresponding physical scale by  $a_{\text{reh}}/a_{\text{bounce}} = e^{N_{\text{tot}}}$ , so a SPHEREx-observable comoving  $k$  today corresponds to a bounce-era physical scale  $k_{\text{bounce}}^{\text{phys}} = k_{\text{obs}} e^{N_{\text{tot}} - N_{\text{exit}}}$  with  $N_{\text{exit}} \sim 60$  the standard CMB horizon-exit  $e$ -fold count, and (iv) reheating preserves comoving  $k$ . The differential  $e^{N_{\text{tot}} - N_{\text{exit}}} \sim e^{32}$  pushes the SPHEREx-relevant modes to bounce-era *physical* scales  $e^{32} \times k_{\text{SPHEREx}}^{\text{phys}}$ , which lie deep inside the inflationary subhorizon regime at the bounce time; the surviving observable bispectrum is dominated by the vacuum-inflationary mode functions amplified between  $t_{\text{cross}}^{\text{gen}}$  and today, not by the matter-bounce contraction-mode functions that sourced  $f_{\text{NL}} = -35/8$ . A fully quan-

titative transfer function tracking the suppression coefficient across the four epochs (vacuum-inflationary amplification vs matter-bounce contraction-mode survival probability) is beyond the scope of this no-go and is reserved for a companion forecast (Paper II [2]); the present argument is the scale-history bookkeeping, not the transfer-function calculation. This tension is presented here as a *robustness check* on the four-route amplitude-level no-go of Sec. IV and the 14-barrier closure of Sec. IX, not as a co-equal closure mechanism: the no-go has already closed the four amplitude routes by which minimal ECH could source dark energy, so the structural-tension argument has nothing remaining to bind against at the route-amplitude level and reads instead as an independent consistency check from the surviving matter-bounce science case (Sec. XIII). DESI DR2 evidence for equation-of-state crossing at  $3.1 - 4.2\sigma$  [10] motivates dynamical-dark-energy parameterizations (including  $w_0 w_a$  and quintom-class scenarios) that can unify bounce and dark energy through mechanisms outside the ECH minimal-route catalog; these non-minimal-ECH mechanisms are not addressed by the present no-go.

### E. Channel-Level Closure

The 13 mechanism-class structural constraints (14 historical catalog entries) catalog the four enumerated minimal-ECH dark-energy channels and close each under the stated assumptions (Scope and Limitations paragraph, Sec. I). The surviving science case rests on the matter-bounce  $f_{\text{NL}}$  prediction, which is compatible with the ECH framework but not derived from it (Sec. XIII).

## XV. CONCLUSIONS

We have investigated whether Einstein-Cartan-Holst spin-torsion gravity can produce late-time dark energy or distinctive cosmological signatures. The answer is a channel-level closure: under the stated assumptions, the 14 mechanism-class constraints (Table IV; B8 is the observational consequence of the perturbation-transparency result B14 and is retained for historical mechanism-class completeness) constrain each of the four enumerated minimal-ECH dark-energy routes. Route R1 closes at the amplitude level via a standard torsion-elimination derivation; Routes R2–R3 close at the amplitude level under explicitly-labeled scaling ansätze; route R4 is closed instead by a naturalness / cosmological-constant fine-tuning objection (Sec. IV F) rather than by an amplitude mismatch, because a free-coupling spectator-ALP fit can simultaneously reproduce  $\beta_{\text{obs}}$  and  $\rho_{\Lambda}$  only at  $m_{\theta} \sim H_0$ , re-importing the CC problem rather than solving it.

*Central result: perturbation transparency.*—For canonical scalar field matter, the Holst sector decouples completely from all scalar and tensor perturbation equations

of motion (Sec. X). Torsion vanishes at all perturbation orders; the Holst dual contraction  $e^{\mu\nu\rho\sigma}R_{\mu\nu\rho\sigma}$  vanishes identically on the Levi-Civita connection ( $T = 0$ ) by the first (algebraic) Bianchi identity  $R_{\mu[\nu\rho\sigma]} = 0$  (distinct from — and not equal to — the Pontryagin density  $\propto R\tilde{R}$ , which involves two curvatures and is a separate topological invariant; see Sec. X footnote for the  $e\wedge e\wedge R = -NY + T\wedge T$  decomposition). This is a positive structural result: it identifies the nonperturbative parity-violating channels (ALP birefringence, primordial GWs) as parity-sensitive channels (model-dependent tests of  $\gamma_{\text{BI}}$  only under a derived  $\gamma_{\text{BI}}$ -dependent photon or tensor-parity coupling).

*The 13 mechanism-class constraints (14 historical catalog entries).*—Systematic analysis across 7 foundations (A–G) and 6 observational branches (H, J, L, M, N, O) established 14 mechanism-class constraints (one of which, B8, is the observational consequence of the perturbation-transparency result B14 and is retained in the catalog for historical mechanism-class completeness) on the minimal ECH dark-energy parameter space (Sec. IX). These constraints are ECH-specific: other bouncing cosmologies (notably quintom scenarios) can in principle unify bounce with late-time dark energy through mechanisms outside the ECH minimal-route catalog.

*Surviving tests.*—Two ECH-independent class-level predictions of the broader bounce/ALP landscape survive the channel-level closure and are testable:

1.  $f_{\text{NL}} = -35/8$  (matter-bounce class): SPHEREx tests at 2.6–5 $\sigma$  realistic significance by  $\sim 2028$ , discriminating from inflation ( $f_{\text{NL}} \approx 0.015$ ) and the Cuscuton bounce ( $f_{\text{NL}} \approx 0$ ).
2. Spectator-ALP birefringence  $\beta \approx 0.27^\circ$ : LiteBIRD ( $\sigma(\beta) \approx 0.03^\circ$ , early 2030s) detects non-zero  $\beta$  at  $\sim 9\sigma$  (a  $0.27^\circ/0.03^\circ$  overall sensitivity number). The relevant model-discrimination test, however, is the differential against the prior central value  $\beta_{\text{obs}} = 0.342^\circ \pm 0.094^\circ$ : LiteBIRD will distinguish the spectator-ALP-derived  $0.27^\circ$  from the observed  $0.342^\circ$  at  $|0.342 - 0.27|/\sqrt{0.03^2 + 0.094^2} \approx 0.072^\circ/0.0987^\circ \approx 0.73\sigma$  (this is a heuristic combining the current Planck uncertainty  $\pm 0.094^\circ$  and the projected LiteBIRD uncertainty  $\pm 0.03^\circ$  in quadrature; the test is dominated by the current Planck term, so under the current Planck error alone the separation is  $|0.342 - 0.27|/0.094^\circ \approx 0.77\sigma$ ; the  $0.73\sigma$  figure is therefore not a well-defined joint-posterior significance but a rough lower bound), NOT at the naive  $|0.342 - 0.27|/0.03 = 2.4\sigma$  which would ignore the prior measurement’s  $\pm 0.094^\circ$  uncertainty; in other words LiteBIRD’s  $\sigma(\beta) = 0.03^\circ$  will not by itself separate the spectator-ALP value from the current WMAP+Planck birefringence central value in a model-discrimination test (a future tightening of the observational central value’s uncertainty below  $\sim 0.05^\circ$  would be needed for LiteBIRD-vs-current-central tension to cross  $1\sigma$ ). The two numbers correspond to distinct null hypotheses (zero vs.

WMAP+Planck-central); the  $\sim 9\sigma$  test will not by itself separate the spectator-ALP class from generic-ALP fits to the observed signal.

Neither is a distinctive ECH prediction; both are shared with other UV completions.

*Known limitations.*—This work does not derive the IR effective vacuum term from first principles:  $w = -1$  is assumed, not derived; the birefringence prediction lacks a derived photon-torsion coupling;  $\alpha/M$  is a phenomenological parameter; and the MCMC uses stock CAMB (not a bespoke torsion-modified Boltzmann code). Full MCMC diagnostics, ALP parameter fitting, and NaMaster pipeline validation are in Paper I(b) (in preparation [6]).

*Forward.*—The program continues with direct tests of the bounce framework: SPHEREx  $f_{\text{NL}}$  forecast (Paper II [2]), multi-survey anomaly catalog including the NANOGrav 15-yr free-spectrum real-KDE GPU MCMC reanalysis used here for  $\gamma_{\text{PTA}}$  (Paper III [48]), and galaxy chirality catalog (Paper IV [23]).

## Data and Code Availability

Minimal-ECH structural calculations, Cobaya YAML configurations, galaxy-spin pipeline code, and the implementation map are publicly available at:

<https://github.com/Hubify-Projects/bigbounce/tree/main/reproducibility>

Code and data are available at the repository above; a Zenodo-archived release will pin all artifacts to the submitted-version snapshot. The frozen MCMC chains backing the cosmology tables are committed in the bundle (under `reproducibility/cosmology/frozen/`); fresh re-verification chains must be regenerated from the supplied Cobaya configurations. The NaMaster pipeline and ALP parameter fitting are documented in companion Paper I(b) [6] and are not duplicated in the present bundle.

## ACKNOWLEDGMENTS

We thank the Planck, CMB-S4, LiteBIRD, LSST, and DESI collaborations for providing the observational foundation for this work. We particularly acknowledge the foundational contributions of Nikodem Poplawski, Simone Mercuri, Laurent Freidel, Djordje Minic, and Tatsuo Takeuchi for their fundamental derivations connecting the Barbero-Immirzi parameter to parity-violating interactions in LQG. We acknowledge Lior Shamir for providing aggregate CW/CCW galaxy spin counts for the  $A(z)$  comparison.

The author acknowledges the use of Claude (Anthropic) as an AI research assistant during systematic barrier-cataloging, perturbation-gate verification, and

manuscript preparation. The author takes sole responsibility for all scientific claims, derivations, numerical results, and bibliographic attributions in this paper. No external funding was received for this research. Computational resources were self-funded (RunPod H200 and H100 instances).

## Appendix A: Complete Parameter Summary

### Appendix B: Dimensional Status of the Parity-Odd Operator

The parity-odd operator (Eq. 6) has off-shell mass dimension +1, not the +4 required for a local Lagrangian density:

$$\begin{aligned} [\alpha/M] &= -1, \quad [\varepsilon^{\mu\nu\rho\sigma} e_\mu^I e_\nu^J \mathcal{F}_{IJ\rho\sigma}] = +2 \\ \implies [\mathcal{L}_{\text{odd}}] &= +1. \end{aligned} \quad (\text{B1})$$

We acknowledge openly that this operator, as written, is not a controlled dimension-+4 EFT operator. Inserting on-shell background curvature factors or a phenomenological “volume-integration-density” factor of  $M_{\text{Pl}}^2$  does not constitute a derivation; the missing powers of mass do not arise from off-shell EFT counting but from *on-shell scaling assumptions* applied to a Planck-scale bounce geometry. We therefore treat the relation

$$\rho_\Lambda^{\text{bounce}} \sim (\alpha/M) M_{\text{Pl}}^5 \sim 10^{-2} M_{\text{Pl}}^4, \quad (\text{B2})$$

as a phenomenological on-shell scaling *ansatz*, not a controlled EFT result. Equivalently: if Eq. (6) is to map to a dimension-+4 local operator without on-shell curvature insertions, the coupling must carry three additional powers of  $M_{\text{Pl}}$  in its coefficient ( $\alpha/M \rightarrow \alpha M_{\text{Pl}}^3/M$ ), promoting the operator to  $\alpha M_{\text{Pl}}^3 \varepsilon e e \mathcal{F}/M$  (which has  $[\alpha/M] + [M_{\text{Pl}}^3] + [\varepsilon e e \mathcal{F}] = -1 + 3 + 2 = +4$  as required for a dimension-+4 local operator). Either reading is a *phenomenological dimensional assignment*, not a derivation; we make that status explicit here.

*Why the ansatz is a conservative bound, not a circular assumption.*—One might worry that adopting Eq. (B2) as an on-shell scaling relation quietly *assumes* the dark-energy mapping it is then used to constrain, making the closure circular. It does not, for three reasons. First, Eq. (B2) is a *conservative upper bound* on the bounce-scale parity-odd density: on-shell evaluation at Planck-scale bounce curvature returns  $\rho_\Lambda^{\text{bounce}} \sim 10^{-2} M_{\text{Pl}}^4$ , within two orders of magnitude of the largest density  $\sim M_{\text{Pl}}^4$  the geometry can support, so no plausible completion of the dimension-+1 operator can *increase* the available amplitude by a factor that matters against the  $\sim 120$ -order hierarchy. Adopting the largest defensible source density makes the required dilution  $\mathcal{D}_{\text{inf}}$  and the  $N_{\text{tot}}$  e-fold budget *harder* to satisfy, not easier; a circular assumption would instead choose the value that delivers the desired conclusion. Second, the closure conclusion is insensitive to the ansatz: whether  $\rho_\Lambda^{\text{bounce}}$  is  $M_{\text{Pl}}^4$ ,

$10^{-2} M_{\text{Pl}}^4$ , or  $10^{-4} M_{\text{Pl}}^4$  shifts  $N_{\text{tot}}$  by  $\mathcal{O}(\text{a few})$ , not by orders of magnitude (the *Sharper dependency statement* below), so the ansatz supplies a bookkeeping placeholder for an amplitude *ceiling*, not the load-bearing content of the barriers. Third, and most directly, the R4 closure that this mapping feeds *makes no positive amplitude derivation at all*: R4 is closed by a naturalness / explanatory-deficit objection (Sec. IV F, Tier II in Table III), not by an amplitude no-go. A charge of circularity requires a claimed derivation of the conclusion from an assumption of that same conclusion; here there is no derived amplitude to be circular about — the ansatz bounds a source density from above, and the closure rests on the observation that minimal ECH supplies neither  $m_\theta \sim H_0$  nor the fitted  $\alpha/M$ . The honest residual limitation is the disclosed one: a controlled dimension-+4 operator-basis derivation is left to a companion treatment, and every R4 / dark-energy claim is stated as conditional on Eq. (B2).

Inflationary dilution ( $\mathcal{D}_{\text{inf}} \sim e^{-3N_{\text{tot}}}$ ) then yields  $\rho_\Lambda = \Xi M_{\text{Pl}}^4$  with  $\Xi = (\alpha/M) M_{\text{Pl}} \mathcal{D}_{\text{inf}}$  under Eq. (B2). The genuine cosmological-constant hierarchy is  $M_{\text{Pl}}^4/\rho_\Lambda^{\text{obs}} \sim 10^{19 \text{ GeV} \times 4}/(10^{-3} \text{ eV})^4 \sim 10^{122}$ , i.e.  $\sim 120$  orders of magnitude (the bounce-scale density entering this hierarchy is  $\rho_{\text{bounce}} \sim M_{\text{Pl}}^4$ , not the local pseudo-density  $\rho_\Lambda^{\text{bounce}} \sim 10^{-2} M_{\text{Pl}}^4$  that Eq. (B2) labels). The dilution factor required to bridge  $\sim 10^{122}$  from  $M_{\text{Pl}}^4$  down to the observed  $\rho_\Lambda$  is  $\mathcal{D}_{\text{inf}} \sim e^{-3N_{\text{tot}}} \sim 10^{-122}$ , giving  $N_{\text{tot}} \approx 122 \ln 10/3 \approx 94$  e-folds (consistent at the  $\sim 2\%$  level with the structural-tension  $N_{\text{tot}} \approx 92$  quoted in Sec. XIV D; the small offset reflects that the structural tension uses Eq. (B2) as the input ansatz, while the genuine  $M_{\text{Pl}}^4$ -to- $\rho_\Lambda^{\text{obs}}$  hierarchy uses the unrescaled Planck density).

*Sharper dependency statement.*—The precise value  $N_{\text{tot}} \approx 92$  vs the independent  $M_{\text{Pl}}^4$ -to- $\rho_\Lambda^{\text{obs}}$  estimate  $N_{\text{tot}} \approx 94$  (a  $\sim 2\%$  offset) *does* depend on the ansatz choice in Eq. (B2); however, the *overall scale separation* between  $\rho_\Lambda^{\text{bounce}}$  and  $\rho_\Lambda^{\text{obs}}$  is  $\sim 120$  orders of magnitude under *any* non-cancellation assumption (whether the bounce-scale density is  $M_{\text{Pl}}^4$ ,  $10^{-2} M_{\text{Pl}}^4$ , or  $10^{-4} M_{\text{Pl}}^4$  shifts the required e-fold count by  $\mathcal{O}(\text{a few})$ , not by orders of magnitude), and this scale separation is what drives the 13 mechanism-class structural barriers (Sec. IX). The barriers close the bounce-to-dark-energy route on amplitude-budget and operator-counting grounds whose qualitative conclusions are ansatz-independent; only the  $\sim 2\%$  precision of the headline  $N_{\text{tot}}$  figure is ansatz-dependent. Readers should therefore treat  $N_{\text{tot}} \approx 92$  as an order-of-magnitude estimate ( $N_{\text{tot}} = 92 \pm 2$  accounting for the ansatz-choice systematic), not as a precise number; the broader structural closure does not depend on the precise e-fold value.

We emphasize that the present treatment labels the on-shell scaling explicitly as a phenomenological ansatz rather than as a derivation: a controlled EFT-level construction (an operator-basis closure for a local dimension-+4 parity-odd interaction with all required  $M_{\text{Pl}}$  factors in the coupling coefficient) remains left to a separate com-

TABLE VI. Complete parameter summary with priors, reference values, and physical interpretations. Rows marked † cite the companion internal MCMC analysis (in preparation [6]) and are not independently peer-reviewable until that work is publicly posted. The  $\gamma$  row uses the SU(2) full-counting scheme value  $\gamma_{\text{SU}(2)} \approx 0.274$  [18, 19]; the scheme range  $\sim 0.037$  (SU(2)–DLM spread) denotes LQG area-spectrum scheme dependence, *not* a statistical error.

Parameter	Description	Prior	Reference value	Notes
<i>Fundamental theory parameters</i>				
$\gamma_{\text{BI}}$	Barbero-Immirzi	Fixed: 0.274	0.274 (scheme range $\sim 0.037$ )	LQG area spectrum (Eq. 2)
$\alpha/M$	Parity-odd coefficient	Log-flat	$\sim 10^{-21} \text{ GeV}^{-1}$	One-loop motivated
$N_{\text{tot}}$	Total e-folds	[60, 120] flat	$\approx 92$ (fitted)	Controls $\Xi$
<i>Cosmological parameters (companion internal MCMC†)</i>				
$H_0^\dagger$	Hubble constant	From Planck prior	$67.68 \pm 1.06 \text{ km/s/Mpc}$	Recovers $\Lambda\text{CDM}$
$\Delta N_{\text{eff}}^\dagger$	Radiation proxy	[-3, 3] flat	$-0.020 \pm 0.169$ (full-tension)	Consistent with 0
$\sigma_8^\dagger$	Clustering amplitude	Derived	$0.803 \pm 0.008$	
$\Omega_m$	Matter density	Derived	$0.308 \pm 0.005$	
<i>Observational channel parameters</i>				
$\beta$	ALP birefringence	—	$0.27^\circ$ (midpoint)	Spectator ALP, not ECH
$f_{\text{NL}}$	Non-Gaussianity	—	$-35/8 = -4.375$	Matter bounce class <sup>a</sup>
$\gamma_{\text{PTA}}$	PTA spectral index	—	$2.567 \pm 0.382$ (real-KDE GPU MCMC)	Bounce $\gamma = 3.0$ at $+1.13\sigma$

<sup>a</sup> Survives only in bounce scenarios *not* invoking the  $N_{\text{tot}} \approx 92$  dark-energy dilution; under that dilution it is erased at SPHEREx-accessible scales (Sec. XIV D).

panion treatment.

### Appendix C: Line-of-Sight Birefringence from the Maxwell–Chern–Simons Operator

This appendix derives the rotation-angle mapping  $\beta = (\alpha/2M) \Delta\phi = (\alpha f_a/2M) \Delta\theta$  used in Eq. (19), fixing the factor of 1/2 from first principles in the operator normalization used throughout this paper.

*Setup.*—For the spectator-ALP benchmark used in Sec. IV F, assume the Maxwell–Chern–Simons form

$$\mathcal{L} \supset -\frac{1}{4} F_{\mu\nu} F^{\mu\nu} - \frac{1}{4} \frac{\alpha}{M} \phi F_{\mu\nu} \tilde{F}^{\mu\nu}, \quad (\text{C1})$$

with  $\tilde{F}^{\mu\nu} = \frac{1}{2} \epsilon^{\mu\nu\rho\sigma} F_{\rho\sigma}$  and  $\phi$  the dim-+1 canonical pseudoscalar (homogeneous: spatial gradients negligible for the cosmological background field considered here) [49, 50]. Throughout this appendix we use the dimensionless angle  $\theta \equiv \phi/f_a$  for evolution equations and quote  $\Delta\theta$  or  $\Delta\phi = f_a \Delta\theta$  interchangeably for the line-of-sight excursion; the single-convention bridge  $\phi = f_a \theta$  is recorded in the footnote at the operator’s first appearance in Sec. IV F.

*Field equation in FRW.*—Varying  $\theta$ ’s canonical action with potential  $V = m_\theta^2 f^2 (1 - \cos\theta)$  in a flat FRW background gives

$$\ddot{\theta} + 3H\dot{\theta} + m_\theta^2 \sin\theta = 0, \quad (\text{C2})$$

the equation integrated numerically by the released pipeline (`research/branch_R_alp_birefringence/phase2_mcmc/alp_ode.py`; frozen initial condition  $\theta(t_{\text{init}}) = 0$  at  $z_{\text{init}} = 3000$ ).

*Helicity dispersion.*—In conformal time ( $ds^2 = a^2(-d\eta^2 + d\vec{x}^2)$ ) the Maxwell sector of Eq. (C1) is conformally invariant, and the  $\theta F \tilde{F}$  term, being topological

up to the  $\theta$  prefactor, carries no additional factors of  $a$ . In Coulomb–temporal gauge ( $A_0 = 0$ ,  $\partial_i A^i = 0$ ; because  $\partial_\mu \theta = \theta' \delta_\mu^0$  for the homogeneous background field, the parity-odd term contributes only through the spatial  $\epsilon^{ijk} A_j \partial_k$  structure and the longitudinal mode stays non-dynamical), decomposing the transverse field into circular-polarization modes  $A_\pm(\eta, k)$ , the modified wave equation reads

$$A''_\pm + \left[ k^2 \mp \frac{\alpha}{M} \phi' k \right] A_\pm = 0, \quad (\text{C3})$$

where  $' \equiv d/d\eta$ ,  $k$  is comoving, and  $\phi' \equiv d\phi/d\eta = f_a \theta'$ ; with  $[\alpha/M] = -1$ ,  $[\phi'] = +2$ , each bracketed term carries dimension +2 as required for consistency with  $k^2$ . For  $k \gg (\alpha/M)\phi'$  (satisfied by  $\sim 30$  orders of magnitude for CMB photons against the cosmological field considered here:  $(\alpha/M)\phi' \sim 10^{-30} \text{ eV}^{-1} \times [\mathcal{O}(1) f_a] \times H_0 \sim 10^{-35} \text{ eV}$  for an  $\mathcal{O}(1)$  dimensionless excursion  $\Delta\theta$  accumulated over a Hubble time at  $f_a \sim M_{\text{Pl}}$  and the cosmological-tuning condition  $m_\theta \sim H_0$  that sets  $\dot{\theta} \sim H_0$  (in conformal time, with  $\phi' \equiv d\phi/d\eta$ ), versus a CMB photon  $k \sim 6 \times 10^{-4} \text{ eV}$  at 150 GHz, a ratio of  $\sim 10^{31}$ ) the WKB phase of each helicity is  $\int \omega_\pm d\eta$  with  $\omega_\pm \simeq k \mp \frac{1}{2}(\alpha/M)\phi'$ .

*Rotation angle.*—A linear polarization is a fixed-phase superposition of the two helicities; its position angle rotates by half the accumulated helicity phase difference:

$$\begin{aligned} \beta &= \frac{1}{2} \int_{\eta_{\text{em}}}^{\eta_{\text{obs}}} (\omega_- - \omega_+) d\eta = \frac{1}{2} \frac{\alpha}{M} \int_{\eta_{\text{em}}}^{\eta_{\text{obs}}} \phi' d\eta \\ &= \frac{\alpha}{2M} [\phi(\eta_{\text{obs}}) - \phi(\eta_{\text{em}})] \equiv \frac{\alpha}{2M} \Delta\phi = \frac{\alpha f_a}{2M} \Delta\theta. \end{aligned} \quad (\text{C4})$$

The result is achromatic (no  $k$  dependence), independent of the expansion history except through the endpoint values of  $\phi$  (equivalently the dimensionless angle

$\theta = \phi/f_a$ ; a total derivative along the line of sight — the well-known “ $2\beta = g \Delta\phi$ ” property [50]), and exact at leading WKB order. This is Eq. (19)’s mapping; with the spectator-ALP identification  $\alpha/M \equiv C_{a\gamma} \alpha_{\text{em}}/(2\pi f_a)$  (cf. the basis-conversion footnote at the first quote of  $\alpha/M = 10^{-21} \text{ GeV}^{-1}$  in Sec. IV F for the  $1/(2\pi)$ -vs- $1/(4\pi)$  normalization gap) and  $\Delta\theta = \Delta\phi/f_a$  it reproduces the com-

panion pipeline’s  $\beta = (\alpha_{\text{em}} C_{a\gamma}/4\pi)(\Delta\phi/f_a)$  (the convention block of the companion’s §VI<sup>8</sup>), closing the normalization chain from the Lagrangian to the numerical prediction; this mapping is what Eq. (19) and the Route-2 estimates of Sec. IV use. The overall sign of  $\beta$  matches the WMAP+Planck convention of Eskilt–Komatsu, in which a freely rolling field with  $\theta(\eta_{\text{obs}}) > \theta(\eta_{\text{em}})$  produces  $\beta > 0$ .

- 
- [1] Y.-F. Cai, W. Xue, R. Brandenberger, and X. Zhang, Non-gaussianity in a matter bounce, *JCAP* **0905**, 011, arXiv:0903.0631.
- [2] H. Golden,  $f_{\text{NL}} = -35/8$  Forecast: SPHEREx Discrimination of Bounce vs. Inflation, (2026), companion paper, posted concurrently on arXiv.
- [3] Y. Minami and E. Komatsu, New extraction of the cosmic birefringence from the Planck 2018 polarization data, *Physical Review Letters* **125**, 221301 (2020), arXiv:2011.11254 [astro-ph.CO].
- [4] J. R. Eskilt and E. Komatsu, Improved constraints on cosmic birefringence from the WMAP and Planck cosmic microwave background polarization data, *Phys. Rev. D* **106**, 063503 (2022), arXiv:2205.13962 [astro-ph.CO].
- [5] P. Diego-Palazuelos and E. Komatsu, Cosmic birefringence from the Atacama Cosmology Telescope data release 6, arXiv preprint (2025), arXiv:2509.13654 [astro-ph.CO].
- [6] H. Golden, Cobaya MCMC + NaMaster Birefringence + ALP Companion: Computational Verification for ECH Structural Closure, (2026), companion paper, posted concurrently on arXiv.
- [7] Planck Collaboration, N. Aghanim, *et al.*, Planck 2018 results. VI. cosmological parameters, *Astronomy & Astrophysics* **641**, A6 (2020), arXiv:1807.06209 [astro-ph.CO].
- [8] S. Weinberg, The cosmological constant problem, *Reviews of Modern Physics* **61**, 1 (1989).
- [9] DESI Collaboration, A. G. Adame, *et al.*, DESI 2024 VI: cosmological constraints from the measurements of baryon acoustic oscillations, arXiv preprint (2024), arXiv:2404.03002 [astro-ph.CO].
- [10] DESI Collaboration, M. Abdul-Karim, *et al.*, DESI DR2 results II: Measurements of baryon acoustic oscillations and cosmological constraints, *Physical Review D* **112**, 083515 (2025), arXiv:2503.14738 [astro-ph.CO].
- [11] A. Ashtekar and P. Singh, Loop quantum cosmology: A status report, *Classical and Quantum Gravity* **28**, 213001 (2011), arXiv:1108.0893 [gr-qc].
- [12] F. W. Hehl, P. von der Heyde, G. D. Kerlick, and J. M. Nester, General relativity with spin and torsion: Foundations and prospects, *Reviews of Modern Physics* **48**, 393 (1976).
- [13] N. J. Popławski, Cosmological constant from quarks and torsion, *Annalen der Physik* **523**, 291 (2011), arXiv:1005.0893 [gr-qc].
- [14] N. J. Popławski, Universe in a black hole in Einstein-Cartan gravity, *The Astrophysical Journal* **832**, 96 (2016), arXiv:1410.3881 [gr-qc].
- [15] S. Mercuri, Peci-quin mechanism in gravity and the nature of the Barbero-Immirzi parameter, *Physical Review Letters* **103**, 081302 (2009), arXiv:0902.2764 [gr-qc].
- [16] L. Freidel, D. Minic, and T. Takeuchi, Quantum gravity, torsion, parity violation and all that, *Physical Review D* **72**, 104002 (2005), arXiv:hep-th/0507253 [hep-th].
- [17] A. Ashtekar, J. C. Baez, A. Corichi, and K. Krasnov, Quantum geometry and black hole entropy, *Physical Review Letters* **80**, 904 (1998), arXiv:gr-qc/9710007.
- [18] M. Domagała and J. Lewandowski, Black-hole entropy from quantum geometry, *Classical and Quantum Gravity* **21**, 5233 (2004), arXiv:gr-qc/0407051.
- [19] K. A. Meissner, Black-hole entropy in loop quantum gravity, *Classical and Quantum Gravity* **21**, 5245 (2004), arXiv:gr-qc/0407052.
- [20] I. L. Shapiro and P. M. Teixeira, Quantum Einstein-Cartan theory with the Holst term, *Classical and Quantum Gravity* **31**, 185002 (2014), arXiv:1402.4854 [gr-qc].
- [21] D. Saadeh, S. M. Feeney, A. Pontzen, H. V. Peiris, and J. D. McEwen, How isotropic is the universe?, *Physical Review Letters* **117**, 131302 (2016), arXiv:1605.07178 [astro-ph.CO].
- [22] V. A. Kuzmin, V. A. Rubakov, and M. E. Shaposhnikov, On anomalous electroweak baryon-number non-conservation in the early universe, *Phys. Lett. B* **155**, 36 (1985).
- [23] H. Golden, Galaxy Chirality at Scale: 8.47M Galaxies Classified, Hemisphere Null at  $p_{\text{LEE}} < 10^{-4}$ , (2026), companion paper, posted concurrently on arXiv.
- [24] F. W. Hehl and B. K. Datta, Nonlinear spinor equation and asymmetric connection in general relativity, *J. Math. Phys.* **12**, 1334 (1971).
- [25] R. Jackiw and S.-Y. Pi, Chern-simons modification of general relativity, *Physical Review D* **68**, 104012 (2003).
- [26] S. Holst, Barbero’s Hamiltonian derived from a generalized Hilbert-Palatini action, *Physical Review D* **53**, 5966 (1996), arXiv:gr-qc/9511026 [gr-qc].
- [27] G. Date, R. K. Kaul, and S. Sengupta, Topological interpretation of Barbero-Immirzi parameter, *Phys. Rev. D* **79**, 044008 (2009), arXiv:0811.4496 [gr-qc].
- [28] D. Benedetti and S. Speziale, Perturbative quantum gravity with the Immirzi parameter, *JHEP* **06**, 107, arXiv:1104.4028 [hep-th].
- [29] D. Benedetti and S. Speziale, Perturbative running of the Immirzi parameter, *J. Phys. Conf. Ser.* **360**, 012011

---

<sup>8</sup> The WKB condition  $k \gg (\alpha/M)\phi'$  entering this appendix is satisfied by  $\sim 30$  orders of magnitude:  $(\alpha/M)\phi' \sim 10^{-35} \text{ eV}$  vs.  $k \sim 6 \times 10^{-4} \text{ eV}$  for a 150 GHz CMB photon (see computation block above Eq. (C3)). This recomputation is self-contained within App. C; no companion result is required to establish the WKB approximation.

- (2012), [arXiv:1111.0884 \[hep-th\]](#).
- [30] A. Lue, L. Wang, and M. Kamionkowski, Cosmological signature of new parity violating interactions, *Phys. Rev. Lett.* **83**, 1506 (1999), [arXiv:astro-ph/9812088 \[astro-ph\]](#).
- [31] LiteBIRD Collaboration, E. Allys, *et al.*, Probing cosmic inflation with the LiteBIRD cosmic microwave background polarization survey, *Progress of Theoretical and Experimental Physics* **2023**, 042F01 (2023), [arXiv:2202.02773 \[astro-ph.IM\]](#).
- [32] S. M. Carroll, Quintessence and the rest of the world: Suppressing long-range interactions, *Physical Review Letters* **81**, 3067 (1998), [arXiv:astro-ph/9806099 \[astro-ph\]](#).
- [33] Y.-F. Cai, E. N. Saridakis, M. R. Setare, and J.-Q. Xia, Quintom Cosmology: Theoretical implications and observations, *Phys. Rept.* **493**, 1 (2010), [arXiv:0909.2776 \[hep-th\]](#).
- [34] L. Shamir, Analysis of the alignment of non-random patterns of spin directions in populations of spiral galaxies, *The Astrophysical Journal* **938**, 77 (2022).
- [35] L. Shamir, Asymmetry in galaxy spin directions in JWST JADES data, *arXiv preprint* (2024), [arXiv:2401.09450 \[astro-ph.GA\]](#).
- [36] D. Patel and H. Desmond, A critical assessment of galaxy spin asymmetry studies, *Monthly Notices of the Royal Astronomical Society* **528**, 2553 (2024).
- [37] O. H. E. Philcox and J. Ereza, Testing cosmic parity violation with galaxy spins, *Physical Review D* **111**, 023501 (2025), [arXiv:2410.18185 \[astro-ph.CO\]](#).
- [38] C. Heinrich, O. Dore, and E. Krause, Measuring  $f_{nl}$  with the spherex multi-tracer redshift space bispectrum, *JCAP* **2024** (04), 074, [arXiv:2311.13082 \[astro-ph.CO\]](#).
- [39] S. Dehghani, G. Geshnizjani, and J. Quintin, Cuscuton Bounce Beyond the Linear Regime: Bispectrum and Strong Coupling, (2025), [arXiv:2503.01992 \[gr-qc\]](#).
- [40] K. Gödel, An Example of a New Type of Cosmological Solutions of Einstein's Field Equations of Gravitation, *Rev. Mod. Phys.* **21**, 447 (1949).
- [41] N. J. Popławski, Cosmology with torsion: An alternative to cosmic inflation, *Physics Letters B* **694**, 181 (2010), [arXiv:1007.0587 \[astro-ph.CO\]](#).
- [42] S. Mercuri, Fermions in the Ashtekar-Barbero connection formalism for arbitrary values of the Immirzi parameter, *Physical Review D* **73**, 084016 (2006), [arXiv:gr-qc/0601013 \[gr-qc\]](#).
- [43] T. Liu, X. Li, T. Xu, M. Biesiada, and J. Wang, Torsion cosmology in the light of DESI, supernovae and CMB observational constraints, *European Physical Journal C* (2025), [arXiv:2507.04265 \[gr-qc\]](#).
- [44] S. Legner, W. Handley, and W. Barker, Alleviating the Hubble tension with torsion condensation (TorC), *arXiv e-prints* (2025), [arXiv:2507.09228 \[astro-ph.CO\]](#).
- [45] S. Alam, S. Sen, and S. Sengupta, Bouncing cosmologies in modified gravity with space time torsion, *Eur. Phys. J. C* (2025), [arXiv:2509.03508 \[gr-qc\]](#).
- [46] Y.-F. Cai and J.-H. Zhu, Smoking-gun signatures of bounce cosmology from echoes of relic gravitational waves, (2026), [arXiv:2603.13924 \[astro-ph.CO\]](#).
- [47] T. Papanikolaou, S. Banerjee, Y.-F. Cai, S. Capozziello, and E. N. Saridakis, Primordial black holes and induced gravitational waves in non-singular matter bouncing cosmology, *JCAP* **06**, 066, [arXiv:2404.03779 \[gr-qc\]](#).
- [48] H. Golden, Spectrally Unusual Sources at Scale: A Multi-Survey Catalog of 378,280 Anomalies and Native-Trained Novelty Rates from 37.3 Million Sources, (2026), companion paper, posted concurrently on arXiv.
- [49] S. M. Carroll, G. B. Field, and R. Jackiw, Limits on a Lorentz- and parity-violating modification of electrodynamics, *Physical Review D* **41**, 1231 (1990).
- [50] D. Harari and P. Sikivie, Effects of a nambu-goldstone boson on the polarization of radio galaxies and the cosmic microwave background, *Phys. Lett. B* **289**, 67 (1992).

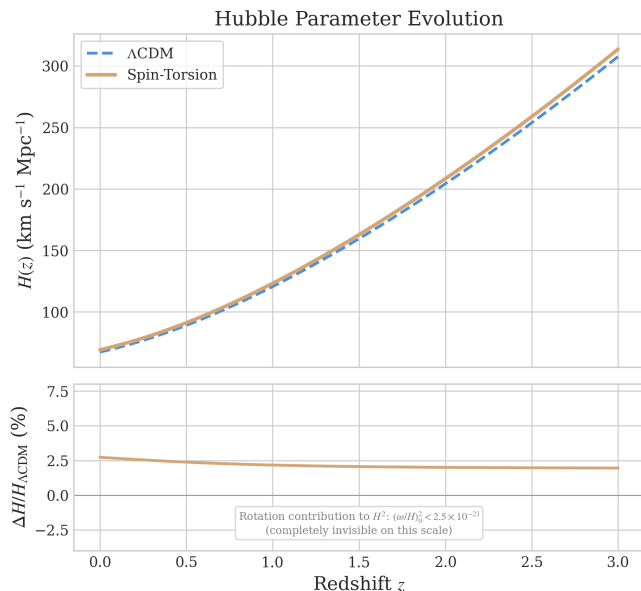


**FIG. 3. ECH dark-energy model vs.  $\Lambda$ CDM Hubble evolution.** Upper panel ( $y$ -axis:  $H(z)$  [ $\text{km s}^{-1} \text{Mpc}^{-1}$ ]): Hubble parameter for the full ECH dark-energy model (orange;  $\Xi M_{\text{Pl}}^2$  term from Eq. 10) versus  $\Lambda$ CDM (blue). Lower panel ( $y$ -axis:  $\Delta H/H_{\Lambda\text{CDM}}$  [%]): percent deviation between the spin-torsion benchmark cosmology and a Planck-VI  $\Lambda$ CDM reference; an illustrative parameter-set comparison under the  $\Xi M_{\text{Pl}}^2$  phenomenological on-shell scaling ansatz (Appendix B), not a derived prediction. The Lite-BIRD/SPHEREx falsification windows (§III, Sec. X G; 2027–early-2030s) carry the load-bearing testable predictions. The rotation contribution  $c_\omega \omega^2$  is a *distinct* and negligible term, confined to  $\lesssim 10^{-21} \rho_\Lambda^{\text{obs}}$  ( $(\omega/H)_0^2 < 2.5 \times 10^{-21}$ ; dividing by  $3\Omega_\Lambda \approx 2.1$  gives  $\sim 1.2 \times 10^{-21}$  of  $\rho_\Lambda^{\text{obs}}$ ) — completely invisible on the scale plotted. The dark-energy mechanism is therefore the  $\Xi M_{\text{Pl}}^2$  term sourced by the parity-odd contorsion sector (§II A 2), *not* the rotation component. The orange ECH curve uses  $\Xi$  set to reproduce  $\rho_\Lambda$  (i.e.  $\Xi = \rho_\Lambda/M_{\text{Pl}}^4 = \Lambda_{\text{eff}}/M_{\text{Pl}}^2 \approx 10^{-123}$ , consistent with the dimensionless-ratio derivation in the body below) with spin-torsion benchmark cosmology  $H_0 = 69.2 \text{ km/s/Mpc}$ ,  $\Omega_m = 0.310$ , and enhanced radiation density  $\Omega_r^{\text{ext}} = \Omega_r^{\text{std}}(1 + 0.3\frac{7}{8}(\frac{4}{11})^{4/3})$  as a  $\Delta N_{\text{eff}}$  proxy for the extra-radiation ECH channel; the  $\Lambda$ CDM reference uses  $H_0 = 67.36 \text{ km/s/Mpc}$ ,  $\Omega_m = 0.315$  (Planck-VI best-fit). The  $\Delta H/H_{\Lambda\text{CDM}}$  deviation is  $\sim 2$ – $3\%$  across  $z = 0$ – $3$ , but *this deviation is dominated by the differing  $H_0$  baselines, not by spin-torsion dynamics*: because  $H(0) \equiv H_0$  for both models, the  $z = 0$  residual is exactly the  $H_0$  offset,  $(69.2 - 67.36)/67.36 \approx 2.7\%$ , independent of the  $\Xi M_{\text{Pl}}^2$  sector. An  $H_0$ -matched comparison (identical  $H_0, \Omega_m$  for both curves) isolates the genuine dynamical effect of the spin-torsion dark-energy term, a sub-percent residual sourced by the  $\Omega_m$  and  $\Delta N_{\text{eff}}$  differences alone; the figure is thus an illustrative benchmark-parameter overlay, *not* a measure of the spin-torsion signal, and the 2–3% figure must not be read as a bounce signature. The benchmark  $H_0 = 69.2$  used here is a deliberately high illustrative value and differs from the paper’s adopted  $H_0 = 67.68 \pm 1.06$  (Table I, Table VI). The  $(\omega/H)_0 < 5 \times 10^{-11}$  bound (Saadeh *et al.* [21]) applies under the Bianchi IX isotropized cosmological model and is adopted here as a conservative bookkeeping upper limit on  $c_\omega \omega^2$ .

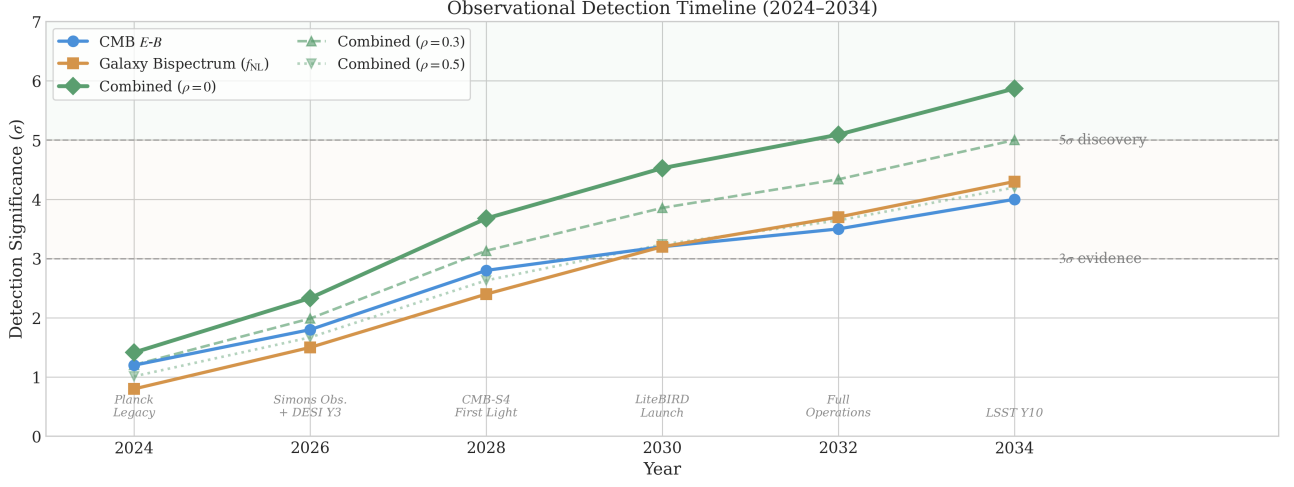


FIG. 4. **Observational decision timeline for the two surviving ECH-independent class-level falsification paths.** Top: LiteBIRD CMB birefringence ( $\sigma(\beta) \approx 0.03^\circ$ , launch early 2030s) testing the spectator-ALP route 4. Bottom: SPHEREx galaxy bispectrum ( $\sim 2028$  first cosmological data release) testing the matter-bounce  $f_{NL} = -35/8$  prediction at  $2.6\text{--}5\sigma$  realistic significance (footnote 6). Both surveys deliver ECH-independent class-level discrimination tests; under the stated ansätze they can falsify the relevant matter-bounce and uniform spectator-ALP benchmarks, but they do not identify a unique surviving minimal-ECH channel. Curve families labeled  $\rho = 0, 0.3, 0.5$  correspond to the assumed cross-correlation coefficient  $\rho$  between the  $f_{NL}$  and  $\beta$  joint-forecast estimators (with  $\rho = 0$  the uncorrelated baseline;  $\rho > 0$  combinations track the gain in joint significance under a positive between-estimator correlation).

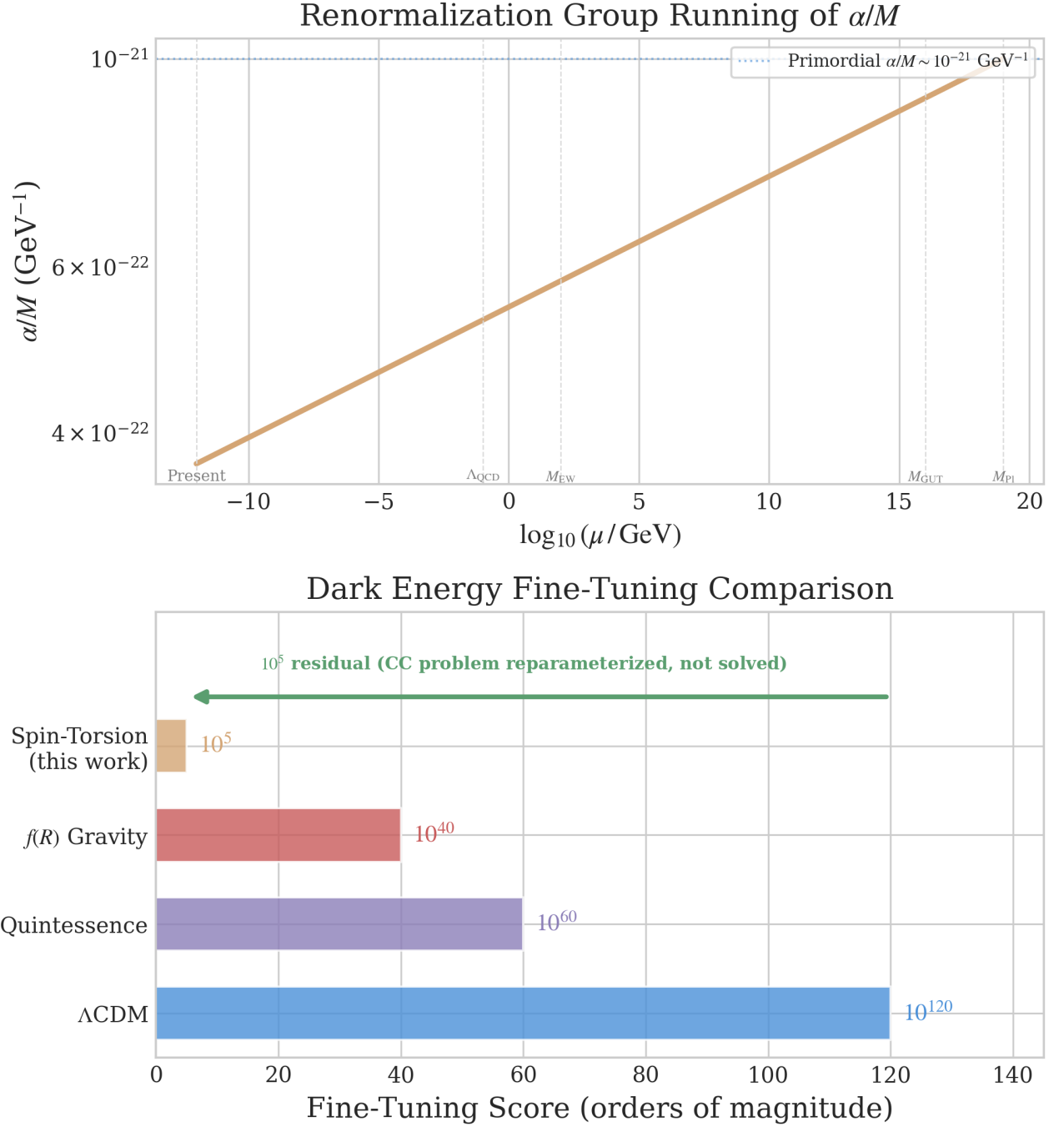
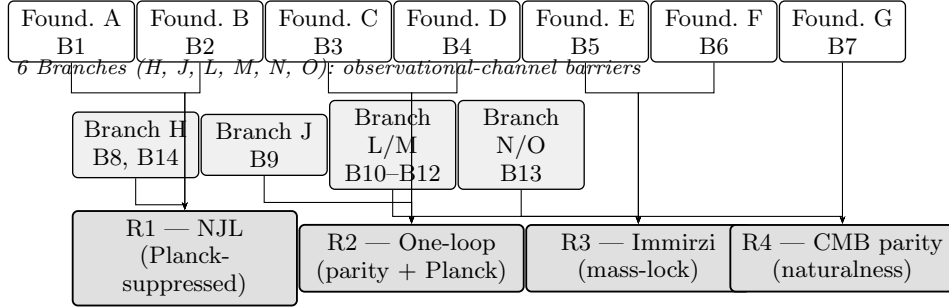


FIG. 5. **Parameter-naturalness diagnostics for the minimal-ECH dark-energy parameterization.** *Top* ( $y$ -axis:  $\alpha/M$  [ $\text{GeV}^{-1}$ ]): renormalization-group running of the parity-odd coupling from the present epoch to the Planck scale, anchored at the primordial benchmark  $\alpha/M \sim 10^{-21} \text{ GeV}^{-1}$  (Sec. IV F). *Bottom* ( $y$ -axis: fine-tuning score [orders of magnitude]): comparison of residual tuning (unreduced  $M_{\text{Pl}}$  convention throughout):  $\Lambda\text{CDM}$  ( $10^{122}$ ), quintessence ( $10^{60}$ ),  $f(R)$  gravity ( $10^{40}$ ), and the spin-torsion  $N_{\text{tot}}$  parameterization of this work ( $10^5$ ). The  $\Lambda\text{CDM}$  ( $10^{122}$ ) and spin-torsion ( $10^5$ ) scores are derived in this paper (Appendix B and Sec. XII A); the quintessence ( $10^{60}$ ) and  $f(R)$  ( $10^{40}$ ) entries are illustrative order-of-magnitude literature-level comparators, not derived here. The  $10^5$  residual annotation is the score under the  $N_{\text{tot}}$  reparameterization; per Sec. XII A this is a reparameterization of the cosmological-constant problem as sensitivity to  $N_{\text{tot}}$ , *not* a resolution. All four enumerated routes either sit outside their naturalness windows or require a  $m_\theta \sim H_0$  tuning that re-imports the cosmological-constant problem; the 13 mechanism-class constraints (Table IV) constrain the routes at the amplitude level. ( $\sigma$  values across panels use different null procedures; see text.)

## 7 Foundations (A–G): mechanism-class barriers



All four routes closed (13 mechanism-class constraints)

FIG. 6. **Structure of the 14-barrier closure.** The 7 foundation mechanism classes (Foundations A–G, top row; Barriers 1–7) and 6 observational-channel branches (Branches H, J, L, M, N, O, middle row; Barriers 8–14) feed collectively into the four closed dark-energy routes R1–R4 (bottom row). Arrows indicate which barrier classes constrain each route. B8 (Branch H, parity-even interaction) is subsumed by B14 (perturbation transparency) and they are grouped together. Thirteen mechanism-class constraints are shown (several share the scaling ansatz but each probes a distinct physical failure mode); B8 is not counted separately.

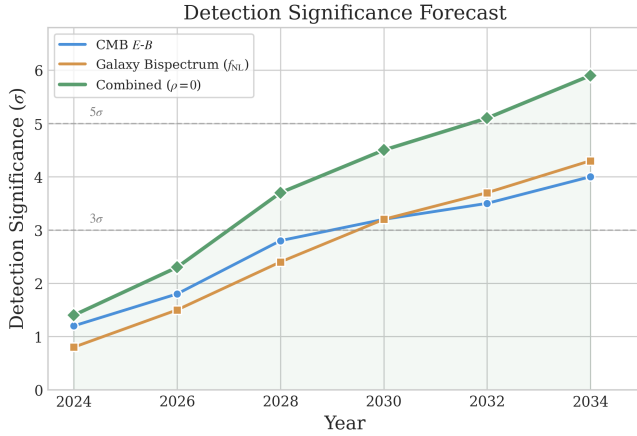


FIG. 7. **Detection forecast for the two surviving ECH-independent class tests.** Top: matter-bounce  $f_{\text{NL}} = -35/8$  in the SPHEREx multi-tracer  $f_{\text{NL}}$  Fisher landscape (in preparation [2], 2.6–5 $\sigma$  projection). Bottom: spectator-ALP cosmic birefringence in the LiteBIRD  $\sigma(\beta) \approx 0.03^\circ$  window (in preparation [6]); the WMAP+Planck  $\beta = 0.342^\circ \pm 0.094^\circ$  and ACT DR6  $\beta = 0.215^\circ \pm 0.074^\circ$  points are shown for reference. The SPHEREx  $f_{\text{NL}}$  forecast is potentially decisive in optimistic configurations; 2.6–5 $\sigma$  after the stated systematic budget (Table I footnote b) against  $f_{\text{NL}} = 0$ ; the LiteBIRD birefringence forecast targets a non-zero- $\beta$  detection at its  $\sigma(\beta) \approx 0.03^\circ$  sensitivity but does not separate  $\beta = 0.27^\circ$  from the published  $\beta = 0.342^\circ \pm 0.094^\circ$  at high significance (the discrimination runs at  $\sim 0.7\sigma$  given current central values); neither is uniquely an ECH prediction (§XIII). The significance tracks duplicate the  $\rho = 0$  combination of Fig. 4 ( $\rho$  here is the cross-correlation coefficient between the  $f_{\text{NL}}$  and  $\beta$  joint-forecast estimators; see the Fig. 4 caption for the precise definition); this panel is the summary view retained for the surviving-tests discussion, while Fig. 4 additionally shows the correlated ( $\rho = 0.3, 0.5$ ) combinations and milestone annotations. ( $\sigma$  values across panels use different null procedures; see text.)